

Hong Duc Ta

**A Kinetic Analysis of Ester Hydrolysis Reactions
Considering Volume and Enthalpy Changes Due to Mixing**



Fakultät für Verfahrens- und Systemtechnik
Otto-von-Guericke-Universität Magdeburg

A Kinetic Analysis of Ester Hydrolysis Reactions Considering Volume and Enthalpy Changes Due to Mixing

Dissertation

zur Erlangung des Akademischen Grades

Doktoringenieur (Dr.-Ing.)

von: M.Sc. Hong Duc Ta
geb. am: 20.02.1977
in: Vinh Phuc, Viet Nam

genehmigt durch die
Fakultät für Verfahrens- und Systemtechnik
der Otto-von-Guericke-Universität Magdeburg

Gutachter: Prof. Dr.-Ing. Andreas Seidel-Morgenstern
Prof. Dr.-Ing. Stephan Scholl (TU Braunschweig)
Prof. Dr.-Ing. Dorota Antos (TU Rzeszów)

eingereicht am: 10.01.2012
Promotionskolloquium am: 20.03.2012

Acknowledgements

I am deeply indebted to a number of people who have helped me to make this doctoral thesis possible.

First and foremost, I would like to extend my deepest gratitude to my supervisor, Prof. Andreas Seidel-Morgenstern, for giving me excellent academic guidance and leading me to the right track of research. Without his expert advice, great patience and generous support, this research would not have come to fruition.

Enormous thanks are due to Prof. Stephan Scholl and Prof. Dorota Antos for reviewing my dissertation and giving me constructive comments and suggestions.

My appreciation also goes to all my colleagues of the Chair of Chemical Process Engineering, Otto-von-Guericke-University and the Group of Physical and Chemical Foundations of Process Engineering, Max Planck Institute Magdeburg. I am particularly indebted to Dr. Christof Hamel, Tino Lehmann, Frau Marlis Chrobog, Frau Marion Hesse, Frau Anett Raasch and Frau Nancy Ziebell for all the useful discussions and sharing with me my beautiful PhD years in Germany.

I would also like to acknowledge the financial support provided by Vietnamese Government, German Academic Exchange Service - DAAD, Project 3 Network of Otto-von-Guericke-University Magdeburg and Max Planck Society.

Initial guidance and continuous encouragement of Prof. Mai Xuan Ky and Prof. Ha Thi An are acknowledged personally.

Last but not least, I would like to thank my wife Cam Le for her dedication, understanding and love during the past years. I thank my parents for their support and encouragement throughout my life. Also, my parents-in-law, my sisters-in-law, my brother and my son receive my deepest gratitude for their constant love, encouragement and immeasurable compassion.

Abstract

Liquid phase reactions are frequently performed in conventional well-mixed batch reactors. Hereby volume changes can occur even for ideal solutions due to composition changes caused by the reactions. Pronounced additional effects are possible in case of real mixtures, in which significant volume and temperature changes can happen due to mixing. However, these changes are often not considered in quantifying the kinetics of liquid phase reactions and in modelling and optimizing reactor behaviour.

An established theory to describe excess molar volumes and excess molar enthalpies is provided in the thermodynamic literature. This theory is based on Gibbs energy and activity coefficient models. To account for mixing effects the parameters in these models are needed as a function of temperature and pressure. However, for most liquid solutions these dependencies are not well known. In this study, excess molar volumes and excess molar enthalpies were quantified experimentally.

In order to acquire an understanding of the relevance of mixing effects in real reacting liquid mixtures, volume changes due to mixing were incorporated into a batch reactor model. This model was applied to estimate kinetic parameters from experimentally determined concentration courses. The reversible hydrolysis of two esters (methyl formate and ethyl formate) were investigated as model reactions. To follow the courses of these reactions the concentration profiles of the alcohols and the corresponding heat fluxes were measured as a function of time. The chemical reaction equilibrium constants were determined from measured concentrations for various temperatures at equilibrium. To describe the reaction equilibria based on activities, activity coefficients were computed using the UNIFAC method.

Kinetic parameters of the two hydrolysis reactions were estimated analysing the observed transients based on *i)* neglecting and *ii)* incorporating volume changes of the reaction mixture due to both reaction and mixing. The obtained kinetic parameters were compared and the differences evaluated and interpreted. The results based on incorporating the mentioned effects were found to be capable of describing the measured data well. The kinetic parameters were used to simulate transient temperature profiles in a batch reactor under adiabatic conditions based on incorporating heat changes due to both reaction and mixing.

Conclusions regarding the importance of incorporating volume changes in analysing and predicting liquid phase reactions are drawn. The results of the study performed illustrate *i)* how the relevance of mixing effects can be evaluated for reactive liquid phases and in case of significance *ii)* how the property changes due to mixing can be described.

Zusammenfassung

Flüssigphasenreaktionen werden häufig in konventionellen, intensiv durchmischten Rührkessel-reaktoren durchgeführt. Selbst in idealen Lösungen kann es infolge der reaktionsbedingten Veränderung der Stoffzusammensetzung zu Volumenänderungen kommen. Zusätzliche Effekte sind in realen Mixturen möglich, in denen es zu Änderungen des Volumens und der Temperatur durch das Vermischen von Komponenten kommt. Diese Einflüsse werden jedoch bei der Quantifizierung der Kinetik von Flüssigphasenreaktionen, der Modellierung des Verhaltens von Reaktoren und der Optimierung ihrer Leistungsfähigkeit oft nicht betrachtet.

In der Literatur zur Thermodynamik findet sich eine etablierte Theorie zur Beschreibung von molaren Exzess volumina und Exzess enthalpien. Diese Theorie basiert auf der Analyse der Gibbs-Energie und der Aktivitätskoeffizienten. Um Mischeffekte zu berücksichtigen, werden die in diesen Modellen enthaltenen Parameter in Abhängigkeit der Temperatur und des Drucks benötigt. Für die meisten Lösungen sind diese Zusammenhänge weitgehend unbekannt. In der vorliegenden Untersuchung werden molare Exzess volumina und molare Exzess enthalpien experimentell ermittelt.

Um die Relevanz von Mischeffekten in realen reagierenden Flüssigphasen zu verstehen, wurde die Volumenänderung infolge des Mischens der Komponenten in ein *Batch*-Reaktor-Modell einbezogen. Dieses Modell wurde verwendet, um kinetische Parameter aus experimentell bestimmten Konzentrationsverläufen zu berechnen. Die reversible Hydrolyse von zwei Estern (Methylformiat und Ethylformiat) wurden als Modellreaktionen untersucht. Um die Reaktionsverläufe zu verfolgen, wurden die Konzentrationsprofile der Alkohole und die dazugehörigen Wärmeströme als Funktion der Zeit gemessen. Die chemischen Gleichgewichtskonstanten wurden aus den bei verschiedenen Temperaturen im Gleichgewicht gemessenen Konzentrationen ermittelt. Um die Reaktionsgleichgewichte aktivitätsbasiert zu beschreiben, wurden Aktivitätskoeffizienten mittels der UNIFAC-Methode berechnet.

Die kinetischen Parameter der zwei Hydrolysereaktionen wurden berechnet, indem die beobachteten Prozesse *i*) unter Vernachlässigung bzw. *ii*) unter Berücksichtigung der Volumenänderung der Reaktionsmischungen infolge der Reaktion und des Mischens analysiert wurden. Die erhaltenen kinetischen Parameter wurden miteinander verglichen und Abweichungen bewertet und interpretiert. Die Berücksichtigung der erwähnten Effekte erlaubte eine gute Beschreibung der gemessenen Daten. Die erhaltenen kinetischen Parameter wurden verwendet, um transiente Temperaturprofile für adiabate Bedingungen unter Einbeziehung von Einflüssen des Mischens und der Reaktion zu simulieren.

Es wurden allgemeine Schlussfolgerungen bezüglich der Bedeutung der Berücksichtigung der Volumenänderungen für die Vorhersage und Analyse von Flüssigphasenreaktionen gezogen. Die Ergebnisse dieser Studie zeigen *i*) wie die Relevanz von Mischeffekten bewertet und *ii*) wie im Fall der Signifikanz der Effekte Veränderung von Eigenschaften infolge des Mischens beschrieben werden können.

CONTENTS

1. INTRODUCTION	1
1.1 THERMODYNAMICS	1
1.2 KINETICS OF REACTIONS	2
1.3 BATCH REACTORS.....	3
1.4 RESEARCH OBJECTIVES AND OUTLINE.....	4
2. FUNDAMENTAL ASPECTS	7
2.1 THERMODYNAMICS	7
2.1.1 Ideal Solutions	7
2.1.2 Real Solutions.....	12
2.1.2.1 Models for the excess Gibbs energy and corresponding activity coefficients ...	18
2.1.2.2 Models for excess volumes due to mixing effects.....	26
2.1.2.3. Model for excess enthalpies due to mixing effects	30
2.1.3 Chemical reaction equilibria.....	32
2.2 CHEMICAL KINETICS	38
2.3 REACTOR MODELS	41
2.3.1 Mass balance of chemical reactors	41
2.3.1.1 Batch Reactors with constant - volume	42
2.3.1.2 Batch Reactors with varying – volume	42
2.3.2. Energy balance of chemical reactors.....	46
2.3.3 Numerical aspects of solving the mass and energy balances	51
2.4 ILLUSTRATION OF NON-IDEAL BEHAVIOUR.....	52
2.4.1 Non-reactive system	52
2.4.2 Transient reactive system	59
2.4.2.1 Isothermal varying volume and constant volume BR	60
2.4.2.2 Adiabatic and isothermal BR	63
3. MODEL REACTIONS	68
3.1 MODEL REACTIONS	68
3.2 PHYSICAL AND THERMODYNAMIC PROPERTIES	69
3.2.1 Physical properties.....	69
3.2.2 Thermodynamic properties.....	70
3.3 CHEMICAL EQUILIBRIA	73
3.3.1 Chemical reaction equilibrium	73
3.3.2 Dissociation equilibrium	74
4. EXPERIMENTAL INVESTIGATIONS	76
4.1 EXPERIMENTAL EQUIPMENT	76
4.1.1 Equipments to determine molar excess volumes.....	76

4.1.2 Equipments to measure molar excess enthalpies and reaction enthalpies.....	77
4.1.3 Batch reactor and equipment to measure heat fluxes	80
4.1.4 Concentration analysis.....	82
4.2 EXPERIMENTAL PROCEDURES AND PROGRAM.....	83
4.2.1 Measurement of molar excess volumes V^E	83
4.2.2 Measurement of molar excess enthalpies H^E	84
4.2.3 Measurement of reaction enthalpies ΔH_R	86
4.2.4 FTIR calibration	86
4.2.5 Measurement of reaction equilibrium constants.....	87
4.2.6 Reaction kinetics experiments in batch reactor	87
5. RESULTS AND DISCUSSION.....	89
5.1 EXPERIMENTAL RESULTS	89
5.1.1 Molar excess volumes	89
5.1.2 Molar excess enthalpies.....	93
5.1.3 Reaction equilibrium constants and reaction enthalpies	95
5.1.4 Reaction enthalpies from calorimetric measurements.....	97
5.2 ESTIMATION OF REACTION KINETIC PARAMETERS FROM CONCENTRATION PROFILES.....	98
5.2.1 Constant volume (“ <i>Const</i> ”)	99
5.2.2 Varying volume due to reaction (“ <i>Ideal</i> ”).....	99
5.2.3 Varying volume due to mixing and reaction (“ <i>Real</i> ”).....	100
5.2.4 Parameter fitting	101
5.2.5 Determined reaction rate constants	101
5.3 SENSITIVITY OF KINETIC PARAMETERS	109
5.4 CORRECTION OF THE REACTION HEAT BY THE HEAT OF MIXING AND SIMULATION OF TEMPERATURE PROFILES	111
5.4.1 Correction of the reaction heat by the heat of mixing	111
5.4.2 Adiabatic conditions.....	114
6. CONCLUSIONS AND OUTLOOK	116
Nomenclature	119
References	122
APPENDIX	
A. Calculation of Gibbs energies of formation.	128
B. Molar excess volume V^E	129
C. Molar excess enthalpy H^E	133
D. IR spectra of pure components	137
E. FTIR calibration curves	139

CHAPTER 1

INTRODUCTION

Chemical thermodynamics is an important field of science that studies two questions relevant for reaction engineering. It tells us if a reaction will spontaneously happen or not. Furthermore, it quantifies energetic effects connected with the course of chemical reactions. Thus, thermodynamics plays a key role in phase and chemical equilibrium.

In contrast, chemical kinetics quantitatively study the rates at which chemical reactions happen. This field is concerned with composition changes and the energy and mass fluxes associated therewith. Kinetics of reaction aims to understand the mechanisms of reactions. Studies of reaction rates provide the way to describe chemical reactions quantitatively and to design and optimize reactors.

Chemical engineering thermodynamics and kinetics have been widely investigated and are described extensively in the literature, e.g. [Smith05], [Ness82], [Leve99], [Miss99], [Weste90].

For many years, investigations of the kinetics of liquid phase reactions are based on analyzing data assuming constant volume conditions. However, there is broad evidence that there are significant volume and temperature changes due to mixing in liquid system [Smith05], [Robe87], [Tsao53], etc. Moreover, even in ideal reactive solutions volume changes can occur due to composition changes caused by chemical reactions progressing with time.

In order to gain a better understanding of mixing effects of real solutions on reaction kinetics, this research aims to provide a quantitative evaluation by performing a kinetic analysis of hydrolysis reactions of esters considering volume and enthalpy changes due to mixing.

1.1 THERMODYNAMICS

The application of thermodynamics to any real problem starts with the identification of a particular body which may be a specified volume in space or a quantity of matter as the focus of attention. This body of matter is called the *system*; the rest of the universe is its

surroundings and between the system and its surrounding is a boundary. To describe system the term *state* is used which referring to the thermodynamic state of a system with given properties: pressure P , temperature T , volume V , molar number of species i n_i , mass m , etc. The state of agglomeration of the system like gas, liquid, or solid, is called its *phase*.

Systems can be identified as open, closed or isolated. If mass can flow into or out of thermodynamic system through boundary, then it is an *open* system; if not it is a *closed* system. If a system does not change as a result of changes in its surrounding, the system is said to be *isolated*. An *adiabatic* system is not in thermal contact, but may be in mechanical contact, with its surroundings, this system is one that is thermally isolated from its surroundings [Sand99].

The state of a system is characterized by its properties such as temperature, pressure, and composition. The equilibrium state of a system is one of the most important concepts in thermodynamics. Equilibrium state means that there is no change with time in any of the measurable properties of the system [Never02]. For instance, if a system is not subjected to a continuous forced flow of mass, heat, or work, the system will eventually evolve to a time-invariant state in which there are no internal or external flows of heat or mass and no change in composition as a result of chemical reactions. This state of system is called the equilibrium state [Sand99].

The research described in this thesis deals with non-ideal or real solution system. The simple relationships valid in ideal solutions are not applicable to non-ideal solutions which need modification because of the change in thermodynamic properties of real solutions. The additional properties introduced are called *excess properties* [Smith05], [Ness82], [Abbot89]. The changes of volume and heat, excess volume and enthalpy, due to mixing inside the reaction mixture directly influence the values of chemical kinetic parameters.

This dissertation will concentrate on two important areas of chemical thermodynamics:

- (1) Solution thermodynamics of ideal and non-ideal solutions, particularly changes of volumes and enthalpies due to mixing
- (2) Chemical reaction equilibria of mixtures of liquids

Information provided by thermodynamics will be used and incorporated to determine kinetic parameters in real reactive liquid solutions.

1.2 KINETICS OF REACTIONS

Kinetics analyses are devoted to study rates of chemical processes and all factors effecting these rates, e.g. [Leve99], [Miss99], [Weste90], [Smith81], [Coop71]. The kinetics reactions depend on concentrations and temperature. For heterogeneously catalysed reactions the concentrations and type of the catalyst are additional factors influencing rates. For multi-phase reactions, transport processes interface effects have to be considered. The kinetics of

heterogeneous systems depend on both the intrinsic chemical reactions (micro kinetics) and on transport phenomena (macro kinetics).

Rate equations are mathematical models that describe the kinetics of chemical reactions. The parameters of these models can only be determined by experiments.

The identification of suitable rate equations is often a two-step procedure [Leve99]; first the concentration dependency is found at a given constant temperature and then the temperature dependence of the rate constants is estimated, yielding the complete rate equation.

Approaches to study reaction rates differ typically in the following aspects [Miss99]

- (1) Type of reactors applied (e.g., a batch reactor)
- (2) Species (reactant or product) followed during the experiments (e.g., by chemical analysis)
- (3) Methods used to follow the extent of reaction with respect to time (e.g., by Fourier transform infrared (FTIR) spectroscopy or chromatographic analysis)
- (4) Methods applied to determine numerically the value of the parameters, and hence to establish the form of the rate law

To gain an insight into a chemical process, thermodynamics must be applied in combination with chemical kinetics in an appropriate reactor model. The reactor used in this dissertation is the Batch Reactor (BR) described below.

1.3 BATCH REACTORS

Figure 1.1 illustrates a classical Batch Reactor (BR). A first application of these discontinuously operated reactors is to perform laboratory scale experiments and to determine parameters of reaction rate equation [Leve99], [Miss99], [Coop71]. The reactor is defined as a closed spatially uniform system which has concentration parameters that are typically specified at time zero by an initial recipe [Schm98]. Homogeneity requires that the system is typically stirred rapidly by a mixer.

It is assumed that also the reaction temperature is the same in the whole reactor. To maintain thermal conditions in transient period a heating or cooling jacket is used. If the temperature in this heating or cooling jacket can be controlled to be the same as in the reactor, an adiabatic operation of the BR can be realized.

Batch Reactors are applied for relatively slow reactions and slightly exothermic reaction.

They are used extensively in industrial plants. The selection of a BR over a continuous system is based on considering aspects as product amounts and process economics. The size of batch reactors ranges from 19 L in small industrial pilot plants to 38,000-76,000 L in large plants

[Coke01]. In the pharmaceutical and biochemical industries multi-product batch reactors are frequently applied.

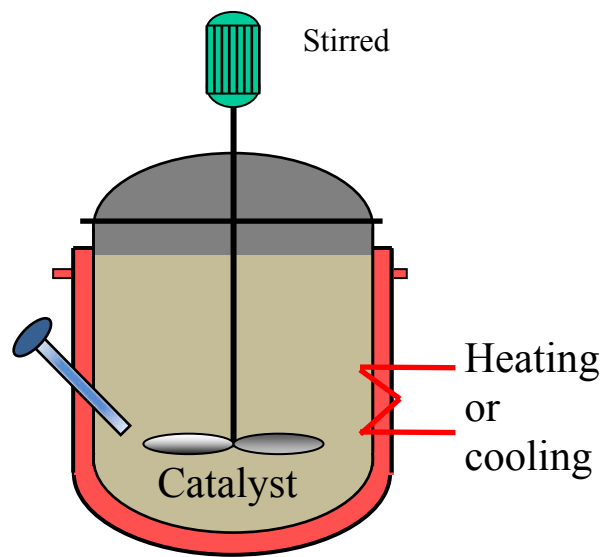


Figure 1.1 Batch Reactor (BR).

In small industrial pilot plants, a batch system may be also employed just for acquiring preliminary information. Furthermore, batch reactors can be used to obtain small quantities of a new product for further evaluation.

Advantages of Batch Reactors are:

- (1) Simple in construction
- (2) Small instrumentation and cost
- (3) Flexibility of operation and ability to perform different reactions
- (4) The possibility to reach high conversion (if “long” reaction time is used)

Disadvantages of Batch Reactors are:

- (1) The labor cost
- (2) Very time consuming (filling, running reaction, emptying, cleaning)
- (3) Successful and reliable operation and high product quality require considerable control efforts
- (4) A precise operation is needed to guarantee a constant product quality

1.4 RESEARCH OBJECTIVES AND OUTLINE

Liquid phase reactions are typically described in a simplified manner assuming constant reaction volumes and neglecting heat effects connected with mixing processes. Consequently, changes in reaction volumes and heats of mixing are often not considered in quantifying the kinetics of reactions taking place in liquid phases. These are questionable assumptions, because

significant volume and temperature changes can be caused in real reaction mixtures just by mixing.

The aim of this dissertation is to investigate theoretically and experimentally the thermodynamics and chemical kinetics of liquid phase reactions in more detail. Hereby, in particular the behavior of ideal and non-ideal solutions is studied. The behavior of ideal and real liquid solutions should be quantified based on molar excess volumes and heats. Appropriate relationships for ideal and real solutions should be incorporated into a batch reactor model which is applied to find out kinetic parameters for two model reactions based on analyzing corresponding transient data.

The reversible hydrolysis reactions of two esters (methyl formate and ethyl formate) are selected for the experimental study. To follow the courses of the reactions, the concentrations of the alcohols produced and heat fluxes occurring over the reactor wall should be measured as a function of time. Volume changes of mixing should be quantified and considered during the evaluation of kinetics. For this, kinetic parameters of the hydrolysis reactions should be determined analyzing the transients measured based on alternative sets of *i)* neglecting and *ii)* incorporating the volume changes due to mixing. The obtained kinetic parameters should be compared and differences should be evaluated and interpreted. General conclusions regarding the importance of neglecting or incorporating volume changes of mixing should be drawn. The results should be validated by comparing concentrations measured in other experiments and with predictions based the kinetic parameters obtained. Finally, the effects of the heats of mixing should be represented by simulations of temperature profiles.

After this introduction, chapter 2 discusses fundamental aspects of thermodynamics and kinetics of chemical reactions. The chapter begins by describing basics of solution thermodynamics, i.e. ideal and real solutions, volume changes and heats of mixing, followed by a presentation of expressions capable to quantify chemical kinetics. Afterwards, the relevant batch reactor models are introduced. Two assumptions are made: assuming inherently constant volumes of the reacting mixtures and assuming varying-volumes. The models capable to simulate concentration changes and heat fluxes the batch reactors contain the mass and energy balances for ideal and real conditions. To describe the non-ideal behavior of the liquid phases the concept of activities and activity coefficients is used.

The two model reactions investigated experimentally and the main details regarding the components involved are presented in chapter 3. This chapter also describes main data of physical chemistry of these components.

Chapter 4 illustrates the equipment applied to carry out the measurements. The experimental procedures applied to reach the goal of this thesis are also introduced in this chapter.

The results obtained are provided and discussed in chapter 5. This chapter summarizes first the determined molar excess volumes and enthalpies. Then estimated rate constants of the

hydrolysis reactions are given based on neglecting and considering the volume changes due to mixing. These results are obtained from comparing the experimental data and model predictions. “Best model” will be identified and discussed. Advantages and disadvantages related to incorporating volume and heat changes in kinetic analysis are evaluated based on the results achieved. Finally, corresponding reaction temperature profiles are calculated.

Chapter 6 presents a summary of the results obtained from this work. A discussion of the relevance considering and neglecting molar excess volumes and enthalpies is given.

CHAPTER 2

FUNDAMENTAL ASPECTS

The aim of this chapter is to describe the basics of chemical thermodynamics and reaction kinetics which are relevant for the purpose of this work. Thermodynamics considerations reveal the direction of a reaction system and its equilibrium state but do not evaluate the rates of chemical or physical processes. To determine these rate constants, reaction kinetics must be identified. Therefore, thermodynamics and kinetics must be jointly used to quantify a chemical reaction process.

This chapter presents fundamental equations and necessary definitions regarding solution thermodynamics, chemical kinetics and standard reactor models. The content of ideal solutions is introduced first. Then volume and heat changes due to mixing in non-ideal solutions are evaluated in section 2.1.2. Afterwards, chemical reaction equilibria and reaction kinetics are discussed. In section 2.3, standard batch reactor models are presented together with concepts capable to solve the corresponding mass and heat balance equations. Finally, excess properties and their effects in real solution are illustrated and interpreted.

2.1 THERMODYNAMICS

The thermodynamic properties of systems depend on temperature, pressure and composition. This holds also for mixtures of several components, which undergo composition changes as a result of mixing, transfer of species from one phase to another or chemical reactions. The main tasks in this section are to develop fundamental property relations for an ideal solution of variable composition and to present a treatment of excess properties characterizing real solutions. The discussion mainly follows classical textbook knowledge summarized e.g. in [Smith05], [Ness82], [Sand99], [Gmeh02], [Robe87], [Abbot89], [John99].

2.1.1 Ideal Solutions

According to Poling et al. [Robe87], ideal solutions are mixtures in which the molecules of different species are distinguishable (they have different masses or different structures or both). However, unlike in an ideal gas, in an ideal solution the molecules exert forces on each other.

When those forces are the same for all molecules, independent of the species considered, a solution is called ideal.

In this work, at first symbols for the properties of individual species as they exist in the pure state at temperature T and pressure P is required. These molar properties are identified by subscript and superscript, the symbol is Ω_i^0 . In order to clarify the three kinds of properties used in solution thermodynamics, the following symbolism is used

Properties of a pure species i	Ω_i^0	for example $H_i^0, S_i^0, V_i^0, G_i^0$
Solution properties	Ω	for example H, S, V, G
Partial properties of species i in solution	Ω_i	for example H_i, S_i, V_i, G_i
Total properties	ω	for example $\mathcal{H}, \mathcal{S}, \mathcal{V}, \mathcal{G}$

For real solution properties, no superscript is used. For instance, in a liquid solution of methanol and water with the molar volume of the solution V , the partial molar volumes for methanol and water in the solution are $V_{Methanol}$ and V_{Water} respectively. These values are different from the molar volumes of pure methanol, $V_{Methanol}^0$, and of pure water, V_{Water}^0 , at the same temperature and pressure.

The total Gibbs energy \mathcal{G} is a function of temperature T , pressure P and composition

$$\mathcal{G} = nG = \mathcal{G}(P, T, n_1, n_2, \dots, n_N) \quad (2.1)$$

where n_i are mole numbers of species i in a N -component mixture and $n = \sum_{i=1}^N n_i$. The total differential of \mathcal{G} is

$$d\mathcal{G} = \left[\frac{\partial \mathcal{G}}{\partial P} \right]_{T, n} dP + \left[\frac{\partial \mathcal{G}}{\partial T} \right]_{P, n} dT + \sum_{i=1}^N \left[\frac{\partial \mathcal{G}}{\partial n_i} \right]_{P, T, n_{j \neq i}} dn_i \quad (2.2)$$

In any closed system, the basic relation connecting the total Gibbs energy to the temperature T and pressure P [Smith05] is:

$$d\mathcal{G} = (nV)dP - (nS)dT \quad (2.3)$$

Eq. (2.3) applies for closed systems with constant composition, i.e. the case of a single phase fluid that does not undergo chemical reaction, with:

$$\left[\frac{\partial \mathcal{G}}{\partial P} \right]_{T, n} = nV \quad \text{and} \quad \left[\frac{\partial \mathcal{G}}{\partial T} \right]_{P, n} = -nS \quad (2.4)$$

Substituting eq. (2.4) into eq. (2.2) we obtain, for a system which the composition can change

$$d\mathcal{G} = (nV)dP - (nS)dT + \sum_{i=1}^N \left[\frac{\partial \mathcal{G}}{\partial n_i} \right]_{P,T,n_{j \neq i}} dn_i \quad (2.5)$$

The partial derivative with respect to the mole numbers n_i are of the chemical potential of species i in the mixture

$$\mu_i \equiv \left[\frac{\partial \mathcal{G}}{\partial n_i} \right]_{P,T,n_{j \neq i}} \quad (2.6)$$

The following expression defines any partial molar property Ω_i of species i in the solution

$$\Omega_i = \left[\frac{\partial (n\Omega)}{\partial n_i} \right]_{P,T,n_{j \neq i}} \quad (2.7)$$

Comparing of eq. (2.7) and eq. (2.6) reveals that the partial molar Gibbs G_i and the chemical potentials μ_i energy are identical

$$\mu_i = G_i \quad (2.8)$$

So, eq. (2.5) can be written as

$$d\mathcal{G} = (nV)dP - (nS)dT + \sum_{i=1}^N G_i dn_i \quad (2.9)$$

Eq. (2.9) is the fundamental property relation for single-phase fluid systems of variable composition [Smith05]. In case n is considered to be unity ($n = 1[\text{mol}]$), the n_i can be expressed as mole fractions

$$x_i \equiv \frac{n_i}{n} \quad (2.10)$$

with $n = \sum_{i=1}^N n_i$

Leading to

$$dG = VdP - SdT + \sum_{i=1}^N G_i dx_i \quad (2.11)$$

Combining eq. (2.2) and (2.11) we can imply

$$S = - \left[\frac{\partial G}{\partial T} \right]_{P,x} \quad (2.12)$$

and

$$V = \left[\frac{\partial G}{\partial P} \right]_{T,x} \quad (2.13)$$

From eq. (2.9) we have equations

$$\left[\frac{\partial(nG)}{\partial T} \right]_{P,n} = -nS \quad (2.14)$$

Taking partial derivation with respect to the n_i both sides eq. (2.14) and considering eq. (2.7) leads to

$$\left[\frac{\partial G_i}{\partial T} \right]_{P,n} = - \left[\frac{\partial(nS)}{\partial n_i} \right]_{P,T,n_{j \neq i}} \quad (2.15)$$

Similarly, we have

$$\left[\frac{\partial G_i}{\partial P} \right]_{P,n} = \left[\frac{\partial(nV)}{\partial n_i} \right]_{P,T,n_{j \neq i}} \quad (2.16)$$

Considering the last two equations and with regards to eq. (2.7), we obtain,

$$\left[\frac{\partial G_i}{\partial T} \right]_{P,x} = -S_i \quad (2.17)$$

and

$$\left[\frac{\partial G_i}{\partial P} \right]_{T,x} = V_i \quad (2.18)$$

It is known that for an ideal-gas (superscript *idgas*) the chemical potential of a constituent species i in an ideal mixture is characterized as

$$\mu_i^{idgas} \equiv G_i^{idgas} = G_i^{0,idgas} + RT \ln x_i \quad (2.19)$$

and an equation valid for pure species i in ideal case is

$$G_i^{0,idgas} = \Gamma_i(T) + RT \ln P_i^0 \quad (2.20)$$

as described e.g. by [Smith05] where $\Gamma_i(T)$, the integration constant at constant T , depends only on temperature T .

Therefore eq. (2.19) may be written

$$\mu_i^{idgas} = \Gamma_i(T) + RT \ln x_i P_i^0 \quad (2.21)$$

Assuming the same behaviour of constituent species as characterized for an ideal-gas mixture by eq. (2.19), we can define for an ideal solution

$$G_i^{id} = G_i^0 + RT \ln x_i \quad (2.22)$$

where the superscript *id* denotes in this thesis always an ideal-solution property.

Therefore, at constant temperature T and pressure P , combining eq. (2.22) with eq. (2.17) holds for an ideal solution,

$$S_i^{id} = - \left[\frac{\partial G_i^{id}}{\partial T} \right]_{P,x} = - \left[\frac{\partial G_i^0}{\partial T} \right]_P - R \ln x_i \quad (2.23)$$

Replacing $(\partial G_i / \partial T)_P$ by S using eq. (2.12), yields

$$S_i^{id} = S_i^0 - R \ln x_i \quad (2.24)$$

Similarly, from eq. (2.13), we have

$$V_i^{id} = \left[\frac{\partial G_i^{id}}{\partial P} \right]_{T,x} = \left[\frac{\partial G_i^0}{\partial P} \right]_T \quad (2.25)$$

and with eq. (2.13)

$$V_i^{id} = V_i^0 \quad (2.26)$$

In general for the Gibbs energy in a mixture holds [Smith05]

$$G = H - TS \quad (2.27)$$

From eq. (2.27), in an ideal solution, consider the more specific form of this equation, $H_i^{id} = G_i^{id} + TS_i^{id}$, and substituting eq. (2.22) and eq. (2.24) into this, we obtain

$$H_i^{id} = G_i^0 + TR \ln x_i + TS_i^0 - TR \ln x_i \quad (2.28)$$

or

$$H_i^{id} = G_i^0 + TS_i^0 = H_i^0 \quad (2.29)$$

Application of the summability relation in the general form

$$\Omega = \sum_{i=1}^N x_i \Omega_i \quad (2.30)$$

eq. (2.30) can be written for an ideal case

$$\Omega^{id} = \sum_{i=1}^N x_i \Omega_i^{id} \quad (2.31)$$

Thus using eq. (2.26) holds

$$V^{id} = \sum_{i=1}^N x_i V_i^{id} = \sum_{i=1}^N x_i V_i^0 \quad (2.32)$$

and analogously

$$H^{id} = \sum_{i=1}^N x_i H_i^0 \quad (2.33)$$

Thus, for ideal solutions the volumes and enthalpies can be calculated simply from the corresponding volumes and enthalpies of the pure species present in the solution.

2.1.2 Real Solutions

A well known empirical observation is the after mixing, 1 mL alcohol is mixed with 1mL water, the total volume of the mixture is less than 2 mL. This means the mixture volume is not necessarily equal to the total volume of all ideal components inside the solution. Thus, the ideal-solution behaviour does not apply in real solutions. However, the ideal solution is a useful model concept, which serves as a standard to which real solutions can be compared [Smith05]. The real solution behaviour can be quantified based on so-called excess properties.

a) Excess properties and activity coefficients

The relationships for pure components are not applicable to real solutions, so a quantitative description requires modifications because of the changes in thermodynamic properties of solution.

The pressure, temperature and amount of various constituents determine the extensive and intensive state of a system. As above, Ω represents again the molar value of any extensive thermodynamic property (e.g. V , H , G , etc.). Now an excess property Ω^E is defined as the difference between the actual property value of a solution and the value it would have in corresponding ideal system at the same temperature, pressure, and composition [Smith05]. This can be described in eqs. (2.34) and (2.35) for any partial molar property:

$$\Omega^E \equiv \Omega - \Omega^{id} \quad (2.34)$$

$$\Omega_i^E \equiv \Omega_i - \Omega_i^{id} \quad (2.35)$$

Specific excess relations come from the application of eq. (2.34) and the ideal case expressions (2.32) and (2.33):

$$V^E = V - \sum_{i=1}^N x_i V_i^0 \quad (2.36)$$

and

$$H^E = H - \sum_{i=1}^N x_i H_i^0 \quad (2.37)$$

In addition, from eq. (2.26) and (2.29), applying eq. (2.35) yields the following partial molar excess property relations

$$V_i^E = V_i - V_i^0 \quad (2.38)$$

and

$$H_i^E = H_i - H_i^0 \quad (2.39)$$

From eq. (2.3), expresses the functional relation to phases of constant composition

$$\mathcal{G} = \mathcal{G}(P, T) \quad (2.40)$$

Then, the fundamental property relation is restricted to systems of constant composition, follows from the mathematical identity:

$$d\left(\frac{\mathcal{G}}{RT}\right) \equiv \frac{1}{RT} d\mathcal{G} - \frac{\mathcal{G}}{RT^2} dT \quad (2.41)$$

Consider that $\mathcal{G} = nG$, substitution of $d(\mathcal{G})$ by eq. (2.9) and G by eq. (2.27), eq. (2.41) becomes

$$d\left(\frac{\mathcal{G}}{RT}\right) = \frac{nV}{RT} dP - \frac{nH}{RT^2} dT + \sum_{i=1}^N \frac{G_i}{RT} dn_i \quad (2.42)$$

This equation is general, in an ideal case it may be written as

$$d\left(\frac{\mathcal{G}^{id}}{RT}\right) = \frac{nV^{id}}{RT} dP - \frac{nH^{id}}{RT^2} dT + \sum_{i=1}^N \frac{G_i^{id}}{RT} dn_i \quad (2.43)$$

In view of eqs. (2.34) and (2.35), this equation may be subtracted from eq. (2.42) to give

$$d\left(\frac{\mathcal{G}^E}{RT}\right) = \frac{nV^E}{RT} dP - \frac{nH^E}{RT^2} dT + \sum_{i=1}^N \frac{G_i^E}{RT} dn_i \quad (2.44)$$

For real fluid, replacing in the equation for a pure species in the ideal-gas state eq. (2.20) P_i^0 by fugacity f_i^0 we obtain

$$G_i^0 \equiv \Gamma_i(T) + RT \ln f_i^0 \quad (2.45)$$

The definition of the fugacity of a species in solution, f_i , corresponds to the case using the pure-species fugacity f_i^0 . Replacing $x_i P$ in eq. (2.21) by f_i we have

$$\mu_i \equiv \Gamma_i(T) + RT \ln f_i \quad (2.46)$$

The Gibbs energy is of particular interest, eq. (2.46) may be written as

$$G_i \equiv \Gamma_i(T) + RT \ln f_i \quad (2.47)$$

When this equation and eq. (2.45) combine with eq. (2.22) to eliminate $\Gamma_i(T)$ and the resulting expression reduces to,

$$f_i^{id} = x_i f_i^0 \quad (2.48)$$

Eq. (2.47) becomes for an ideal solution

$$G_i^{id} \equiv \Gamma_i(T) + RT \ln x_i f_i^0 \quad (2.49)$$

Specifying the difference between G_i and G_i^{id} follows for the free excess Gibbs energy:

$$G_i^E = G_i - G_i^{id} = RT \ln \frac{f_i}{x_i f_i^0} \quad (2.50)$$

The definition of the activity coefficient of species i is

$$\gamma_i \equiv \frac{f_i}{x_i f_i^0} \quad (2.51)$$

Finally, the important relation between the excess Gibbs energy and the activity coefficient of component i results

$$G_i^E = RT \ln \gamma_i \quad (2.52)$$

For an ideal solution holds, $G_i^E = 0$, and therefore $\gamma_i = 1$

Substitution of eq. (2.52) into eq. (2.44) yields

$$d\left(\frac{G^E}{RT}\right) = \frac{nV^E}{RT} dP - \frac{nH^E}{RT^2} dT + \sum_{i=1}^N \ln \gamma_i dn_i \quad (2.53)$$

This equation is called the fundamental excess-property relation [Ness82].

Applying the fundamental excess property relation (2.53), molar excess volumes V^E can be determined by

$$V^E = \frac{\partial G^E}{\partial P}_{T,x} \quad (2.54)$$

Typically G^E values for liquid mixtures are not easily accessible.

Furthermore, excess enthalpies can be determined also from eq. (2.53). Inspecting the coefficient of dT yields

$$H^E = -RT^2 \left[\frac{\partial(G^E / RT)}{\partial T} \right]_{P,x} \quad (2.55)$$

Excess enthalpy data for mixtures are important both in theory and practice.

Obviously, if excess Gibbs energy and activity coefficients are allowed to depend on temperature T , and pressure P . This leads to nontrivial expression for molar excess volumes and enthalpies via eq. (2.54) and (2.55). Thus numerically we can compute V^E if the pressure dependence of the excess Gibbs energy is known and H^E if the temperature dependence of excess Gibbs energy is known.

The partial property with respect to G^E/RT is $\ln \gamma_i$

$$\ln \gamma_i = \left[\frac{\partial (nG^E / RT)}{\partial n_i} \right]_{P,T,n_{j \neq i}} \quad (2.56)$$

The partial property analogues of eqs. (2.54) and (2.55) are

$$\frac{V_i^E}{RT} = \left[\frac{\partial (G_i^E / RT)}{\partial P} \right]_{T,x} = \left[\frac{\partial \ln \gamma_i}{\partial P} \right]_{T,x} \quad (2.57)$$

and

$$\frac{H_i^E}{RT^2} = - \left[\frac{\partial (G_i^E / RT)}{\partial T} \right]_{P,x} = - \left[\frac{\partial \ln \gamma_i}{\partial T} \right]_{P,x} \quad (2.58)$$

Combining eqs. (2.30) and (2.52) gives the important relation for the topic of this work

$$G^E = RT \sum_{i=1}^N x_i \ln \gamma_i \quad (2.59)$$

Eq. (2.59) is very important in chemical and engineering thermodynamics. There are many modern theoretical developments to calculate activity coefficients. Important equations are based on the Redlich/Kister expansion, Margules equation, van Laar equation, NRTL eq. of Renon and Prausnitz [Reno68], the UNIQUAC equation of Abrams and Prausnitz [Robe87]. Moreover, the UNIFAC method [Gmeh02] is seen as a significant development based on the UNIQUAC equation. Activity coefficients frequently are determined analyzing vapour/liquid equilibrium data.

Furthermore, we need an equation which relates partial molar excess properties to the molar excess solution properties and to mole fractions x_i . Van Ness and Abbott [Ness82] presented corresponding equations for multicomponent systems in detail.

Expansion of eq. (2.7) for the excess properties gives

$$\Omega_i^E = \Omega^E + n \left[\frac{\partial \Omega^E}{\partial n_i} \right]_{T,P,n_{j \neq i}} \quad i = 1, N \quad (2.60)$$

Also molar excess properties of homogeneous mixtures existing at equilibrium depend on temperature, pressure, and composition. Thus, the molar excess property Ω^E can be expressed as

$$\Omega^E = \Omega^E(T, P, x_1, x_2, \dots, x_k, \dots, x_N) \quad (2.61)$$

These properties are intensive i.e. they do not depend on the amount of matter that is present. That means that the Ω^E are independent of the total amount of mixture present.

At constant T and P , the total differential $d\Omega^E$ is given by

$$d\Omega^E = \sum_{k=1}^N \left[\frac{\partial \Omega^E}{\partial x_k} \right]_{T,P,x_{j \neq k}} dx_k \quad (2.62)$$

Division by dn_i and restriction to constant n_j ($j \neq i$) yields

$$\left[\frac{\partial \Omega^E}{\partial n_i} \right]_{T,P,n_{j \neq i}} = \sum_{k=1}^N \left[\frac{\partial \Omega^E}{\partial x_k} \right]_{T,P,n_{j \neq i}} \left[\frac{\partial x_k}{\partial n_i} \right]_{n_{j \neq i}} \quad (2.63)$$

From eq. (2.10) we have

$$\left[\frac{\partial x_k}{\partial n_i} \right]_{n_{j \neq i}} = \frac{1}{n} \left[\frac{\partial n_k}{\partial n_i} \right]_{n_{j \neq i}} - \frac{n_k}{n^2} \left[\frac{\partial n}{\partial n_i} \right]_{n_{j \neq i}} \quad k = 1, N \quad i = 1, N \quad (2.64)$$

Obviously, $(\partial n / \partial n_i)_{n_j} = 1$. Therefore the equation becomes

$$\left[\frac{\partial x_k}{\partial n_i} \right]_{n_{j \neq i}} = \frac{1}{n} \left[\frac{\partial n_k}{\partial n_i} \right]_{n_{j \neq i}} - x_k \quad (2.65)$$

Substitution this equation into eq. (2.63) gives

$$\left[\frac{\partial \Omega^E}{\partial n_i} \right]_{T,P,n_{j \neq i}} = \frac{1}{n} \sum_{k=1}^N \left[\frac{\partial \Omega^E}{\partial x_k} \right]_{T,P,x_{j \neq i}} \left[\left[\frac{\partial n_k}{\partial n_i} \right]_{n_{j \neq i}} - x_k \right] \quad (2.66)$$

or

$$n \left[\frac{\partial \Omega^E}{\partial n_i} \right]_{T,P,n_{j \neq i}} = \sum_{k=1}^N \left[\frac{\partial \Omega^E}{\partial x_k} \right]_{T,P,x_{j \neq i}} \left[\frac{\partial n_k}{\partial n_i} \right]_{n_{j \neq i}} - \sum_{k=1}^N x_k \left[\frac{\partial \Omega^E}{\partial x_k} \right]_{T,P,x_{j \neq i}} \quad (2.67)$$

Since the derivatives $(\partial n_k / \partial n_i)_{n_{j \neq i}} = 1$ for $k = i$ and $(\partial n_k / \partial n_i)_{n_{j \neq i}} = 0$ for all terms in the first sum of eq. (2.67). Therefore holds

$$n \left[\frac{\partial \Omega^E}{\partial n_i} \right]_{T,P,n_{j \neq i}} = \left[\frac{\partial \Omega^E}{\partial x_i} \right]_{T,P,x_{j \neq i}} - \sum_{k=1}^N x_k \left[\frac{\partial \Omega^E}{\partial x_k} \right]_{T,P,x_{j \neq i}} \quad (2.68)$$

and eq. (2.60) finally becomes

$$\Omega_i^E = \Omega^E + \left[\frac{\partial \Omega^E}{\partial x_i} \right]_{T,P,x_{j \neq i}} - \sum_{k=1}^N x_k \left[\frac{\partial \Omega^E}{\partial x_k} \right]_{T,P,x_{j \neq i}} \quad (2.69)$$

b) Excess properties of binary solutions

Applying for illustration eq. (2.69) to a binary solution yields

$$\Omega_1^E = \Omega^E + \left[\frac{\partial \Omega_1^E}{\partial x_1} \right]_{T,P,x_2} - \left[x_1 \left[\frac{\partial \Omega^E}{\partial x_1} \right]_{T,P,x_2} + x_2 \left[\frac{\partial \Omega^E}{\partial x_2} \right]_{T,P,x_1} \right] \quad (2.70)$$

Multiplying both sides of eq. (2.70) by dx_1 leads to

$$\Omega_1^E dx_1 = \Omega^E dx_1 + \left[\frac{\partial \Omega_1^E}{\partial x_1} \right]_{T,P,x_2} dx_1 - \left[x_1 \left[\frac{\partial \Omega^E}{\partial x_1} \right]_{T,P,x_2} + x_2 \left[\frac{\partial \Omega^E}{\partial x_2} \right]_{T,P,x_1} \right] dx_1 \quad (2.71)$$

Because $x_1 + x_2 = 1$, it follows that $x_1 = 1 - x_2$ and $dx_2 = -dx_1$. Thus, eq. (2.71) can be rewritten

$$\Omega_1^E dx_1 = \Omega^E dx_1 + \left[\frac{\partial \Omega_1^E}{\partial x_1} \right]_{T,P,x_2} dx_1 - (1 - x_2) \left[\frac{\partial \Omega^E}{\partial x_1} \right]_{T,P,x_2} dx_1 + x_2 \left[\frac{\partial \Omega^E}{\partial x_2} \right]_{T,P,x_1} dx_2 \quad (2.72)$$

Eliminating $\left(\frac{\partial \Omega_1^E}{\partial x_1} \right)_{T,P,x_2} dx_1$ gives

$$\Omega_1^E dx_1 = \Omega^E dx_1 + x_2 \left[\left[\frac{\partial \Omega^E}{\partial x_1} \right]_{T,P,x_2} dx_1 + \left[\frac{\partial \Omega^E}{\partial x_2} \right]_{T,P,x_1} dx_2 \right] \quad (2.73)$$

Thus, total differential $d\Omega^E$ of binary system is given by

$$d\Omega^E = \left[\frac{\partial \Omega^E}{\partial x_1} \right]_{T,P,x_2} dx_1 + \left[\frac{\partial \Omega^E}{\partial x_2} \right]_{T,P,x_1} dx_2 \quad (2.74)$$

or

$$\Omega_1^E dx_1 = \Omega^E dx_1 + x_2 d\Omega^E \quad (2.75)$$

Dividing again by dx_1 and using $x_2 = 1 - x_1$ follows for Ω_1^E

$$\Omega_1^E = \Omega^E + (1 - x_1) \frac{d\Omega^E}{dx_1} \quad (2.76)$$

Similarly, for Ω_2^E can be derived

$$\Omega_2^E = \Omega^E - x_1 \frac{d\Omega^E}{dx_1} \quad (2.77)$$

Thus, at constant T and pressure P for binary systems, the partial excess properties Ω_i^E can be readily calculated directly from an expression for the excess property Ω^E as a function of composition given by x_1 .

c) Change of properties due to mixing

A frequently used definition of property change of mixing is [Smith05]:

$$\Delta\Omega \equiv \Omega - \sum_{i=1}^N x_i \Omega_i^0 \quad (2.78)$$

Where Ω is the molar or unit mass property of a solution and Ω_i^0 is the partial molar or unit mass properties of the pure species at the same temperature and pressure.

Equation (2.78) is a quite general definition of properties changes due to mixing. From the equations specified of excess properties given above (2.36) and (2.37) can be obtained:

$$V^E = \Delta V = V - \sum_{i=1}^N x_i V_i^0 \quad (2.79)$$

and

$$H^E = \Delta H = H - \sum_{i=1}^N x_i H_i^0 \quad (2.80)$$

The equations (2.79) and (2.80) are important equations for this work because they describe that the changes of volume and enthalpy due to mixing in a non-ideal situation are equal to the volumes and enthalpies of excess.

For the case of an ideal solution, each excess property is zero. Therefore, the corresponding properties of ideal mixing are the following:

$$\Delta V^{id} = 0 \quad (2.81)$$

and

$$\Delta H^{id} = 0 \quad (2.82)$$

2.1.2.1 Models for the excess Gibbs energy and corresponding activity coefficients

The excess Gibbs energy G^E present in the important equation (2.59) depends on temperature T , pressure P , and composition. For liquids at low to moderate pressures it is only a very weak function of P [Smith05]. Therefore also the activity coefficients depend only weakly on pressure P , which leads to relative small molar excess volume eq. (2.57).

There are numerous models to describe the excess Gibbs energy such as the models of Redlich/Kister, Margules, Van Laar, Non-Random-Two-Liquid (NRTL) for binary systems. Model treating ternary systems were suggested by Kohler, Jacob and Fitzner, Tsao-Smith, Toop. Multicomponent systems were treated by the models of Wilson [Smith05], UNIQUAC (UNIversal QUAsi-Chemical), UNIFAC [Robe87].

a) Binary systems

Below are given models for the excess Gibbs energy G^E in binary systems. They allow to calculate corresponding activity coefficients using eq. (2.56).

a1) Redlich/Kister equation [Smith05]

For binary system, a well-known equation is the Redlich/Kister expansion

$$\frac{G_{12}^E}{x_1 x_2 RT} = A_{12,0}(x_1 - x_2)^0 + A_{12,1}(x_1 - x_2) + A_{12,2}(x_1 - x_2)^2 + \dots \quad (2.83)$$

When $A_{12,i} = 0$ for $i \geq 1$, follows most simple nontrivial expression for G_{12}^E

$$\frac{G_{12}^E}{RT} = A_{12,0} x_1 x_2 \quad (2.84)$$

where $A_{12,0}$ is constant for a given temperature. Replacing x_1 by $n_1/(n_1 + n_2)$, and x_2 by $n_2/(n_1 + n_2)$. Since $n \equiv n_1 + n_2$, this gives

$$\frac{nG_{12}^E}{RT} = \frac{A_{12,0} n_1 n_2}{n_1 + n_2} \quad (2.85)$$

From eq. (2.56), differentiating with respect to n_1 provides

$$\ln \gamma_1 = \left[\frac{\partial(nG^E / RT)}{\partial n_1} \right]_{P,T,n_2} = \frac{A_{12,0} n_2 (n_1 + n_2) - A_{12,0} n_1 n_2}{(n_1 + n_2)^2} \quad (2.86)$$

or

$$\ln \gamma_1 = A_{12,0} \left(\frac{n_2}{n_1 + n_2} \right)^2 \quad (2.87)$$

Reconversion of the n_i 's to x_i 's and noting that $x_2 = 1 - x_1$, the corresponding final equations for the activity coefficients are

$$\ln \gamma_1 = A_{12,0} x_2^2 \quad (2.88)$$

$$\ln \gamma_2 = A_{12,0} x_1^2 \quad (2.89)$$

a2) Margules equation [Smith05]

Another well-known equation is the Margules equation

$$\frac{G_{12}^E}{RT} = (A_{21} x_1 + A_{12} x_2) x_1 x_2 \quad (2.90)$$

where A_{12} , A_{21} are specific dimensionless. As above, corresponding activity coefficients could be derived leading to the follow expression:

$$\ln \gamma_1 = x_2^2 [A_{12} + 2(A_{21} - A_{12})x_1] \quad (2.91)$$

$$\ln \gamma_2 = x_1^2 [A_{21} + 2(A_{12} - A_{21})x_2] \quad (2.92)$$

a3) van Laar equation [Smith05]

The van Laar equation is provided as

$$\frac{G_{12}^E}{x_1 x_2 RT} = \frac{A'_{12} A'_{21}}{A'_{12} x_1 + A'_{21} x_2} \quad (2.93)$$

The activity coefficients related to this equation are given by

$$\ln \gamma_1 = A'_{12} \left(1 + \frac{A'_{12} x_1}{A'_{21} x_2} \right)^{-2} \quad (2.94)$$

$$\ln \gamma_2 = A'_{21} \left(1 + \frac{A'_{21} x_2}{A'_{12} x_1} \right)^{-2} \quad (2.95)$$

a4) Wilson equation [Smith05]

The Wilson equation, like the Margules and van Laar equations, contains just two parameters Λ_{12} and Λ_{21} for binary system.

$$\frac{G_{12}^E}{RT} = -x_1 \ln(x_1 + \Lambda_{12} x_2) - x_2 \ln(x_2 + \Lambda_{21} x_1) \quad (2.96)$$

The activity coefficients derived from this equation are presented as

$$\ln \gamma_1 = -\ln(x_1 + \Lambda_{12} x_2) + x_2 \left(\frac{\Lambda_{12}}{x_1 + \Lambda_{12} x_2} - \frac{\Lambda_{21}}{\Lambda_{21} x_1 + x_2} \right) \quad (2.97)$$

$$\ln \gamma_2 = -\ln(x_2 + \Lambda_{21} x_1) + x_1 \left(\frac{\Lambda_{12}}{x_1 + \Lambda_{12} x_2} - \frac{\Lambda_{21}}{\Lambda_{21} x_1 + x_2} \right) \quad (2.98)$$

a5) NRTL equation [Smith05]

The NRTL (Non-Random-Two-Liquid) equation was developed by Renon and Prausnitz, based on Scott's two liquid theories and on an assumption of nonrandomness, similar to that used by Wilson. This equation contains three parameters for a binary system and is written as

$$\frac{G_{12}^E}{x_1 x_2 RT} = \frac{G_{21} \tau_{21}}{x_1 + x_2 G_{21}} + \frac{G_{12} \tau_{12}}{x_2 + x_1 G_{12}} \quad (2.99)$$

$$\ln \gamma_1 = x_2^2 \left[\tau_{21} \left(\frac{G_{21}}{x_1 + x_2 G_{21}} \right)^2 + \frac{G_{12} \tau_{12}}{(x_2 + x_1 G_{12})^2} \right] \quad (2.100)$$

$$\ln \gamma_2 = x_1^2 \left[\tau_{12} \left(\frac{G_{12}}{x_2 + x_1 G_{12}} \right)^2 + \frac{G_{21} \tau_{21}}{(x_1 + x_2 G_{21})^2} \right] \quad (2.101)$$

Here

$$G_{12} = \exp(-\alpha\tau_{12}) \quad G_{21} = \exp(-\alpha\tau_{21}) \quad (2.102)$$

and

$$\tau_{12} = \frac{b_{12}}{RT} \quad \tau_{21} = \frac{b_{21}}{RT} \quad (2.103)$$

b) Ternary systems

Also for ternary systems, several explicit models to quantify the Gibbs energy G^E were suggested. Typically, they use specific binary model parameters explained above. Below are given examples.

b1) Kohler equation [Kohl60]

$$G_{123}^E = (1-x_1)^2 G_{23}^E + (1-x_2)^2 G_{13}^E + (1-x_3)^2 G_{12}^E \quad (2.104)$$

where G_{ij}^E refers to the corresponding excess Gibbs energies of the binary system

b2) Tsao and Smith equation [Tsao53]

$$G_{123}^E = \frac{x_2 G_{12}^E}{1-x_1} + \frac{x_3 G_{13}^E}{1-x_1} + (1-x_1) G_{23}^E \quad (2.105)$$

where G_{ij}^E refers to again the binary excess Gibbs energies.

b3) Singh et al. [Singh84]

$$\frac{G_{123}^E}{RT} = \frac{1}{RT} (G_{12}^E + G_{23}^E + G_{31}^E) + x_1 x_2 x_3 [A_{123} + B_{123} x_1 (x_2 - x_3) + C_{123} x_1^2 (x_2 - x_3)^2] \quad (2.106)$$

If $B_{123} = C_{123} = 0$, then the following simplified equation holds

$$\frac{G_{123}^E}{RT} = \frac{1}{RT} (G_{12}^E + G_{23}^E + G_{31}^E) + A_{123} x_1 x_2 x_3 \quad (2.107)$$

c) Multicomponent systems

In the analysis of multicomponent data, the local-composition models have limited flexibility. Here, the generalized Wilson equation, the UNIQUAC equation and the UNIFAC method provide models of greater complexity.

c1) Generalized Wilson equation [Smith05]

The model proposed by Wilson, based on the concept of local compositions is as follows

$$\frac{G^E}{RT} = -\sum_{i=1}^N x_i \ln \sum_{j=1}^N x_j \Lambda_{ij} \quad (2.108)$$

and

$$\ln \gamma_i = 1 - \ln \sum_{j=1}^N x_j \Lambda_{ij} - \sum_{k=1}^N \frac{x_k \Lambda_{ki}}{\sum_{j=1}^N x_j \Lambda_{kj}} \quad (2.109)$$

where $\Lambda_{ij} = 1$ for $i = j$.

The temperature dependence of the parameters is given by

$$\Lambda_{ij} = \frac{V_j}{V_i} \exp \frac{-a_{ij}}{RT} \quad (i \neq j) \quad (2.110)$$

where V_j and V_i are the molar volumes at temperature T of pure liquids j and i , and a_{ij} is a constant independent of composition and temperature.

c2) UNIQUAC method [Robe87]

The UNIQUAC equation is known to often give a good representation of both vapour-liquid and liquid-liquid equilibria for binary and multicomponent mixtures containing a variety of nonelectrolytes such as hydrocarbons, esters, water, amines, alcohols, etc. [Robe87]. In a multicomponent mixture, the basic UNIQUAC equation treats G^E / RT as comprised of two additive parts, a combinatorial term, G_C^E , to account for molecular size and shape differences, and a residual term, G_R^E , to account for molecular interactions:

$$\frac{G^E}{RT} \equiv G_C^E + G_R^E \quad (2.111)$$

The function G^C contains pure-species parameters only, whereas the function G^R incorporates two binary parameters for each pair of molecules. For a multicomponent system holds

$$G_C^E = \sum_{i=1}^N x_i \ln \frac{\phi_i}{x_i} + 5 \sum_{i=1}^N q_i x_i \ln \frac{\theta_i}{\phi_i} \quad (2.112)$$

and

$$G_R^E = - \sum_{i=1}^N q_i x_i \ln \left(\sum_{j=1}^N \theta_j \tau_{ji} \right) \quad (2.113)$$

where

$$\phi_i \equiv \frac{x_i r_i}{\sum_{j=1}^N x_j r_j} \quad (2.114)$$

and

$$\theta_i \equiv \frac{x_i q_i}{\sum_{j=1}^N x_j q_j} \quad (2.115)$$

The subscript i identifies the species, and j is just a dummy index. Note that typically $\tau_{ji} \neq \tau_{ij}$. However, when $i = j$, then $\tau_{ii} = \tau_{jj} = 1$. The influence of temperature on G^E enters through the interaction parameters τ_{ij} of eq. (2.113), which are also follows temperature dependent:

$$\tau_{ji} = \exp \frac{-(u_{ji} - u_{ii})}{RT} \quad (2.116)$$

Key parameters for the UNIQUAC equations are therefore values for $(u_{ji} - u_{ii})$.

The expression for the calculation of $\ln \gamma_i$ was given before eq. (2.56). The UNIQUAC equations provide the following equations:

$$\ln \gamma_i = \ln \gamma_i^C + \ln \gamma_i^R \quad (2.117)$$

$$\ln \gamma_i^C = 1 - J_i + \ln J_i - 5q_i \left(1 - \frac{J_i}{L_i} + \ln \frac{J_i}{L_i} \right) \quad (2.118)$$

and

$$\ln \gamma_i^R = q_i \left(1 - \ln s_i - \sum_{j=1}^N \theta_j \frac{\tau_{ij}}{s_j} \right) \quad (2.119)$$

$$\ln \gamma_i^R = q_i \left(1 - \ln s_i - \sum_{j=1}^N \theta_j \frac{\tau_{ij}}{s_j} \right) \quad (2.120)$$

where in addition to equation (2.115) and (2.116)

$$J_i = \frac{r_i}{\sum_{j=1}^N r_j x_j} \quad (2.121)$$

$$L_i = \frac{q_i}{\sum_{j=1}^N q_j x_j} \quad (2.122)$$

$$s_i = \sum_{l=1}^N \theta_l \tau_{li} \quad (2.123)$$

Again subscript i identifies species, and j and l are dummy indices. All summations are over all species and $\tau_{ij} = 1$ for $i = j$. Value for the parameters $(u_{ij} - u_{ii})$ are found often by regression of binary VLE data as given e.g. by Gmehling et al. [Gmeh02].

c3) UNIFAC method [Robe87]

The UNIFAC method based on the UNIQUAC equation, the activity coefficient of (molecular) component i is again directly presented as:

$$\ln \gamma_i = \ln \gamma_i^C + \ln \gamma_i^R \quad i = 1, N \quad (2.124)$$

where γ_i^C is the combinatorial contribution to γ_i and γ_i^R is the residual contribution. The combinatorial contribution to γ_i depends on the model fractions, x , the area fractions, θ , and the segment fractions, φ , and may be expressed as

$$\ln \gamma_i^C = \ln \frac{\varphi_i}{x_i} + \frac{z}{2} q_i \ln \frac{\theta}{\varphi} + l_i - \frac{\varphi}{x_i} \sum_{j=1}^N x_j l_j \quad (2.125)$$

and

$$\ln \gamma_i^R = q_i \left[1 - \ln \left(\sum_{j=1}^N \theta_j \tau_{ji} \right) - \sum_{j=1}^N \frac{\theta_j \tau_{ij}}{\sum_{k=1}^N \theta_k \tau_{kj}} \right] \quad (2.126)$$

Where z is the coordination number which is set equal to 10 [Smith05], l_i depends on the parameters r_i and q_i . These parameters r_i and q_i are pure component constants which depend on molecular structure, molecular size and external surface areas. l_i is given by

$$l_i = \frac{z}{2} (r_i - q_i) - (r_i - 1) \quad (2.127)$$

θ_i , φ_i and τ_{ji} are given by

$$\theta_i = \frac{q_i x_i}{\sum_{j=1}^N q_j x_j} \quad (2.128)$$

$$\varphi_i = \frac{r_i x_i}{\sum_{j=1}^N r_j x_j} \quad (2.129)$$

$$\tau_{ji} = \exp \left(- \frac{u_{ji} - u_{ii}}{RT} \right) \quad (2.130)$$

Parameters r_i and q_i are calculated as the sum of the group volume and area parameters R_k and Q_k

$$r_i = \sum_{k=1}^M \eta_k^{(i)} R_k \quad \text{and} \quad q_i = \sum_{k=1}^M \eta_k^{(i)} Q_k \quad (2.131)$$

where $\eta_k^{(i)}$ is the number of groups of type k in molecule i . M is the number of groups. Group parameters R_k and Q_k can be obtained from van der Waals group volumes and surface areas V_{wk} and A_{wk} , as given by Bondi [Robe87]

$$R_k = \frac{V_{wk}}{15.17} \quad \text{and} \quad Q_k = \frac{A_{wk}}{2.5 \times 10^9} \quad (2.132)$$

The normalization factors 15.17 and 2.5×10^9 were determined by the volume and external surface of a CH_2 unit in polyethylene [Robe87].

The residual contribution γ_i^R is

$$\ln \gamma_i^R = \sum_{k=1}^M \eta_k^{(i)} \left[\ln \Gamma_k - \ln \Gamma_k^{(i)} \right] \quad (M \text{ groups}) \quad (2.133)$$

Where Γ_k is the activity coefficient of group k at mixture composition, and $\Gamma_k^{(i)}$ is the activity coefficient of group k at a group composition corresponding to pure component i . Hereby, Γ_k and $\Gamma_k^{(i)}$ are given as

$$\ln \Gamma_k = Q_k \left[1 - \ln \left(\sum_{m=1}^M \theta_m \psi_{mk} \right) - \sum_{m=1}^M \left(\frac{\theta_m \psi_{km}}{\sum_{n=1}^M \theta_n \psi_{kn}} \right) \right] \quad (2.134)$$

Where θ_m and ψ_{mk} depend on the group surface areas θ_m , the group fractions X_m and the group interaction parameters a_{nm}

$$\theta_m = \frac{Q_m X_m}{\sum_{n=1}^M Q_n X_n}; \quad X_m = \frac{\sum_{j=1}^N \eta_m^{(j)} x_j}{\sum_{j=1}^N \sum_{n=1}^M \eta_n^{(j)} x_j}; \quad \psi = \exp(-a_{nm} / T) \quad (2.135)$$

The excess Gibbs energy G^E is again connected to γ_i as

$$\frac{G^E}{RT} = \sum_{i=1}^N x_i (\ln \gamma_i^C + \ln \gamma_i^R) \quad (2.136)$$

All methods described in this section for calculating G^E values in multicomponent systems can be of course also used just for binary or ternary mixtures.

In principle, the UNIFAC method can be used for estimation of excess enthalpies based on the values of the structural parameters for the groups, and the group-interaction parameters. However values for these parameters are not evaluated from binary enthalpy data [Coto91]. Therefore the parameters built in temperature dependence of the UNIFAC method are not good enough to predict of excess enthalpies.

d) Summary of G^E models

Table 2.1 provides a summary of the models for the excess Gibbs energy G^E described. In these models the parameters A_{12} , A_{21} , Λ_{12} , Λ_{21} , α , b_{12} , b_{21} , etc. are functions of temperature T and pressure P , but not of x . This allows using them to calculate V^E by eq. (2.54) or H^E by eq. (2.55)

Table 2.1 Summary of selected models for the excess Gibbs energy G^E (N: number of component).

System	Model type	Eq.	Number of parameter	Parameter
Binary	Redlich/Kister	(2.83)	-	$A_{12,0}, A_{12,1}, A_{12,2}, \dots$
	Margules	(2.90)	2	A_{12}, A_{21}
	Van Laar	(2.93)	2	A_{12}, A_{21}
	Wilson	(2.96)	2	$\Lambda_{12}, \Lambda_{21}$
	NRTL	(2.99)	3	α, b_{12}, b_{21}
Ternary	Kohler	(2.104)	-	-
	Tsao and Smith	(2.105)	-	-
	Singh	(2.106)	1	Λ_{123}
Multi-component	Wilson	(2.108)	$\frac{N!}{(N-2)!}$	Λ_{ij}
	UNIQUAC &	(2.111)	$\frac{N!}{(N-2)!}$	u_{ij}
	UNIFAC	(2.124)	$\frac{N!}{(N-2)!}$	

2.1.2.2 Models for excess volumes due to mixing effects

Eq. (2.36) states that the difference between the molar volume of real and ideal liquid mixture is the molar excess volume V^E . At a given temperature and pressure, the molar excess volume can be directly determined from measured densities ρ [Tej99], [Luci98]:

$$V^E = V - \sum_{i=1}^N x_i V_i^0 = \frac{\sum_{i=1}^N x_i M_i}{\rho} - \sum_{i=1}^N \left(\frac{x_i M_i}{\rho_i} \right) \quad (2.137)$$

where the M_i are the molar masses of the pure components, the x_i are the respective mole fractions; ρ is the density of mixture and the ρ_i are the densities of the pure components.

a) Binary systems

If the thermodynamic properties of the binary liquid mixture are ideal (i.e. $V^E = 0$), for binary system eq. (2.32) becomes:

$$V_{12}^{id} = x_1 V_1^0 + x_2 V_2^0 \quad (2.138)$$

or

$$V_{12}^{id} = (1-x_2)V_1^0 + x_2 V_2^0 \quad (2.139)$$

Hence,

$$V_{12}^{id} = V_1^0 + x_2(V_2^0 - V_1^0) \quad (2.140)$$

where V_{12}^0 , V_1^0 and V_2^0 are the molar volume of the ideal mixture, the molar volume of pure component 1 and the molar volume of pure component 2, respectively. The x_1 and x_2 are again the respective mole fractions of components 1, and 2.

Applying eq. (2.30) to a real binary liquid system gives

$$V_{12}^{real} = x_1 V_1 + x_2 V_2 \quad (2.141)$$

Where V_{12}^{real} , V_1 and V_2 are the molar volumes of the real mixture, the partial molar volume of component 1 and the partial molar volume of component 2 in the real mixture, respectively.

From definition (2.36) follows for the molar excess volume V_{12}^E :

$$V_{12}^E = x_1(V_1 - V_1^0) + x_2(V_2 - V_2^0) \quad (2.142)$$

or

$$V_{12}^E = x_1 V_1^E - x_2 V_2^E \quad (2.143)$$

with V_i^E being the partial excess volumes.

The molar excess volume can be determined empirically from measured mixture densities ρ using eq. (2.137)

$$V_{12}^E = V_{12}^{real} - x_1 V_1^0 - x_2 V_2^0 \quad (2.144)$$

with

$$V_{12}^{real} = \frac{M_1 x_1 + M_2 x_2}{\rho} \quad (2.145)$$

$$V_1^0 = \frac{M_1}{\rho_1} \quad (2.146)$$

and

$$V_2^0 = \frac{M_2}{\rho_2} \quad (2.147)$$

Hereby V_{12}^E , V_1^0 and V_2^0 are the molar excess volume of the mixture, the molar volume of component 1 and the molar volume of component 2 respectively. M_1 and M_2 are the molar masses of the pure components. The x_1 and x_2 are the respective mole fractions. The ρ is the density of mixture; ρ_1 , ρ_2 are the densities of the pure components at the same temperature.

As mentioned above eq. (2.54), the molar excess volume V^E can be predicted by taking derivatives of G^E with respect to pressure P . Performing this for example for the simplified first order Redlich/Kister eq. (2.84) on both sides at constant temperature and composition, we obtain:

$$\frac{1}{RT} \left[\frac{\partial G_{12}^E}{\partial P} \right]_T = x_1 x_2 \left[\frac{\partial A_{12,0}}{\partial P} \right]_T \quad (2.148)$$

Substituting these above into equation (2.54) we obtain the corresponding excess volume for the binary system:

$$V_{12}^E = x_1 x_2 RT \left[\frac{\partial A_{12,0}}{\partial P} \right]_T \quad (2.149)$$

Thus, at given T and P , V^E can be evaluated as follows

$$V_{12}^E = RT A_{P,12,0} x_1 x_2 \quad (2.150)$$

where $A_{P,12,0} = \left[\frac{\partial A_{12,0}}{\partial P} \right]_T$ is the essential free parameter that needs to be in agreement with experimental observation.

For the more general Redlich/Kister equation the following expression for the excess volume of a binary systems results:

$$V_{12}^E = RT x_1 x_2 \left[A_{P,12,0} (x_1 - x_2)^0 + A_{P,12,1} (x_1 - x_2) + A_{P,12,2} (x_1 - x_2)^2 + \dots \right] \quad (2.151)$$

the $A_{P,12,i} = \left[\frac{\partial A_{12,i}}{\partial P} \right]_T$ are constants which all depend on pressure.

In a similar manner all G_{12}^E models described above can be exploited to generate corresponding V_{12}^E

In practice, parameters $A_{P,12,i}$ are calculated from experimental data. These parameters are obtained by using the minimization of the objective function given by equation

$$OF = \frac{1}{NUM} \sum_{k=1}^{NUM} \left(V_{12,exp}^E - V_{12,cal}^E \right)_k^2 \longrightarrow \min \quad (2.152)$$

b) Ternary systems

Below a few models suggested for prediction excess volumes for ternary systems are given.

b1) *The Radojkovi'c et al. model [Rado77]*

Radojkovi'c et al. proposed the Redlich/Kister model exploiting just all binary excess volumes as follows:

$$V_{123}^E = V_{12}^E + V_{13}^E + V_{23}^E \quad (2.153)$$

b2) *The Tsao-Smith model [Tsao53]*

Tsao-Smith suggest:

$$V_{123}^E = \frac{x_2 V_{12}^E(x_1^c, x_2^c)}{1 - x_1} + \frac{x_3 V_{13}^E(x_1^c, x_3^c)}{1 - x_1} + (1 - x_1) V_{23}^E(x_2^c, x_3^c) \quad (2.154)$$

The binary contributions of this asymmetric model are evaluated in the following manner:

- $x_i^c = x_1$ and $x_j^c = 1 - x_i^c$ for binary 1-2 and 1-3 and $x_2^c = 1 - x_3^c = \frac{x_2}{x_2 + x_3}$ for binary mixture 2-3
- $x_i^c = x_2$ and $x_j^c = 1 - x_i^c$ for binary 2-1 and 2-3 and $x_1^c = 1 - x_3^c = \frac{x_1}{x_1 + x_3}$ for binary mixture 1-3
- $x_i^c = x_3$ and $x_j^c = 1 - x_i^c$ for binary 3-1 and 3-2 and $x_1^c = 1 - x_2^c = \frac{x_2}{x_2 + x_3}$ for binary mixture 1-2

b3) *Singh et al. [Singh84]*

$$V_{123}^E = V_{12}^E + V_{13}^E + V_{23}^E + RTx_1x_2x_3 \left[A_{123} + B_{123}x_1(x_2 - x_3) + C_{123}x_1^2(x_2 - x_3)^2 \right] \quad (2.155)$$

where A_{123} , B_{123} and C_{123} are free parameters.

c) Multicomponent systems

For the general case of a multicomponent mixture, it is obvious that no simple equation can be expected to describe all situations and no unique equation can represent the diverse types of complex systems in reality.

For generic approach, exemplified here for a quaternary solution, Ulrici *et al.* [Ulri06] proposed the excess volume in form

$$V_{1,4}^E = V_{12}^E + V_{13}^E + V_{14}^E + V_{23}^E + V_{24}^E + V_{34}^E + \delta_{123} + \delta_{124} + \delta_{134} + \delta_{234} + \Delta_{1234} \quad (2.156)$$

where the V_{ij}^E are molar excess volumes of all binary systems of the quaternary system. The parameters δ_{hki} and Δ_{1234} describe ternary and quaternary contributions.

2.1.2.3. Model for excess enthalpies due to mixing effects

In general, the total enthalpy of a mixture at the same pressure and temperature is not equal to the sum of the total enthalpies of the individual components before mixing. When two or more components are mixed isothermally, a significant change in enthalpy (or heat) may occur due to mixing.

As for V^E the partial molar properties of components should be used in the evaluation of enthalpies of a mixture and not only the specific enthalpies of the pure components.

When two components are mixed together, the molar excess enthalpy of the binary mixture can be determined. From eq. (2.37) becomes

$$H_{12}^E = H - x_1H_1 - x_2H_2 \quad (2.157)$$

It can be seen that H_{12}^E depends on the amounts of moles and is different for every mixture composition.

Data for enthalpies of mixing are usually available for a very limited range of temperatures and components. Heats of mixing are similar in many respects to heats of reactions. When a chemical reaction occurs, the energy of the products is different from the energy of the reactants at the same temperature and pressure because of the chemical rearrangement of the atoms. When a mixture is formed, a similar energy change occurs because the interactions between the force fields of like and unlike molecules are different. However, these energy changes are generally much smaller than those associated with chemical bonds. Therefore enthalpies of mixing are generally much smaller than enthalpies of reaction.

a) Binary systems

As for the prediction of the excess volume, the excess enthalpy can be calculated based on a derivation of G^E . In this case the derivation has to be done with respect to temperature at constant pressure and composition eq. (2.55). Doing this for G^E model given by the simple Redlich/Kister eq. (2.84) follows:

$$H_{12}^E = -x_1x_2RT^2 \left[\frac{\partial A_{12,0}}{\partial T} \right]_P \quad (2.158)$$

at given temperature, yields

$$H_{12}^E = -RT^2 A_{T,12,0} x_1x_2 \quad (2.159)$$

where $A_{T,12,0} = \left[\frac{\partial A_{12,0}}{\partial T} \right]_P$ is the only free parameter of the excess enthalpy model.

Note that H^E is a function of the x_i in exactly the same way as valid for G^E . The more general Redlich/Kister equation with more terms for the excess enthalpy is:

$$H_{12}^E = -RT^2 x_1 x_2 \left[A_{T,12,0} (x_1 - x_2)^0 + A_{T,12,1} (x_1 - x_2) + A_{T,12,2} (x_1 - x_2)^2 + \dots \right] \quad (2.160)$$

the $A_{T,12,i} = \left[\frac{\partial A_{12,i}}{\partial T} \right]_P$ are constants which depends on temperature. In practice, parameters $A_{P,12,i}$ are calculated from experimental data. These parameters are obtained by using the minimization of the objective function given by equation

$$OF = \frac{1}{NUM} \sum_{k=1}^{NUM} \left(H_{12,\text{exp}}^E - H_{12,\text{cal}}^E \right)_k^2 \longrightarrow \min \quad (2.161)$$

Again all other G^E models given in Table 2.1 can be exploited in a similar way. In this work, as in most of the journals and papers consulted ([Ben63], [Bouk09], [Don08], [Illiu00], [Medin02], [Tami09] to mention some of them) the simplest model of general Redlich/Kister Equation (2.159) is used to model the binary systems studied experimentally. The model provides a straightforward method to the free parameters.

b) Ternary systems

Some empirical models were suggested to predict the excess enthalpy for ternary systems, based again on the related binary system data. Frequently used expressions for these models are as follows:

b1) Redlich/Kister equation

For a ternary system the already cite authors Redlich and Kister [Kriss96] presented a model to predict molar excess enthalpies

$$H_{123}^E = H_{12} + H_{23} + H_{13} \quad (2.162)$$

Where H_{12} , H_{23} , H_{13} are the binary contributions to ternary H_{123}^E calculated by any suitable binary model.

b2) Tsao and Smith equation

For the excess enthalpy of a ternary system, Tsao and Smith proposed an equation

$$H_{123}^E = \frac{x_2 H_{12}^E}{1 - x_1} + \frac{x_3 H_{13}^E}{1 - x_1} + (1 - x_1) H_{23}^E \quad (2.163)$$

b3) Aguilar equation

Moreover, Aguilar [Agui09] presented an equation to fit H^E measurements based on higher order terms

$$H_{123}^E = H_{12}^E + H_{13}^E + H_{23}^E + x_1 x_2 x_3 \Delta H_{123}^E \quad (2.164)$$

with

$$\Delta H_{123}^E = B_0 + B_1x_1 + B_2x_2 + B_3x_1^2 + B_4x_2^2 + B_5x_1x_2 + B_6x_1^3 + B_7x_2^3 \quad (2.165)$$

where the B_i are the free parameters.

c) Multicomponent systems

In more general case molar excess enthalpies can be calculated e.g. using the Ulrici *et al.* [Ulri06] equation (2.156) as for V^E

$$H_{1,4}^E = H_{12}^E + H_{13}^E + H_{14}^E + H_{23}^E + H_{24}^E + H_{34}^E + \delta_{123} + \delta_{124} + \delta_{134} + \delta_{234} + \Delta_{1234} \quad (2.166)$$

where the H_{ij}^E are molar excess enthalpies of all binary systems of the quaternary system. The parameters δ_{hki} and Δ_{1234} describe ternary and quaternary contributions.

The following section will be devoted to consider reactive systems.

2.1.3 Chemical reaction equilibria

In many mixtures of components chemical reactions can occur. The purpose of this section is to discuss the effect of temperature, pressure and initial composition on the equilibrium composition of reactive mixtures. This an important and extensively studied field of chemical reaction engineering [Smith05].

a) Equilibrium constant

The equilibrium state of a closed system at the given temperature T and pressure P is the state at which the total Gibbs energy has reached a minimum with respect to all possible changes. This criterion of equilibrium provides the way to determine equilibrium states.

For a single-phase system, the fundamental property relation providing an expression for the total differential of the Gibbs energy eqs. (2.8) and (2.9) may be rewritten,

$$d\mathcal{G} = (nV)dP - (nS)dT + \sum_{i=1}^N \mu_i dn_i \quad (2.167)$$

At the equilibrium state differential variations can occur in the system at constant T and P without producing any change in \mathcal{G} . The total Gibbs energy must decrease during an irreversible natural process. Equilibrium is reached when \mathcal{G} attains its minimum value. Thus, at an equilibrium state holds,

$$[d\mathcal{G}]_{T,P} = 0 \quad (2.168)$$

A quantitative analysis of a single chemical reaction can be performed based on following formulation

$$\sum_{i=1}^N \nu_i A_i = 0 \quad (2.169)$$

This equation describes the change of the number of mole of N components (or species) A_1, A_2, \dots, A_N . Hereby the ν_i are the stoichiometric coefficients of component i for the specific reaction.

To calculate changes in the mole number of a component i due to reaction, the following balance has to be respected:

$$n_i = n_i^0 + \nu_i \xi \quad (2.170)$$

In this equation ξ is the extent of reaction which evaluates together with the stoichiometric coefficients the changes of moles of a component i . Taking derivatives on both sides of equation (2.170) gives:

$$dn_i = \nu_i d\xi \quad (2.171)$$

Elimination of dn_i in eq. (2.167) by eq. (2.171) gives the following relation for the total differential of the Gibbs energy:

$$d\mathcal{G} = (nV)dP - (nS)dT + \sum_{i=1}^N \nu_i \mu_i d\xi \quad (2.172)$$

Take derivatives of eq. (2.172) with respect to ξ for constant T and P gives:

$$\left[\frac{\partial \mathcal{G}}{\partial \xi} \right]_{T,P} = \left[\frac{\partial (n\mathcal{G})}{\partial \xi} \right]_{T,P} = \sum_{i=1}^N \nu_i \mu_i \quad (2.173)$$

Thus, the rate of change of the total Gibbs energy of the system with the extent of reaction ξ at given T and P is the quantity $\sum_{i=1}^N \nu_i \mu_i$. At the equilibrium state this quantity becomes zero.

Therefore, the criterion of chemical – reaction equilibrium can be written as

$$\sum_{i=1}^N \nu_i \mu_i = 0 \quad (2.174)$$

The chemical potential of a component in a mixture of real gases or in a solution of real liquids can be expressed by eq. (2.46)

$$\mu_i \equiv \Gamma_i(T) + RT \ln f_i$$

Rewrite eq. (2.45) for pure species i in its standard state at the same temperature

$$G_i^* = \Gamma_i(T) + RT \ln f_i^* \quad (2.175)$$

with property values in the standard state are denote by the star symbol (*)

Taking the difference between eqs. (2.175) and (2.46) follows:

$$\mu_i - G_i^* = RT \ln \frac{f_i}{f_i^*} \quad (2.176)$$

The ratio f_i / f_i^* is called the activity of species i in solution. Thus by definition [Smith05]

$$a_i \equiv \frac{f_i}{f_i^*} \quad (2.177)$$

and

$$a = x_i \gamma_i \quad (2.178)$$

the preceding eq. (2.176) is

$$\mu_i - G_i^* = RT \ln a_i \quad (2.179)$$

Substituting eq. (2.176) into eq. (2.174) to eliminate μ_i gives for the equilibrium state of the reactive system

$$\sum_{i=1}^N \nu_i (G_i^* + RT \ln a_i) = 0 \quad (2.180)$$

or

$$\sum_{i=1}^N \nu_i G_i^* + RT \sum_{i=1}^N \ln a_i^{\nu_i} = 0 \quad (2.181)$$

or

$$\ln \prod_{i=1}^N a_i^{\nu_i} = \frac{\sum_{i=1}^N \nu_i G_i^*}{RT} \quad (2.182)$$

Thus holds

$$\prod_{i=1}^N a_i^{\nu_i} = \exp \left(\frac{\sum_{i=1}^N \nu_i G_i^*}{RT} \right) \equiv K_a \quad (2.183)$$

Hereby K_a is called the chemical equilibrium constant for the reaction at the standard condition.

The difference between the Gibbs energies of the products and reactants of a chemical reaction is called *the standard Gibbs energy change of reaction* ΔG_R^* [Smith05].

$$\Delta G_R^* \equiv \sum_{i=1}^N \nu_i G_i^* \quad (2.184)$$

In the standard state, the values of the Gibbs free energies of formation, G_i^* , which for common compounds can be found in handbooks (e.g., [Perry99], [CRC05])

Combining eq. (2.183) with eq. (2.184) to eliminate $\sum_{i=1}^N \nu_i G_i^*$ gives for the equilibrium constant [Smith05]

$$K_a = \exp\left(-\frac{\Delta G_R^*}{RT}\right) \quad (2.185)$$

In most cases, K_a can be typically determined based on available thermodynamic data.

b) Effect of temperature on the equilibrium constant

Because the G_i^* are properties of pure species i in their standard state at fixed pressure, they are function of temperature T only. Equation (2.183) dealing with K_a shows that then K_a also depends only on temperature T .

In addition, eq. (2.42) can be written using the fundamental property relation for homogeneous fluids of constant composition

$$d\left(\frac{G}{RT}\right) = \frac{V}{RT} dP - \frac{H}{RT^2} dT \quad (2.186)$$

From eq. (2.186) we get

$$\frac{H}{RT} = -T \left[\frac{\partial(G/RT)}{\partial T} \right]_P \quad (2.187)$$

In the standard state eq. (2.187), written for species i , becomes

$$H_i^* = -RT^2 \left[\frac{\partial(G_i^*/RT)}{\partial T} \right]_P \quad (2.188)$$

Multiplication of both sides of this equation by ν_i and summation over all species gives

$$\sum_{i=1}^N \nu_i H_i^* = -RT^2 \frac{d(\sum_{i=1}^N \nu_i G_i^*/RT)}{dT} \quad (2.189)$$

Conventionally, the definition of a standard enthalpy of reaction is

$$\Delta H_R^* = \sum_{i=1}^N \nu_i H_i^* \quad (2.190)$$

The standard state enthalpy of a chemical compound is equal to its heat of formation plus the standard state enthalpies of its constituent elements. By convention the standard state

enthalpies of all elements equal to zero as the basis of calculation. Then the standard state enthalpy of each compound is its enthalpy of formation. In this event,

$$H_i^* = \Delta H_{f,i}^* \quad (2.191)$$

and eq. (2.190) becomes

$$\Delta H_R^* = \sum_{i=1}^N \nu_i \Delta H_{f,i}^* \quad (2.192)$$

Combining the definition of the standard enthalpy of reaction with (2.184), eq. (2.189) becomes

$$\Delta H_R^* = -RT^2 \frac{d(\Delta G_R^* / RT)}{dT} \quad (2.193)$$

or

$$\frac{d(\Delta G_R^* / RT)}{dT} = -\frac{\Delta H_R^*}{RT^2} \quad (2.194)$$

Eq. (2.185) may be rewritten

$$\frac{\Delta G_R^*}{RT} = -\ln K_a \quad (2.195)$$

Thus, the standard heat of reaction is directly connected with the equilibrium constant. This equation is called the van't Hoff equation [Smith05]

$$\frac{d \ln K_a}{dT} = \frac{\Delta H_R^*}{RT^2} \quad (2.196)$$

For a narrow temperature interval, ΔH_R^* can be assumed to be constant. Thus, integrating both side of eq. (2.196) gives

$$\int_{T_1}^T d \ln K_a = \frac{\Delta H_R^*}{R} \int_{T_1}^T \frac{dT}{T} \quad (2.197)$$

and

$$\ln K_a = \ln K_a(T_1) - \frac{\Delta H_R^*}{R} \left(\frac{1}{T} - \frac{1}{T_1} \right) \quad (2.198)$$

This equation shows the effect of temperature on the equilibrium constant. When the reaction is exothermic, i.e. ΔH_R^* is negative, the equilibrium constant decreases due to an increase in temperature. On the other hand, for endothermic reaction, K_a increases with T . However, using this equation to quantify the value of K_a is risky because H_R^* also depends on temperature.

To treat this limitation, from equation (2.27) the expression for the Gibbs energy, $G \equiv H - TS$, can be written for each species involved in the chemical reaction at the standard state and at temperature T

$$G_i^* = H_i^* - TS_i^* \quad (2.199)$$

Multiplying both sides of this equation with ν_i and summing over all species gives

$$\sum_{i=1}^N \nu_i G_i^* = \sum_{i=1}^N \nu_i H_i^* - T \sum_{i=1}^N \nu_i S_i^* \quad (2.200)$$

or

$$\Delta G_R^* = \Delta H_R^* - T \Delta S_R^* \quad (2.201)$$

The value of ΔH_R^* can be calculated by the fundamental equation relating heats of reaction to temperature.

Heat capacity at constantant pressure, $C_{P,i}$, is defined as follows

$$C_{P,i} = \left[\frac{dH_i}{dT} \right]_P \quad (2.202)$$

Multiplying by ν_i and summing over all products and reactants give

$$\sum_{i=1}^N \nu_i dH_i^* = \sum_{i=1}^N \nu_i C_{P,i}^* dT \quad (2.203)$$

Because ν_i is a constant, it can come inside the differential, giving

$$\sum_{i=1}^N d(\nu_i H_i^*) = d \sum_{i=1}^N \nu_i H_i^* = \sum_{i=1}^N \nu_i C_{P,i}^* dT \quad (2.204)$$

As mentioned above the term $\sum_i \nu_i H_i^*$ is the standard heat of reaction, defined by eq. (2.190), and similarly. In addition we express for convenience ΔC_P^* as the standard heat capacity change of the reaction

$$\Delta C_P^* \equiv \sum_{i=1}^N \nu_i C_{P,i}^* \quad (2.205)$$

From definitions (2.190) and (2.205), eq. (2.204) becomes

$$d\Delta H_R^* = \Delta C_P^* dT \quad (2.206)$$

Integrating both sides gives

$$\Delta H_R^* = \Delta H_0^* + R \int_{T_0}^T \frac{\Delta C_P^*}{R} dT \quad (2.207)$$

Where ΔH_R^* and ΔH_0^* are heats of reaction at temperature T and at reference temperature T_0 respectively.

A similar analysis leads for the entropy change of reaction

$$\Delta S_R^* = \Delta S_0^* + R \int_{T_0}^T \frac{\Delta C_P^*}{R} \frac{dT}{T} \quad (2.208)$$

Where ΔS_R^* and ΔS_0^* are standard entropy changes of reaction at temperature T and at the reference temperature T_0 respectively.

Combining eq. (2.201), (2.207) and (2.208) gives

$$\Delta G_R^* = \Delta H_0^* + R \int_{T_0}^T \frac{\Delta C_P^*}{R} dT - T \Delta S_0^* - RT \int_{T_0}^T \frac{\Delta C_P^*}{R} \frac{dT}{T} \quad (2.209)$$

Nevertheless

$$\Delta S_0^* = \frac{\Delta H_0^* - \Delta G_0^*}{T_0} \quad (2.210)$$

and substituting eq. (2.210) into eq. (2.209) yields,

$$\Delta G_R^* = \Delta H_0^* - \frac{T}{T_0} (\Delta H_0^* - \Delta G_0^*) + R \int_{T_0}^T \frac{\Delta C_P^*}{R} dT - RT \int_{T_0}^T \frac{\Delta C_P^*}{R} \frac{dT}{T} \quad (2.211)$$

Division by RT gives,

$$\frac{\Delta G_R^*}{RT} = \frac{\Delta G_0^* - \Delta H_0^*}{RT_0} + \frac{\Delta H_0^*}{RT} + \frac{1}{T} \int_{T_0}^T \frac{\Delta C_P^*}{R} dT - \int_{T_0}^T \frac{\Delta C_P^*}{R} \frac{dT}{T} \quad (2.212)$$

So, at any temperature the equilibrium constant can be quantified from the values of heat of reaction and the standard Gibbs energy change of reaction at a reference temperature (usually 298.15K) by using eq. (2.212) and eq. (2.195).

After considering basic thermodynamic aspects of chemical reactions, in the following section, concepts capable to quantify chemical kinetics are introduced.

2.2 CHEMICAL KINETICS

Knowledge regarding chemical kinetics is the most important requirement to describe chemical reactions and to design real reactors. The kinetics provides the functional relationship between the rates of reactions and all state properties which effect these rates as e.g. compositions,

temperature, pressure, etc. The discussion below follows classical textbooks [Leve99], [Miss99], [Weste90], [Smith81], [Coop71], etc.

For a homogeneous reaction, the kinetics are a function of the concentrations and temperature. In catalysed reactive systems, the kinetics additionally depends on the concentration and the type of the catalyst. Beside, kinetic models of heterogeneous systems need to evaluate the intrinsic chemical reaction (micro kinetics) and also transport phenomena (macro kinetics).

For the description of the rate of a homogeneous reaction in a closed system with N components, the rate quantifies the temporal change of the number of moles of each component i per unit scale of reaction phase and per unit time. The definition for a single reaction is

$$r = \frac{1}{Scale} \frac{1}{\nu_i} \frac{dn_i}{dt} \quad i = 1, N \quad (2.213)$$

with the stoichiometric coefficients of component i ν_i . The *Scale* for liquid phase reactions is often the volume of reaction mixture, V_R . So eq. (2.213) becomes

$$r = \frac{1}{V_R} \frac{1}{\nu_i} \frac{dn_i}{dt} \quad (2.214)$$

For several (M) reactions, which take place simultaneously, the temporal changes of the number of moles of one component i are described by the following equation

$$\frac{dn_i}{dt} = V_R \sum_{j=1}^M \nu_{ij} r_j \quad i = 1, N \quad (2.215)$$

The reaction volume V_R may change due to two causes: one is due to the reaction and the other is due to mixing effects.

It is assumed that the rate of reaction involves the collision or interaction of a single molecule of a reactant with a single molecule of the other reactants. The rate is then proportional to the concentrations of the reactants in the reaction mixture [Miss99], [Smith81]. Thus, for an irreversible reaction the reaction rate can be expressed as

$$r = k(T) \prod_{i=1}^{N_r} c_i^{m_i} \quad (2.216)$$

where N_r is the number of reactants; m_i is the order of the reaction with respect to the component i , and c_i is the concentration of component i defined as

$$c_i = \frac{n_i}{V_R} \quad (2.217)$$

In general, the temperature dependence of the reaction rate constant $k(T)$ can be described empirically by the Arrhenius equation.

$$k(T) = k_0 \exp\left(-\frac{E_A}{RT}\right) \quad (2.218)$$

where E_A is the activation energy for the reaction and k_0 is the pre-exponential factor.

If the reaction is reversible, the rate can be rewritten as

$$r = r_f - r_b = k_f(T) \prod_{i=1}^N c_i^{m_{f,i}} - k_b(T) \prod_{i=1}^N c_i^{m_{b,i}} \quad (2.219)$$

with

$$m_{f,i} = \frac{1}{2}(|\nu_i| - \nu_i) \quad (2.220)$$

$$m_{b,i} = \frac{1}{2}(|\nu_i| + \nu_i) \quad (2.221)$$

The two terms in eq. (2.219) show the kinetic expression for the forward and backward reaction of N components, where k_f and k_b are the rate constants of the forward and backward reactions, respectively. K_c is the concentration-based reaction equilibrium constant Eq. (2.222)

$$K_c = \frac{k_f}{k_b} = \prod_{i=1}^N c_i^{\nu_i} \quad (2.222)$$

Thus, it holds

$$r = k_f(T) \left[\prod_{i=1}^N c_i^{m_{f,i}} - \frac{1}{K_c} \prod_{i=1}^N c_i^{m_{b,i}} \right] \quad (2.223)$$

Alternatively, the reaction rate can be expressed in terms of activities as in Eq. (2.224) in order to take into account the non-idealities of the solution.

$$r = k_{f,a}(T) \left[\prod_{i=1}^N a_i^{m_{f,i}} - \frac{1}{K_a} \prod_{i=1}^N a_i^{m_{b,i}} \right] \quad (2.224)$$

Here a_i is the activity of component i and for K_a holds

$$K_a = \prod_{i=1}^N a_i^{\nu_i} \quad (2.225)$$

with $a_i = x_i \gamma_i$ (eq. (2.178)), where the activity coefficient, γ_i , of component i in the liquid phase can be calculated using the Wilson eq. (2.108), UNIQUAC eq. (2.111) and UNIFAC eq. (2.124), which were introduced in section 2.1.2.1.

This short introduction is sufficient for the needs of this work. More information regarding the large field of chemical kinetics can be found e.g. [Leve99], [Miss99], [Smith81].

Combination of thermodynamics and chemical kinetics provides the platform for analysis of chemical processes using mass and energy balances formulated for specific chemical reactors.

For illustration, in the next section the most simple batch reactor is described in more detail.

2.3 REACTOR MODELS

2.3.1 Mass balance of chemical reactors

Consider a differential volume dV_R depicted as in Figure 2.1, which is exposed to inlet and outlet flows of a component i with molar flow rates \dot{n}_i^{in} and \dot{n}_i^{out} , respectively, and in which a single chemical reaction can take place

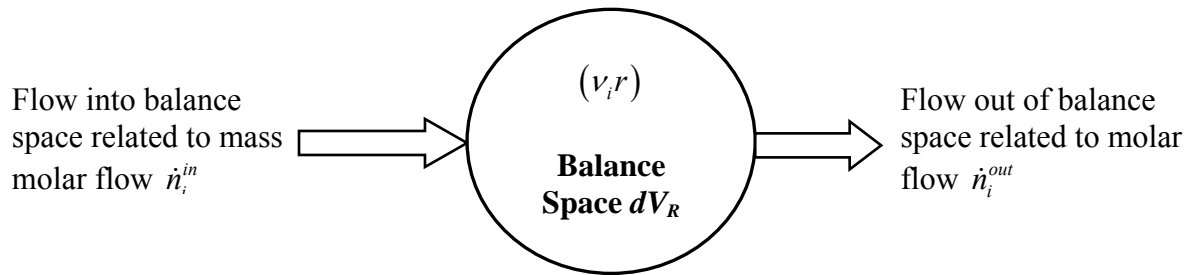


Figure 2.1 Illustration to derive mass balance for a balance space of differential volume dV_R .

A conventional mass balance, written for any chemical component i may be formulated verbally in the following form [Weste90]:

$$\left(\begin{array}{l} \text{Rate of accumulation} \\ \text{of component } i \\ \text{in the volume} \end{array} \right) = \left(\begin{array}{l} \text{Rate of component } i \\ \text{flowing into the} \\ \text{volume} \end{array} \right) - \left(\begin{array}{l} \text{Rate of component } i \\ \text{flowing out of} \\ \text{the volume} \end{array} \right) + \left(\begin{array}{l} \text{Rate of component } i \\ \text{produced or consumed} \\ \text{by chemical reactions} \end{array} \right) \quad (2.226)$$

In general, such balance holds in the differential volumes dV_R , which are considered sufficiently small to be perfectly mixed and homogeneous. For a well-mixed reactor the appropriate balance space is the entire reaction volume V_R . Assuming that only one reaction proceeds in homogeneous phase with rate r holds

$$\frac{dn_i}{dt} = \dot{n}_i^{in} - \dot{n}_i^{out} + v_i r V_R \quad i = 1, N \quad (2.227)$$

For a closed system (BR), there are no inlet and outlet flows. Hence we have

$$\dot{n}_i^{in} = 0 \quad \text{and} \quad \dot{n}_i^{out} = 0 \quad i = 1, N \quad (2.228)$$

and eq. (2.227) becomes

$$\frac{dn_i}{dt} = v_i r V_R \quad i = 1, N \quad (2.229)$$

This equation is exactly the same as eq. (2.214) formulated to define the reaction rate.

2.3.1.1 Batch Reactors with constant - volume

The simplest case of the batch reactor balance is the constant-volume case. Here we are really referring to the volume of reaction mixture and not the volume of reactor, which might not be completely filled. Thus, we actually consider a constant-density situation [Leve99]. Under these conditions for the constant-volume case holds:

$$\frac{dV_R}{dt} = 0 \quad (2.230)$$

Thus, in summary the mass balances of the reactor can be expressed by the following ODE system

“Const” case:

$\begin{aligned} \frac{dn_i}{dt} &= v_i r V_R & i &= 1, N \\ \frac{dV_R}{dt} &= 0 \end{aligned}$	(2.231)
--	---------

To solve eq. (2.231) initial conditions at $t = 0$ are needed

$$t = 0 : \begin{cases} n_i = n_i^{init} \\ V_R = V_R^{id,init} \end{cases} \quad i = 1, N \quad (2.232)$$

In general, the reaction volume is not constant. As stated above, it can change due to two contributions: one is the composition change due to reaction and the other is due to mixing effects. More detailed expressions considering these changes are described in the following parts.

2.3.1.2 Batch Reactors with varying - volume

a) Volume effects due to composition changes caused only by reaction

If excess volumes can be neglected, from eq. (2.26) follows that the molar volume of a pure component i equals to its partial molar volume in solution

$$V_i^{id} = V_i^0 = \frac{M_i}{\rho_i} \quad (2.233)$$

where M_i is the molar mass of component i , and ρ_i is the density of component i .

From eq. (2.32) we have:

$$V_R^{id} = \sum_{i=1}^N n_i V_i^0 \quad (2.234)$$

To calculate changes in the mole number of a component i due to reaction, it is helpful to exploit the extent of reaction as

$$\xi = \frac{n_i - n_i^{init}}{\nu_i} \quad (2.235)$$

Substituting n_i in eq. (2.234) by ξ yields

$$V_R^{id} = \sum_{i=1}^N (n_i^{init} + \nu_i \xi) V_i^0 = \sum_{i=1}^N n_i^{init} V_i^0 + \left(\sum_{i=1}^N \nu_i V_i^0 \right) \xi \quad (2.236)$$

Thus, the reaction volume V_R present at any time can be calculated from the initial reaction volume, V_R^{init} and the extent of reaction by

$$V_R = V_R^{id,init} + \left(\sum_{i=1}^N \nu_i V_i^{init} \right) \times \xi \quad (2.237)$$

Hence, the larger the $\sum_{i=1}^N \nu_i V_i^0$ value, the more volume effects occur due to composition changes caused by reaction. Even, if $\sum_{i=1}^N \nu_i = 0$, since the molar densities of components are different, the above term is not zero. Only if $\sum_{i=1}^N \nu_i V_i^0 = 0$, there will be no volume changes.

Taking derivatives on both sides of eq. (2.237) with respect to time we obtain:

$$\frac{dV_R}{dt} = \left(\sum_{i=1}^N \nu_i V_i^0 \right) \frac{d\xi}{dt} \quad (2.238)$$

From the definition of extent of reaction, eq. (2.235), we have

$$\frac{d\xi}{dt} = \frac{1}{\nu_i} \frac{dn_i}{dt} \quad (2.239)$$

Inserting eq. (2.239) into eq. (2.238) yields

$$\frac{dV_R}{dt} = \left(\sum_{i=1}^N \nu_i V_i^0 \right) \frac{1}{\nu_j} \frac{dn_j}{dt} \quad (2.240)$$

Exploiting the definition of r , we obtain

$$\frac{dV_R}{dt} = r V_R \sum_{i=1}^N \nu_i V_i^0 \quad (2.241)$$

The complete ODE system is built by combining eq. (2.241) instead of eq. (2.230) and the mass balance (2.229) with the identical initial conditions eq. (2.232).

“Ideal” case:

$$\boxed{\begin{aligned} \frac{dn_i}{dt} &= v_i r V_R & i = 1, N \\ \frac{dV_R}{dt} &= r V_R \sum_{i=1}^N v_i V_i^0 \end{aligned}} \quad (2.242)$$

To solve eq. (2.242) initial conditions at $t=0$, eq. (2.232) is used.

Furthermore, from eq. (2.241) one obtains,

$$\frac{d(\ln V_R)}{dt} = r \sum_{i=1}^N v_i V_i^0 \quad (2.243)$$

or

$$\frac{d(\ln V_R)}{dt} = r V^+ \quad (2.244)$$

where $V^+ = \sum_{i=1}^N v_i V_i^0$

Assume for illustration the order of the reaction is zero, i.e. $r = k$, eq. (2.243) may be written as

$$\frac{d(\ln V_R)}{dt} = k V^+ \quad (2.245)$$

After integration of eq. (2.245) follows

$$\ln \frac{V_R}{V_R^0} = k V^+ t \quad (2.246)$$

This equation can be interpreted in Figure 2.2

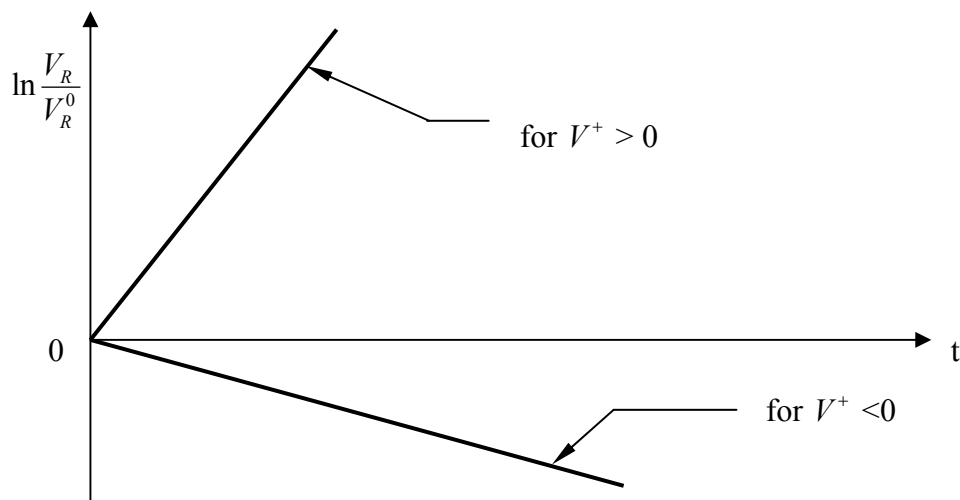


Figure 2.2 Illustration of changes in volume only due to reaction (homogeneous zero-order reaction) based on eq. (2.246).

Not considered so far, the mixing effect can be not negligible so more complicated models must be considered.

b) Volume changes due to reaction and mixing

Section 2.1 was already devoted to evaluate volume changes in nonreactive system due to mixing.

The reaction volume expressed in eq. (2.229) can be more described by

$$V_R = nV^{id} + nV^E \quad (2.247)$$

Taking the derivative with respect to composition n_i we have

$$dV_R = \sum_{i=1}^N \left[\frac{\partial(nV^{id})}{\partial n_i} \right]_{n_{k \neq i}} dn_i + \sum_{i=1}^N \left[\frac{\partial(nV^E)}{\partial n_i} \right]_{n_{k \neq i}} dn_i \quad (2.248)$$

Applying eq. (2.7) to this equation gives

$$dV_R = \sum_{i=1}^N V_i^{id} dn_i + \sum_{i=1}^N V_i^E dn_i \quad (2.249)$$

Thus, the corresponding time derivatives for a real volume can be expressed by

$$\frac{dV_R}{dt} = \sum_{i=1}^N V_i^{id} \frac{dn_i}{dt} + \sum_{i=1}^N V_i^E \frac{dn_i}{dt} \quad (2.250)$$

Exploiting definition of r leads to

$$\frac{dV_R}{dt} = rV_R \sum_{i=1}^N v_i V_i^{id} + rV_R \sum_{i=1}^N v_i V_i^E \quad (2.251)$$

Considering eq. (2.26), we also have

$$\frac{dV_R}{dt} = rV_R \sum_{i=1}^N v_i V_i^0 + rV_R \sum_{i=1}^N v_i V_i^E \quad (2.252)$$

The ODE system for the batch reactor is built by combining eq. (2.252) and the mass balance given already in eq. (2.231)

“Real” case:

$$\boxed{\begin{aligned} \frac{dn_i}{dt} &= v_i r V_R & i &= 1, N \\ \frac{dV_R}{dt} &= rV_R \sum_{i=1}^N v_i V_i^0 + rV_R \sum_{i=1}^N v_i V_i^E \end{aligned}} \quad (2.253)$$

The values for V_i^E and are determined by eq. (2.57)

The initial conditions at $t = 0$, are:

$$t = 0: \begin{cases} n_i = n_i^{init} \\ V_R = V_R^{init} \end{cases} \quad i = 1, N \quad (2.254)$$

In summary, we have three ways to treat volume effects in a different manner:

- Constant-volume case, eq. (2.231): “*Const*”
- Ideal solution just effect of reaction eq. (2.242): “*Ideal*”
- Non-ideal solution joint effects of mixing and reaction eq. (2.253): “*Real*”

Later we will investigate how each of these method effects the results of a kinetic study.

2.3.2. Energy balance of chemical reactors

In practice, industrial reactors work very seldom under isothermal conditions. To quantify joint temperature and concentrations changes, we have to solve simultaneously both the component mass balances and an energy balance.

Compared to the mass balance, the energy balance is more complicated. This is due to the fact that because the reactor walls are closed for mass but not for energy. Therefore, during a chemical reaction, all individual heat supplies from the surrounding to the reaction medium caused by heat transfer through the wall of reactor, heat, heat losses, etc. muss be included.

In this work, an enthalpy balance is considered based on the illustration give in Figure 2.3.

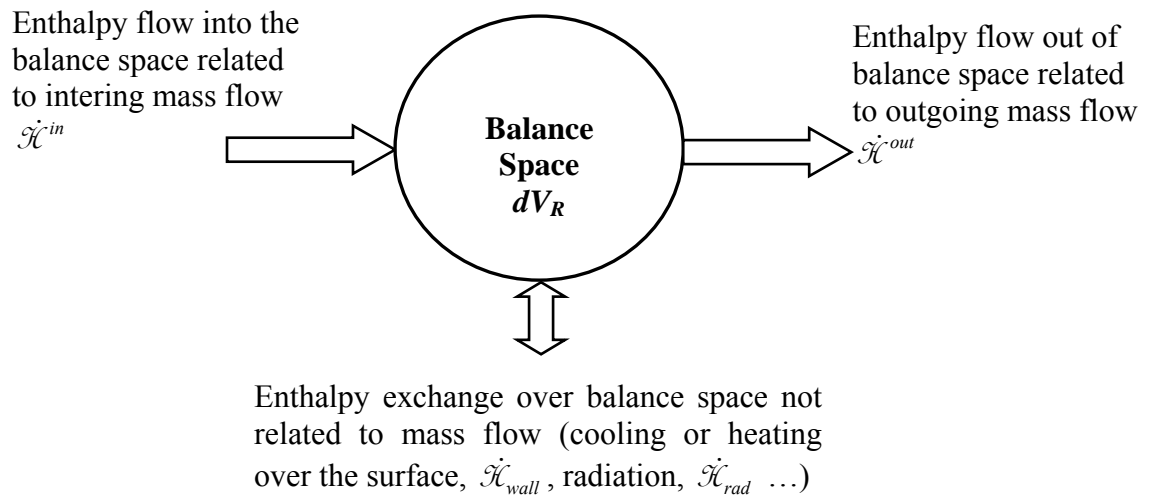


Figure 2.3 Illustration to formulate the enthalpy balance for a differential volume dV_R .

The enthalpy balance can be presented in the following statement

$$\left(\begin{array}{c} \text{Rate of enthalpy} \\ \text{accumulation} \end{array} \right) = \left(\begin{array}{c} \text{Rate of enthalpy} \\ \text{flowing into the volume} \end{array} \right) - \left(\begin{array}{c} \text{Rate of enthalpy} \\ \text{flowing out of the volume} \end{array} \right) + \left(\begin{array}{c} \text{Enthalpy exchange over system} \\ \text{not related to mass flow} \end{array} \right) \quad (2.255)$$

Assuming again a well-mixed (BR) situation an equation similar to the mass balance, eq. (2.255) can be written for the whole reaction volume V_R

$$\frac{d\mathcal{K}}{dt} = \dot{\mathcal{K}}^{in} - \dot{\mathcal{K}}^{out} + (\dot{\mathcal{K}}_{wall} + \dot{\mathcal{K}}_{rad}) \quad (2.256)$$

where \mathcal{K} is the total enthalpy

The terms containing reaction and mixing effects will appear based on the derivation given below.

At moderate temperature level (<500°C), it is justified to assume that radiation effects are negligible ($\dot{\mathcal{K}}_{rad} = 0$), then eq. (2.256) becomes

$$\frac{d\mathcal{K}}{dt} = \dot{\mathcal{K}}^{in} - \dot{\mathcal{K}}^{out} + \dot{\mathcal{K}}_{wall} \quad (2.257)$$

In a single phase system, the total enthalpy \mathcal{K} is a function of temperature T , pressure P and composition. This gives the following total differential as

$$d\mathcal{K}(P, T, n_i) = \left[\frac{\partial \mathcal{K}}{\partial P} \right]_{T, n_i} dP + \left[\frac{\partial \mathcal{K}}{\partial T} \right]_{P, n_i} dT + \sum_{i=1}^N \left[\frac{\partial \mathcal{K}}{\partial n_i} \right]_{T, P, n_{k \neq i}} dn_i \quad (2.258)$$

Above, we denoted the molar enthalpy of a solution by H . Using eq. (2.30) we have for the total enthalpy \mathcal{K} :

$$\mathcal{K} = n \sum_{i=1}^N x_i H_i = \sum_{i=1}^N n_i H_i \quad (2.259)$$

Substituting eq. (2.259) into eq. (2.258) follows

$$d\mathcal{K}(P, T, n_i) = \sum_{i=1}^N n_i \left[\frac{\partial H_i}{\partial P} \right]_{T, n_i} dP + \sum_{i=1}^N n_i \left[\frac{\partial H_i}{\partial T} \right]_{P, n_i} dT + \sum_{i=1}^N \left[\frac{\partial (n_i H_i)}{\partial n_i} \right]_{T, P, n_{k \neq i}} dn_i \quad (2.260)$$

At constant pressure, from eq.(2.202) the heat capacities $C_{p,i}$ are defined

$$\sum_{i=1}^N n_i \left[\frac{\partial H_i}{\partial T} \right]_{P, n_i} = \sum_{i=1}^N n_i C_{p,i} \quad (2.261)$$

For small temperature changes, $C_{p,i}$ can be assumed to be constant. This assumption is made in this dissertation.

As a result of eq. (2.261) and eq. (2.7), at constant pressure, eq. (2.260) becomes

$$d\mathcal{K} = \sum_{i=1}^N n_i C_{p,i} dT + \sum_{i=1}^N H_i dn_i \quad (2.262)$$

In real solutions, we have

$$H_i = H_i^{id} + H_i^E \quad (2.263)$$

Thus, the second term of right side eq. (2.262) can be expressed as

$$\sum_{i=1}^N H_i dn_i = \sum_{i=1}^N H_i^{id} dn_i + \sum_{i=1}^N H_i^E dn_i \quad (2.264)$$

Since $H_i^{id} = H_i^0$ (eq. (2.29)), eq. (2.262) becomes

$$d\mathcal{H} = \sum_{i=1}^N n_i C_{P,i} dT + \sum_{i=1}^N H_i^0 dn_i + \sum_{i=1}^N H_i^E dn_i \quad (2.265)$$

Therefore, the transient of the enthalpy can be expressed by forming the time derivatives from eq. (2.265) gives

$$\frac{d\mathcal{H}}{dt} = \sum_{i=1}^N n_i C_{P,i} \frac{dT}{dt} + \sum_{i=1}^N H_i^0 \frac{dn_i}{dt} + \sum_{i=1}^N H_i^E \frac{dn_i}{dt} \quad (2.266)$$

a) Batch reactor

For a closed system, there are no inlet and outlet flow. This yields

$$\frac{d\mathcal{H}}{dt} = \dot{\mathcal{H}}_{wall} \quad (2.267)$$

Substituting dn_i/dt by the mass balance (2.231) into eq. (2.266), and combination with eq. (2.267) yields

$$\sum_{i=1}^N n_i C_{P,i} \frac{dT}{dt} + rV_R \sum_{i=1}^N v_i H_i^0 + rV_R \sum_{i=1}^N v_i H_i^E = \dot{\mathcal{H}}_{wall} \quad (2.268)$$

Using eq. (2.190) to substitute $\sum_{i=1}^N v_i H_i^0$ by ΔH_R^0 eq. (2.190) we have

$$\sum_{i=1}^N n_i C_{P,i} \frac{dT}{dt} + rV_R \Delta H_R^0 + rV_R \sum_{i=1}^N v_i H_i^E = \dot{\mathcal{H}}_{wall} \quad (2.269)$$

or

$$\sum_{i=1}^N n_i C_{P,i} \frac{dT}{dt} = -rV_R \Delta H_R^0 - rV_R \sum_{i=1}^N v_i H_i^E + \dot{\mathcal{H}}_{wall} \quad (2.270)$$

Finally holds

$$\frac{dT}{dt} = \frac{-rV_R \Delta H_R^0 - rV_R \sum_{i=1}^N v_i H_i^E + \dot{\mathcal{H}}_{wall}}{\sum_{i=1}^N n_i C_{P,i}} \quad (2.271)$$

This equation expresses the changes of the reaction temperature during the joint effects of reaction and mixing together with wall heat transfer.

The final ODE system describing the batch reactor is built by combining this equation and ODEs (eq. (2.229) and eq. (2.252)).

$$\boxed{\begin{aligned} \frac{dn_i}{dt} &= v_i r V_R & i = 1, N \\ \frac{dV_R}{dt} &= r V_R \sum_{i=1}^N v_i V_i^0 + r V_R \sum_{i=1}^N v_i V_i^E \\ \frac{dT}{dt} &= \frac{-r V_R \Delta H_R^0 - r V_R \sum_{i=1}^N v_i H_i^E + \dot{\mathcal{K}}_{wall}}{\sum_{i=1}^N n_i C_{P,i}} \end{aligned}} \quad (2.272)$$

with the initial conditions, at $t = 0$:

$$t = 0 : \begin{cases} n_i = n_i^{init} & i = 1, N \\ V_R = V_R^{init} \\ T = T^{init} \end{cases} \quad (2.273)$$

The values of V_i^E and H_i^E are directly determined by eq. (2.57) and (2.58) leading to V^E and H^E by eq. (2.69). Possible dependences of the pure molar volumes V_i^0 on temperature are neglected in this dissertation.

This ODE system is capable to describe closed batch systems considering volume and enthalpy changes due to reaction and mixing

b) Isothermal batch reactor

Under isothermal condition eq. (2.271) become simply

$$\frac{dT}{dt} = 0 \quad (2.274)$$

then

$$-r V_R \Delta H_R^0 - r V_R \sum_{i=1}^N v_i H_i^E + \dot{\mathcal{K}}_{wall} = 0 \quad (2.275)$$

Thus,

$$\dot{\mathcal{K}}_{wall} = r V_R \Delta H_R^0 + r V_R \sum_{i=1}^N v_i H_i^E \quad (2.276)$$

Finally the wall term can be designated as

$$\dot{\mathcal{K}}_{wall} = -\dot{\mathcal{K}}_{chem-mix} \quad (2.277)$$

with $\dot{\mathcal{K}}_{chem-mix}$ is heat released or consumed jointly by reaction and mixing of products formed in reactive solution

$$\dot{\mathcal{K}}_{chem-mix} = - \left(rV_R \Delta H_R^0 + rV_R \sum_{i=1}^N \nu_i H_i^E \right) \quad (2.278)$$

The enthalpy flow over the reactor wall, $\dot{\mathcal{K}}_{wall}$, is directly related to enthalpies of reaction and mixing during reaction time.

From eq. (2.276), we have

$$\dot{\mathcal{K}}_{wall} = -\dot{\mathcal{K}}_{chem} + rV_R \sum_{i=1}^N \nu_i H_i^E \quad (2.279)$$

Then

$$\dot{\mathcal{K}}_{chem} = -\dot{\mathcal{K}}_{wall} + rV_R \sum_{i=1}^N \nu_i H_i^E \quad (2.280)$$

with $\dot{\mathcal{K}}_{chem} = -rV_R \Delta H_R^0$

c) Adiabatic batch reactor

Under adiabatic conditions, $\dot{\mathcal{K}}_{wall} = 0$, eq. (2.271) simplified to

$$\frac{dT}{dt} = \frac{-rV_R \Delta H_R^0 - rV_R \sum_{i=1}^N \nu_i H_i^E}{\sum_{i=1}^N n C_P} \quad (2.281)$$

d) Semi-batch reactor

Due to the situation encountered in starting experiments here also the case of a semi-batch reactor is consider.

For the semi-batch reactor, there is no flow out the volume eq. (2.257) reduces to

$$\frac{d\mathcal{K}}{dt} = \dot{\mathcal{K}}^{in} + \dot{\mathcal{K}}_{wall} \quad (2.282)$$

and the mass balance for the semi-batch eq. (2.227) becomes

$$\frac{dn_i}{dt} = \dot{n}_i^{in} + \nu_i rV_R \quad i = 1, N \quad (2.283)$$

Substituting eqs. (2.282) and (2.283) into eq. (2.266) yields

$$\sum_{i=1}^N n_i C_{P,i} \frac{dT}{dt} + rV_R \Delta H_R^0 + rV_R \sum_{i=1}^N \nu_i H_i^E + \sum_{i=1}^N \dot{n}_i^{in} H_i^0 + \sum_{i=1}^N \dot{n}_i^{in} H_i^E = \dot{\mathcal{K}}^{in} + \dot{\mathcal{K}}_{wall} \quad (2.284)$$

Rearrangement

$$\sum_{i=1}^N n_i C_{P,i} \frac{dT}{dt} = - \left(r V_R \Delta H_R^0 + r V_R \sum_{i=1}^N \nu_i H_i^E \right) + \sum_{i=1}^N \dot{n}_i^{in} (H_i^{in} - H_i^0) + \sum_{i=1}^N \dot{n}_i^{in} H_i^E + \dot{\mathcal{K}}_{wall} \quad (2.285)$$

If components are quickly introduced at the same temperature as the medium in reactor, it gives $H_i^{in} = H_i^0$, then finally

$$\dot{\mathcal{K}}_{chem-mix} + \dot{\mathcal{K}}_{mix} = \dot{\mathcal{K}}_{wall} + \sum_{i=1}^N n_i C_{P,i} \frac{dT}{dt} \quad (2.286)$$

$\dot{\mathcal{K}}_{mix}$ is the enthalpy flow occurring due to mixing of introduced components

$$\dot{\mathcal{K}}_{mix} = \sum_{i=1}^N \dot{n}_i^{in} H_i^E \quad (2.287)$$

$\dot{\mathcal{K}}_{wall}$ is heat exchange between the reaction mixture and surrounding, which is typically a cooling or heating system

$$\dot{\mathcal{K}}_{wall} = UA(T - T_{jack}) \quad (2.288)$$

where T_{jack} is the temperature of the medium (or the jacket temperature), U is the overall heat transfer coefficient to the reactor wall, and A is the heat transfer area between the reaction mixture and the reactor wall.

If no reaction and mixing occur, eq. (2.286) reduces

$$0 = \dot{\mathcal{K}}_{wall} + \sum_{i=1}^N n_i C_{P,i} \frac{dT}{dt} \quad (2.289)$$

2.3.3 Numerical aspects of solving the mass and energy balances

a) ODE solving

A model consisting of differential equations, such as the mass and energy balance equations, derived above may be shown in the form [Alkis00]

$$\frac{dY}{dx} = g(x, Y, b) \quad (2.290)$$

where dY/dx is the vector of derivatives of Y , g is the vector of functions, x is the independent variable, Y is the vector of dependent variables and b is a vector of parameters.

If the initial conditions, the vector b and the function g are given, the differential equations (2.290) can be integrated numerically or analytically to get the integrated results

$$Y = f(x, b) \quad (2.291)$$

The $(N+2)$ nonlinear differential equation eqs. (2.272) represent the mass and energy balances of a Batch Reactor.

The software tool MATLAB offers efficient ODE solvers, which were employed to solve the equations and determine unknown kinetic parameters fitting predictions to experimental data collected.

b) Optimization

To get the best-fit values of free kinetic parameters, the calculated values of the dependent variables have to be compared with the measured one. Assuming that the model consists of only one dependent variable Y , the sum of squared residual can be described by

$$\phi = (Y_{\text{exp}} - Y)'(Y_{\text{exp}} - Y) \quad (2.292)$$

Where Y_{exp} is vector of experimental observations of the dependent variable, Y is vector of calculated values of the dependent variables obtained from eq. (2.291)

In order to obtain the values of free parameters fitting b , the minimization of the sum of squared residuals given by eq. (2.292) must be performed. In this work, to determine kinetic parameters, the following objective function evaluating measured concentrations is used

$$OF_c = \frac{1}{NUM} \sum_{k=1}^{NUM} \left[\frac{c_i^{\text{exp}}(t_k) - c_i^{\text{cal}}(t_k)}{c_i^{\text{exp}}(t_k)} \right]^2 \longrightarrow \min \quad (2.293)$$

Where $c_i^{\text{cal}}(t_k)$ is computable concentration of component i at NUM times $t = t_k$ and corresponding experimentally determined concentrations $c_i^{\text{exp}}(t_k)$ of component i at $t = t_k$.

In this objective function, the relative errors of concentrations are taken instead of absolute errors, because relative errors are useful for analysing concentrations measured in a larger range.

2.4 ILLUSTRATION OF NON-IDEAL BEHAVIOUR

After introducing the basic theory, the goal of this section is to illustrate the effect of excess properties of non-reactive and reactive mixtures based on reasonable property parameters. Firstly, we demonstrate expressions for G^E , H^E , V^E and the activity coefficients γ_i for a non-reactive ternary mixture. Then a simple reversible liquid phase reaction will be considered evaluating the joint effects of mixing and reaction.

2.4.1 Non-reactive system

The parameters used in the following to simulate the behaviour of a ternary mixture are fictitious but lie in the order of magnitude of real systems. Firstly, just mixing of a ternary non-reactive mixture of three components 1, 2 and 3 is considered. The physical properties of the components assumed for this illustrative purpose are given in Table 2.2.

Table 2.2 Physical properties used for the simulation of the three components non-reactive system.

Component	M_i [g/mol]	ρ_i [g/L]	V_i^0 [L/mol]
1 (A)	100	1100	0.091
2 (B)	18	1000	0.018
3 (C)	60	1050	0.057

To describe the excess Gibbs energy for the ternary system ($N = 3$) the Singh model eq.(2.107) is used

$$\frac{G^E}{RT} = \frac{1}{RT} (G_{12}^E + G_{23}^E + G_{31}^E) + A_{123}x_1x_2x_3$$

Applying the Redlich/Kister eq. (2.84) to describe the binary system excess Gibbs energies $G_{12}^E, G_{23}^E, G_{13}^E$ yields

$$\frac{G^E}{RT} = A_{12}x_1x_2 + A_{23}x_2x_3 + A_{31}x_3x_1 + A_{123}x_1x_2x_3 \quad (2.294)$$

Thus the four parameters A_{ij} and A_{123} are needed to predict G^E values or activity coefficients.

As mentioned earlier, the four Gibbs parameters A_{12} , A_{23} , A_{13} and A_{123} depend on temperature and pressure, but not on composition. We express each of these four parameters as a polynomial function of T and P , not considering influences of term $T \times P$:

$$Par = a_0 + a_1T + a_2T^2 + a_3T^3 + \dots + b_1P + b_2P^2 + b_3P^3 + \dots \quad (2.295)$$

where Par indicates four different empirical functions (2.295) for the four Gibbs parameters (A_{ij} & A_{123}), with a_i and b_i being free coefficients.

The assignment of $a_i = b_i = 0$ for $i \geq 1$, yields the simplest expression for these parameters, namely constant values a_0 :

$$Par = a_0 \quad (2.296)$$

From eq. (2.294) and (2.296) follows

$$\frac{G^E}{RT} = a_{0,12}x_1x_2 + a_{0,23}x_2x_3 + a_{0,31}x_3x_1 + a_{0,123}x_1x_2x_3 \quad (2.297)$$

In case that the sum of $a_{0,12}, a_{0,23}, a_{0,31}$ and $a_{0,123}$ gives zero, then $G^E = 0$ and $\ln \gamma_i = 0$ or $\gamma_i = 1$.

Thus, the solution is ideal. Otherwise, if $G^E \neq 0$ or $\gamma_i \neq 1$, the solution is real. In the special case eq. (2.297) based on eqs. (2.54) and (2.55), there are no excess volumes and excess enthalpies due to mixing ($V^E = 0, H^E = 0$).

To illustrate excess Gibbs energies G^E at a fixed temperature T and a fixed pressure P , arbitrary chosen values of the four specific parameters (Par) are given in Table 2.3

Table 2.3 Assumed fictitious values of parameters Par at fixed T and P using eq. (2.295).

$A_{12} = a_{0,12}$	$A_{23} = a_{0,23}$	$A_{31} = a_{0,31}$	$A_{123} = a_{0,123}$
3	1.5	1	1

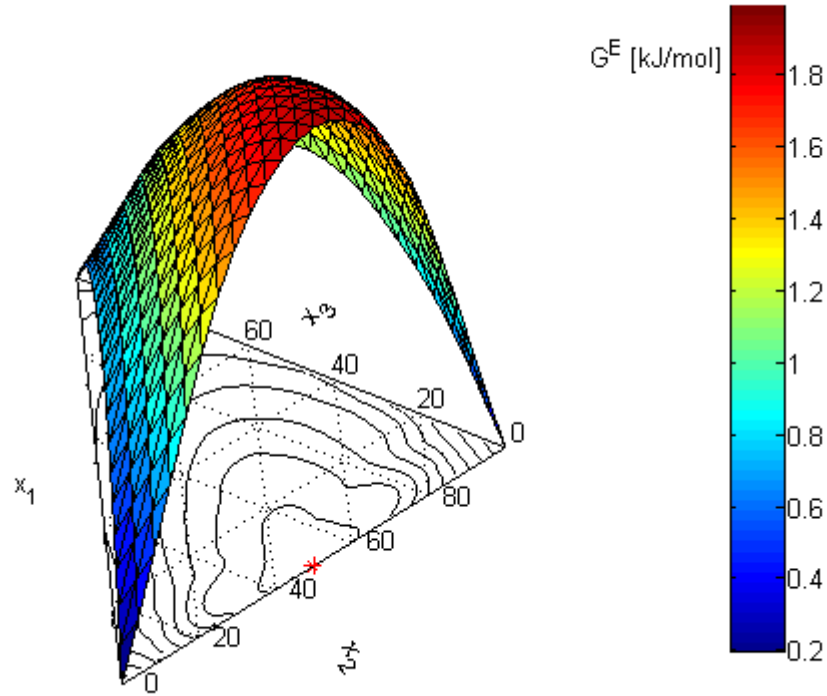


Figure 2.4 Graphical representation of the surface of molar excess Gibbs energies G^E [kJ/mol] for the ternary system (1, 2, 3) based on eq. (2.294) using the parameters given in Table 2.3.

Figure 2.4 illustrates the predicted composition dependence of G^E for the ternary system. For the parameters assumed in Table 2.3, the course of G^E is highly unsymmetrical and shows always positive values over the whole composition range. The maximum occurs on the component 1-2 side at a composition $x_1 = x_2 = 0.5$ and $x_3 = 0$.

The corresponding specific activity coefficients γ_i or the $\ln\gamma_i$ can be calculated by eq. (2.52). In eq. (2.52) the values of $\ln\gamma_i$ are related to the partial Gibbs energies G_i^E . Applying eq. (2.69) at constant temperature and pressure gives

$$\frac{G_i^E}{RT} = \frac{G^E}{RT} + \left[\frac{\partial \left(\frac{G^E}{RT} \right)}{\partial x_i} \right]_{x_j, x_k} - \left[x_i \left[\frac{\partial \left(\frac{G^E}{RT} \right)}{\partial x_i} \right]_{x_j, x_k} + x_j \left[\frac{\partial \left(\frac{G^E}{RT} \right)}{\partial x_j} \right]_{x_i, x_k} + x_k \left[\frac{\partial \left(\frac{G^E}{RT} \right)}{\partial x_k} \right]_{x_i, x_j} \right] \quad (2.298)$$

where $i, j, k = 1, 2, 3$

The expressions for the three partial derivatives for the case described by eq. (2.294) are:

$$\left[\frac{\partial(G^E / RT)}{\partial x_i} \right]_{x_j, x_k} = A_{ij}x_j + A_{ik}x_k + A_{123}x_jx_k \quad (2.299)$$

From these equations we find

$$\sum_{k=1}^3 x_k \left[\frac{\partial(G^E / RT)}{\partial x_k} \right]_{x_j \neq k} = 2[A_{12}x_1x_2 + A_{23}x_2x_3 + A_{31}x_3x_1 + A_{123}x_1x_2x_3] + A_{123}x_1x_2x_3 \quad (2.300)$$

or

$$\sum_{k=1}^3 x_k \left[\frac{\partial(G^E / RT)}{\partial x_k} \right]_{x_j \neq k} = 2(G^E / RT) + A_{123}x_1x_2x_3 \quad (2.301)$$

Inserting the derivatives we have

$$\frac{G_i^E}{RT} = A_{ij}x_j + A_{ik}x_k + A_{123}x_jx_k(1-x_i) - \frac{G^E}{RT} \quad (2.302)$$

Combining eq. (2.302) and (2.52) one obtains

$$\ln \gamma_i = A_{ij}x_j + A_{ik}x_k + A_{123}x_jx_k(1-x_i) - \frac{G^E}{RT} \quad (2.303)$$

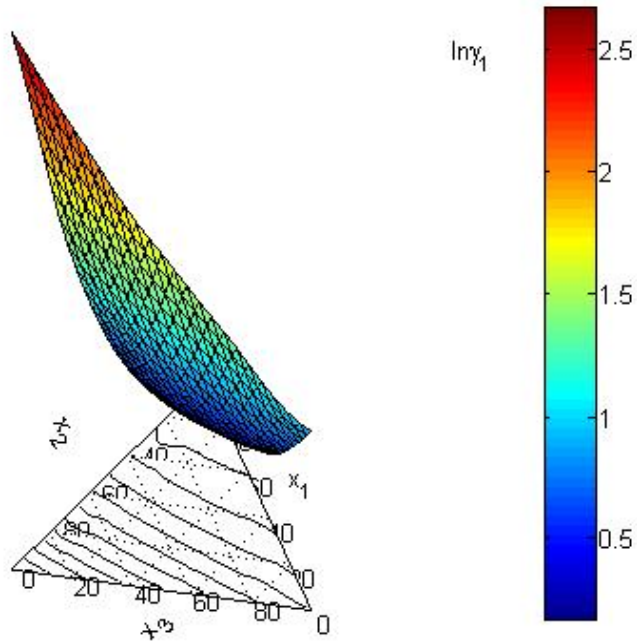


Figure 2.5 Graphical representation of the surfaces of $\ln \gamma_i$ values for the ternary system 1, 2, 3 as a function of composition based on eq. (2.303) using parameters in Table 2.3.

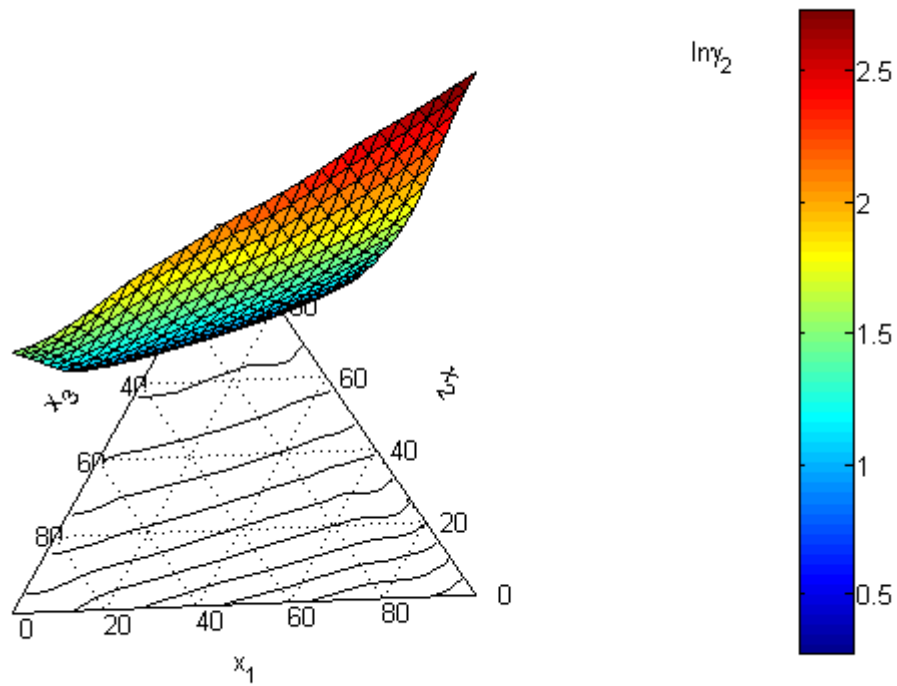


Figure 2.6 Graphical representation of the surfaces of $\ln \gamma_2$ values for the ternary system 1, 2, 3 as a function of composition based on eq. (2.303) using parameters in Table 2.3.

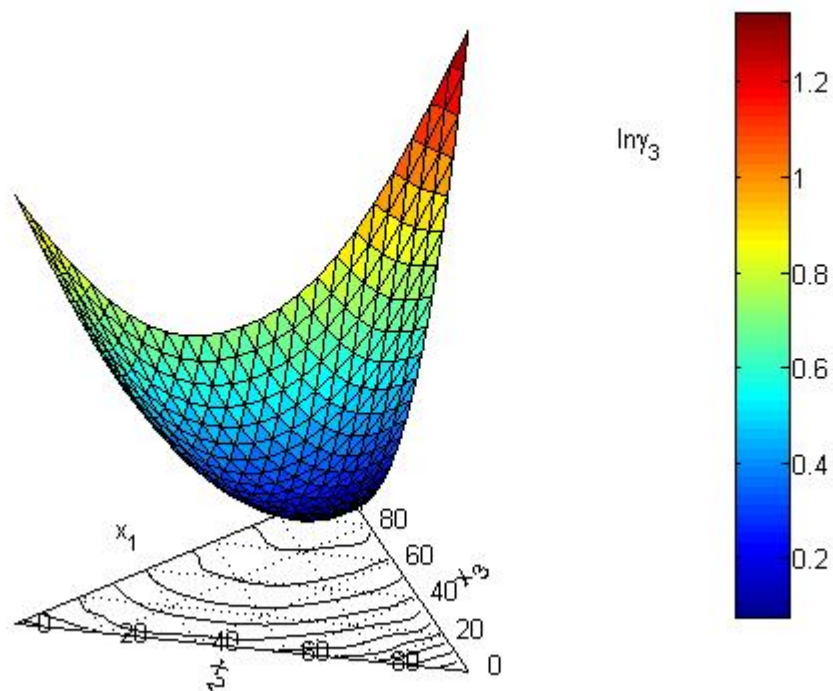


Figure 2.7 Graphical representation of the surfaces of $\ln \gamma_3$ values for the ternary system 1, 2, 3 as a function of composition based on eq. (2.303) using parameters in Table 2.3.

The calculated values of $\ln\gamma_i$ for the three components are illustrated in Figure 2.5, 2.6 and 2.7. Qualitatively, we see that at every composition the values of $\ln\gamma_i$ are from 0 to 2.6. When $x_i \rightarrow 1$ (and $x_j, x_k \rightarrow 0$) and component i becomes infinitely unity, the slope of the $\ln\gamma_i$ curve surface is zero or each $\ln\gamma_i$ curve surface becomes horizontal at $x_i = 1$. At the other limit, where $x_i \rightarrow 0$ and component i becomes infinitely dilute, $\ln\gamma_i$.

After looking at G^E and $\ln\gamma_i$ at a fixed temperature and pressure we evaluate the corresponding magnitude of V^E and H^E . Applying eqs. (2.54) and (2.55) yields

$$\frac{V^E}{RT} = \frac{\partial A_{12}}{\partial P} x_1 x_2 + \frac{\partial A_{23}}{\partial P} x_2 x_3 + \frac{\partial A_{13}}{\partial P} x_1 x_3 + \frac{\partial A_{123}}{\partial P} x_1 x_2 x_3 \quad (2.304)$$

and

$$-\frac{H^E}{RT^2} = \frac{\partial A_{12}}{\partial T} x_1 x_2 + \frac{\partial A_{23}}{\partial T} x_2 x_3 + \frac{\partial A_{13}}{\partial T} x_1 x_3 + \frac{\partial A_{123}}{\partial T} x_1 x_2 x_3 \quad (2.305)$$

For V_i^E, H_i^E , applying eqs. (2.57) and (2.58) and based on eq. (2.303) we have

$$\frac{V_i^E}{RT} = \frac{\partial A_{ij}}{\partial P} x_j + \frac{\partial A_{ik}}{\partial P} x_k + \frac{\partial A_{123}}{\partial P} x_j x_k (1 - x_i) - \frac{V^E}{RT} \quad (2.306)$$

and

$$-\frac{H_i^E}{RT^2} = \frac{\partial A_{ij}}{\partial T} x_j + \frac{\partial A_{ik}}{\partial T} x_k + \frac{\partial A_{123}}{\partial T} x_j x_k (1 - x_i) + \frac{H^E}{RT^2} \quad (2.307)$$

Explicitly, we need to specify the derivatives: $\frac{\partial Par}{\partial P}$ and $\frac{\partial Par}{\partial T}$. They are related to the coefficients a_1, a_2, \dots and b_1, b_2, \dots in eq. (2.295). In contrast to the simple example case discussed above, we now consider more complex behaviour characterized by $a_i \neq 0$ and $b_i \neq 0$ which leads to the follow expression for the Gibbs' parameters:

$$Par = a_0 + a_1 T + b_1 P \quad (2.308)$$

Applying eq. (2.308) yields that pressure and temperature derivatives of the Gibbs parameters are constant. We assume specific parameters again for illustration purposes. They are given in Table 2.4.

It is well know that it takes a relative large pressure change to have similar effect on the excess Gibbs energy as generated by a relative small temperature change [Smith05]. This is the reason that for low pressures the effect of pressure on the Gibbs energy (and therefore on the activity coefficient) is rather small. This also means that the values of pressure derivatives of Gibbs parameters are much smaller than the corresponding values of temperature derivatives.

Table 2.4 Assumed fictitious values of pressure and temperature derivatives of Gibbs' parameters used for simulations using eq. (2.308).

Par	$\frac{\partial Par}{\partial T} \times 10^3 [K^{-1}]$	$\frac{\partial Par}{\partial P} \times 10^9 [bar^{-1}]$
A_{12}	$a_{1,12} = 6$	$b_{1,12} = -2$
A_{23}	$a_{1,23} = 3$	$b_{1,23} = -1$
A_{31}	$a_{1,31} = 2$	$b_{1,31} = -1$
A_{123}	$a_{1,123} = 3$	$b_{1,123} = -2$

In Figures 2.8 and 2.9 a perspective view of the ternary molar excess volumes V^E and enthalpies H^E is shown. We observe that both of them are unsymmetrical and show negative values over the whole composition regions. For V^E , the extreme values occurs near the component 1-2 side with minimum at a composition $x_1 = x_2 = 0.40$ and $x_3 = 0.2$. For H^E , the extreme values occurs also near the component 1-2 side with minimum at a composition $x_1 = x_2 = 0.45$ and $x_3 = 0.1$.

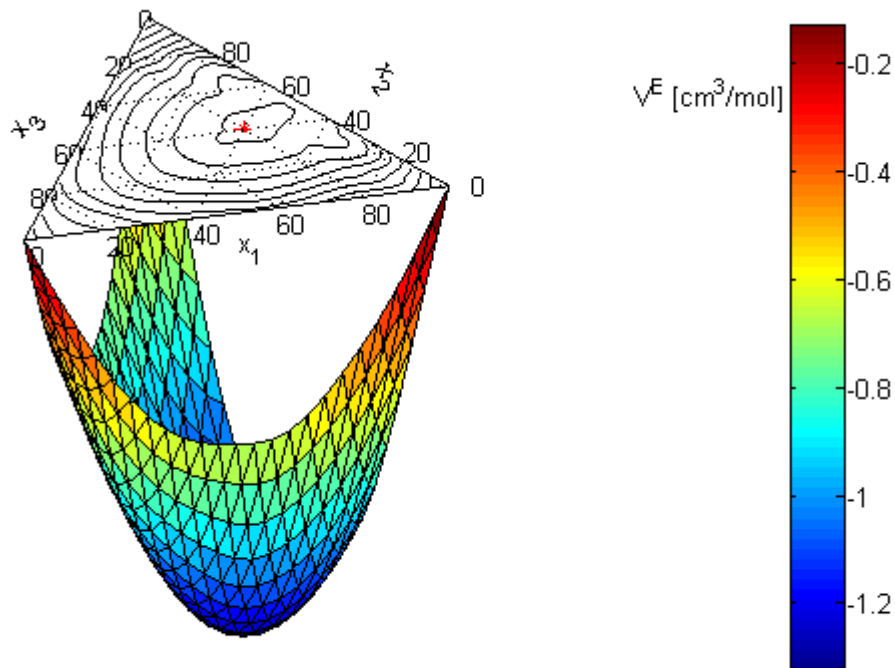


Figure 2.8 Graphical representation of the surfaces of molar excess volumes V^E [cm^3/mol] with minimum at point (*) composition for the ternary system (1, 2, 3) based on eq. (2.304) using parameters in Table 2.4.

To evaluate differences between ideal and real solutions, the values for the molar volumes of the ideal solution V^0 and the real solution V were determined and compared at a composition $x_1 = x_2 = 0.40$; $x_3 = 0.2$ (minimum point). At this composition: $V^0 = 55 \text{ cm}^3/mol$, $V = 53.74$

cm^3/mol and $\Delta V = V^E = 1,26 \text{ cm}^3/\text{mol}$. Thus, in this simulated case the molar excess volume is 2.3 percent of the ideal molar volume.

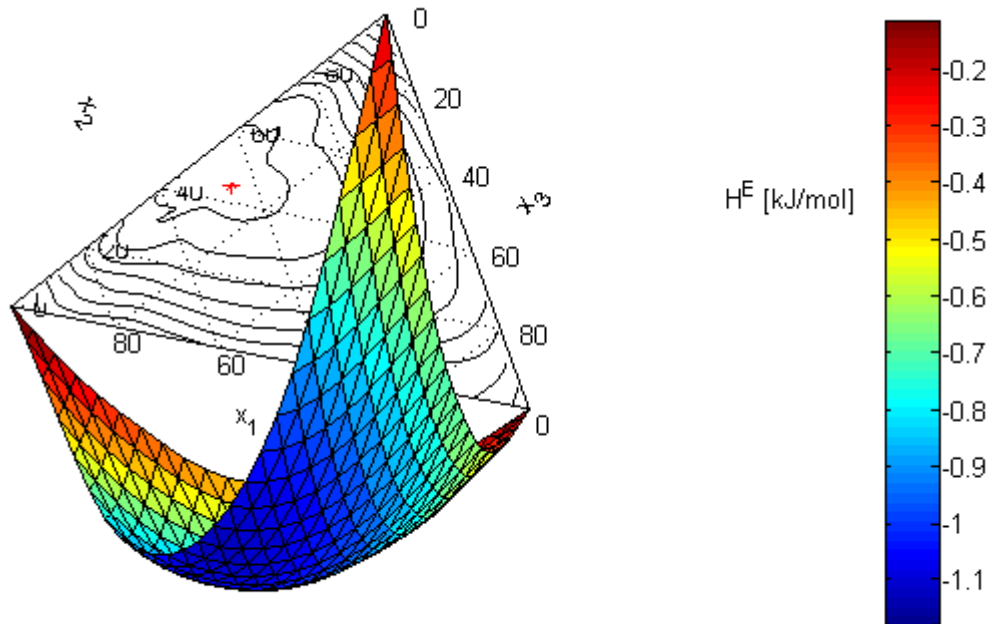


Figure 2.9 Graphical representation of the surfaces of molar excess enthalpies H^E [kJ/mol] with maximum at point (*) composition for the ternary system (1, 2, 3) based on eq. (2.305) using parameters in Table 2.4.

2.4.2 Transient reactive system

Let us turn now to a reactive system with again three components. We designate them by A (component 1), B (component 2), and C (component 2). The components undergo changes due to an irreversible homogeneous chemical reaction carried out in an ideal batch reactor



The simulations are performed based on *i*) neglecting and *ii*) incorporating volume and heat changes due to reaction or/and mixing. The reaction rate is expressed by a standard second order rate law

$$r = k(T)c_A c_B \quad (2.310)$$

Hereby k is the reaction rate constant according to eq. (2.218). The assumed kinetic parameters and the reaction enthalpy are listed in Table 2.5.

Table 2.5 Assumed kinetic parameters used for the simulation of the reaction system.

Activation energy, E_a [kJ/mol]	40
k_0 [Lmol ⁻¹ sec ⁻¹]	2000
ΔH_R [kJ/mol]	-10

Typically heat capacities of components undergo little changes during the course of reactions. Therefore average heat capacities are taken for each component. The values of heat capacities assumed are shown in Table 2.6.

Table 2.6 Assume fictional values of heat capacity of components.

Component	Cp [Jmol ⁻¹ K ⁻¹]
A	190
B	75
C	125

The initial conditions considered are displayed in Table 2.7. Thus, initial there is no product C in the reactor and component A is present in a slightly larger amount than component B.

Table 2.7 Initial conditions of reaction studied theoretically.

Reaction temperature [K]	298
n_A^{init} [mol]	10
n_B^{init} [mol]	9
n_C^{init} [mol]	0
$V_R^{id,init}$ [L]	1.071
$\dot{\mathcal{Q}}_{wall}$ [Jsec ⁻¹]	0
T^{init} [K]	298

The reactor model given in section 2.3 is used, i.e. the ODE system eq. (2.272) is rewritten as

$$\frac{dn_i}{dt} = v_i r V_R \quad i = A, B, C \quad (2.311)$$

$$\frac{dV_R}{dt} = r V_R \sum_{i=1}^3 v_i V_i^0 + r V_R \sum_{i=1}^3 v_i V_i^E \quad (2.312)$$

$$\frac{dT}{dt} = \frac{-V_R r \Delta H_R^0 - V_R r \sum_{i=1}^3 v_i H_i^E + \dot{\mathcal{Q}}_{wall}}{\sum_{i=1}^3 n_i C_{P,i}} \quad (2.313)$$

The V_i^E and H_i^E are calculated through V^E and H^E by eqs. (2.306) and (2.307) respectively using the parameters given in Table 2.4.

2.4.2.1 Isothermal varying volume and constant volume BR

In an isothermal system eq. (2.313) reduces to

$$\frac{dT}{dt} = 0 \quad (2.314)$$

At given temperature and pressure, when the reactants A and B are mixed together, there is an molar excess volume V^E of the mixture A and B. While the reaction occurs with time amounts of reactants A and B are consumed and the product C is formed and mixed following reaction time. Therefore the values of V^E change during the reaction and reach a constant volume at the end of the reaction.

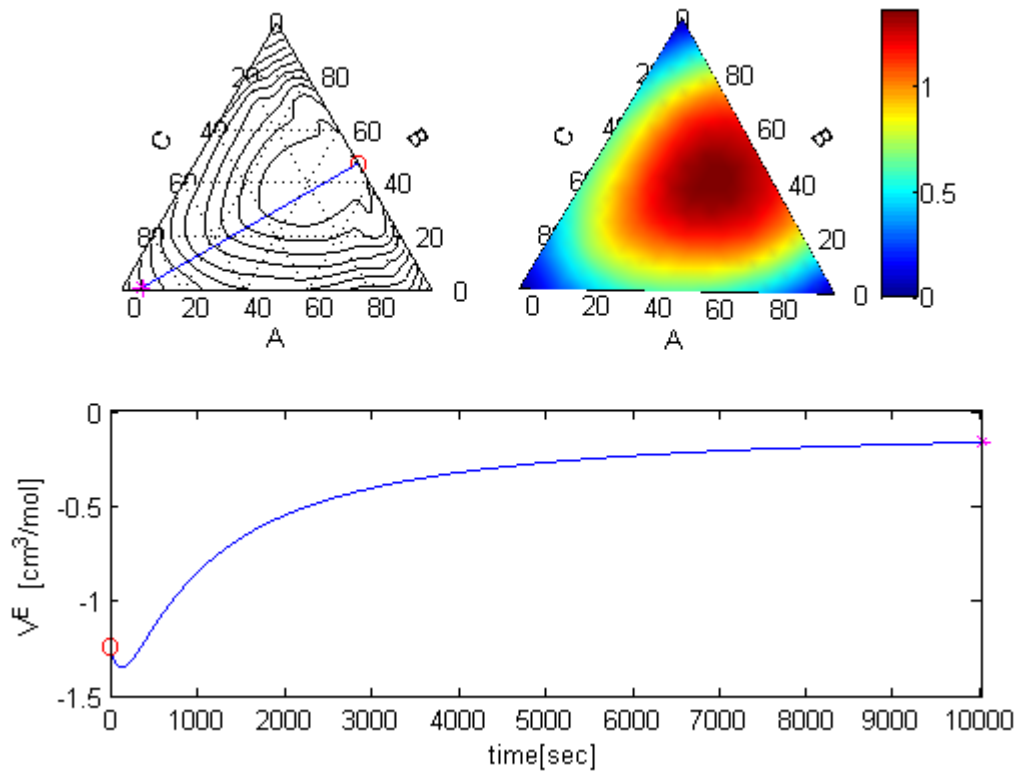


Figure 2.10 Illustration of development of molar excess volume V^E due to mixing with starting point (o) and end point (*).

Figure 2.10 shows that the value of V^E drops immediately at starting point when A and B are mixed. Then it increases slightly when C is formed by the reaction leading to a maximum absolute V^E . After that, the value decreases and comes close to zero at the end of the reaction. At point(*), V^E is approximately zero like for an ideal solution or a pure component. This is understandable, because at the end product C is dominant and exists almost alone.

The change of the reaction volume was studied based on considering 1) just due to the reaction effect 2) just the mixing effect and 3) both reaction and mixing effects. For the first two cases eq. (2.312) becomes eq. (2.315) and (2.316).

Case 1:

$$\frac{dV_R}{dt} = rV_R \sum_{i=1}^3 \nu_i V_i^0 \quad (2.315)$$

Case 2:
$$\frac{dV_R}{dt} = rV_R \sum_{i=1}^3 \nu_i V_i^E \quad (2.316)$$

The results are illustrated in Figures 2.11 and 2.12.

In Figure 2.11, the volume change just due to the reaction (1) is increase because the value of the molar volume of product C (V_C^0) is bigger than the average of the reactants A and B ($(V_A^0 + V_B^0)/2$) (Table 2.2). The volume change just caused by mixing (2) has a similar shape as the molar excess volume V^E of the reaction mixture discussed above (Figure 2.10). The volume change due to both mixing and reaction (3) drops at starting point when A and B are mixed together, then increases and comes near the one just due to reaction (2) at the end of the reaction. It is noteworthy, that the “Real” case deviates remarkably from the “Constant” case. The volume change due to both mixing and reaction is most realistic.

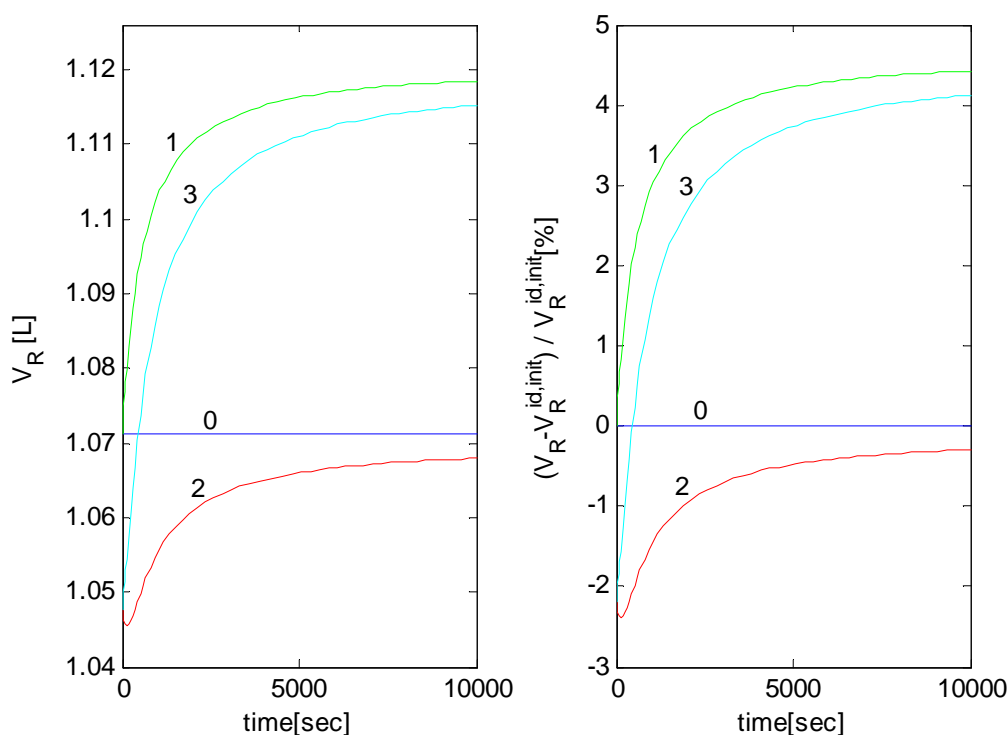


Figure 2.11 Comparison between reaction volume due to differential changing volume cause and ideal constant volume with kinetic parameters given in Table 2.5: 0 – no volume change, 1- volume change just due to reaction, 2 – volume change just caused by mixing, 3 – volume change due to both mixing and reaction.

Figure 2.12 shows that the corresponding concentrations of the reactant A and the product C over the time of reaction. The values for the concentrations based on assuming a constant reaction volume curve (0) is different from the cases assuming effects just due to mixing curve (2) during reaction but they come close at the end of reaction. The values for the concentrations belonging to the case of both mixing and reaction curve (3) are different from the concentrations of the cases assuming effects just due to reaction curve (1) but they come near

at the end of reaction. The reason is that molar excess volumes of the reaction mixture are considerable during reaction and negligible at the end of reaction (Figure 2.10). The concentrations based on considering both mixing and reaction (3) are seen as most reliable.

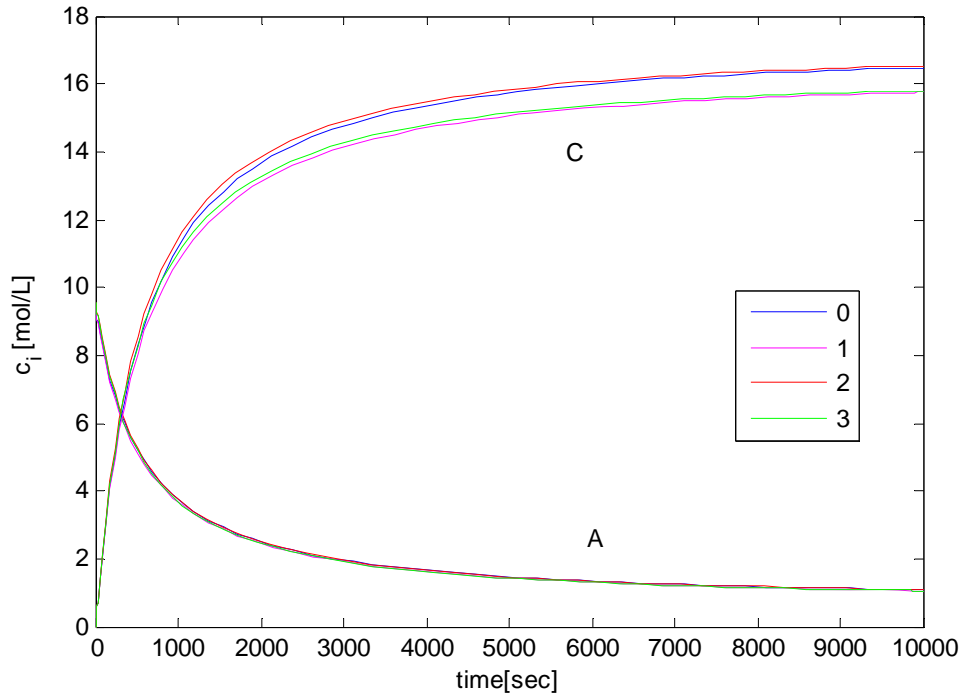


Figure 2.12 Schematic course of concentrations of reactant A and product C versus reaction time: $A + B \rightarrow 2C$, for kinetic parameters given in Table 2.5: 0 - Concentration change due to reaction in constant volume, 1- Concentrations for volume change just due to reaction, 2 – concentrations change just caused by mixing, 3 – concentrations volume change due to both mixing and reaction.

2.4.2.2 Adiabatic and isothermal BR

In this part, the kinetics under adiabatic and isothermal conditions is studied based on mass and energy balance. The mass balance in “Real” case is used to combine with different thermal effect (isothermal, reaction, mixing and reaction & mixing).

An analysis of an adiabatic batch reactor (no heat exchange over the wall of the reactor, i.e. no heating, cooling losses) leads to $\dot{\mathcal{K}}_{wall} = 0$. Then eq. (2.313) becomes

$$\frac{dT}{dt} = \frac{-V_R r \Delta H_R^0 - V_R r \sum_{i=1}^3 v_i H_i^E}{\sum_i n_i C_{P,i}} \quad (2.317)$$

At a given temperature and pressure, when the components A and B are mixed together, there is an initial conditions of the reaction (Table 2.7) that allow to calculate a binary molar excess enthalpy H^E of the mixture A and B at starting point. Then the reaction starts and forms the

component C changing the composition of the mixture over time. Therefore, also the values of H^E change during the course of the reaction. They reach a constant value at the end of the reaction after more than 5000 seconds.

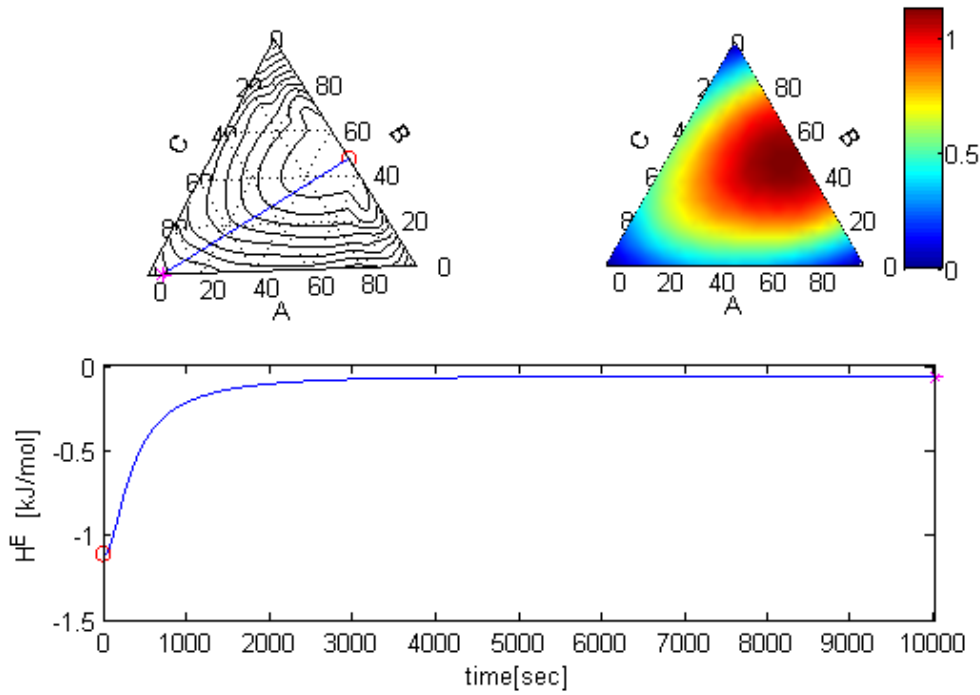


Figure 2.13 Illustration of the temporal development of the molar excess enthalpy H^E of the reaction mixture due to just mixing, starting point at $t = 0s$ (o) and end point at $t = 10000s$ (*).

Figure 2.13 shows that the values of H^E drop immediately at starting point when A and B are mixed and then it decreases because C is formed by the reaction leading the composition changes of the ternary mixture. At the end point (*), H^E is approximately zero like for ideal solutions or pure components. This is because at the end point (*) product C is dominant others (A and B is very dilute). H^E would be reach exactly zero, if both components A and B would be consumed completely to form just product C.

The enthalpy change was then investigated for the adiabatic case based on 1) just considering the effect of reaction (enthalpy of reaction) 2) just considering the effect of mixing (enthalpy of mixing) and 3) both effects of reaction and mixing enthalpies. For the first two cases, the energy balance eq. (2.317) becomes eq. (2.318) or (2.319).

$$\frac{dT}{dt} = \frac{-V_R r \Delta H_R^0}{\sum_{i=1}^3 n_i C_{P,i}} \quad (2.318)$$

$$\frac{dT}{dt} = \frac{-V_R r \sum_{i=1}^3 v_i H_i^E}{\sum_{i=1}^3 n_i C_{P,i}} \quad (2.319)$$

Combining the mass balance, eq. (2.311), the equation for the varying volume, eq. (2.312), and the energy balance of the three cases, provides results illustrated in Figures 2.14, 2.15 and 2.16.

In Figure 2.14, first the normalized temperature change due to just reaction (1) is shown. This relative temperature increases because the reaction is exothermic ($\Delta H_R < 0$) from zero (initial reaction temperature T^{init}) and reaches a constant value at the end of the reaction. The temperature change caused only by enthalpy mixing (2) rises immediately at the beginning point because of exothermic mixing of two components A and B. If no reaction contributes the temperature decreases since the molar excess enthalpy decreases and reach approximately zero at the end of reaction. Obviously, even if the reaction enthalpy is negligible ($\Delta H_R^0 = 0$), the temperature of the mixture can change caused by mixing. The predicted temperature change caused by both mixing and reaction effects (3) is the most realistic scenario. In this case the initial temperature increase due to mixing the reactant A and B is followed by a further relative rapid increase due to the exothermic reaction, slowed down due to mixing with the formed product C. The final volumes of case (1) and (3) come close, differing just by the small remaining molar excess enthalpies in case (3).

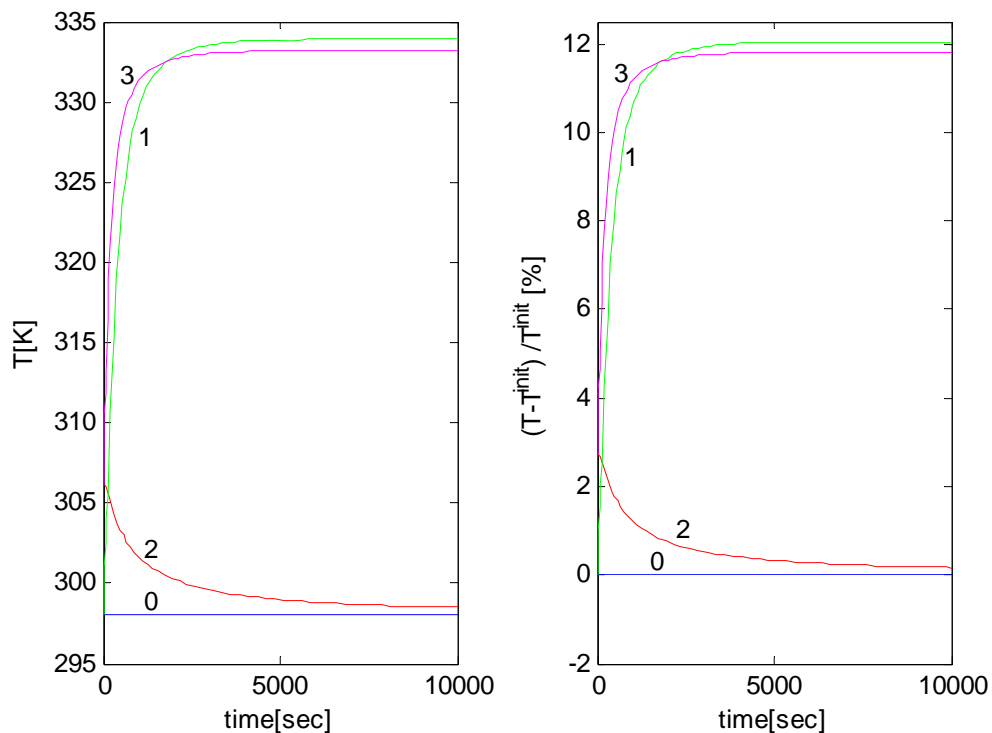


Figure 2.14 Comparison between courses of normalized reactor temperatures due to different thermal effects for the considered case study on the kinetic parameter values given in Table 2.5. 0 – temperature for the isothermal case, 1- temperature change due to just reaction, 2 – temperature change caused by the mixing enthalpy, 3 – temperature change due to both enthalpy mixing and reaction.

In Figure 2.15 the corresponding courses of the reaction volumes are shown. There are similar significant final normalized volume changes of approximately 4 percent predicted for all case considered. The most rapid approach to this final state is reached for the two cases (1) and (3), which correspond to the two highest temperatures shown in Figure 2.14. These higher temperatures increase the reaction rates causing their acceleration. This explains also why the approach to the final value is slowest for the isothermal case (0).

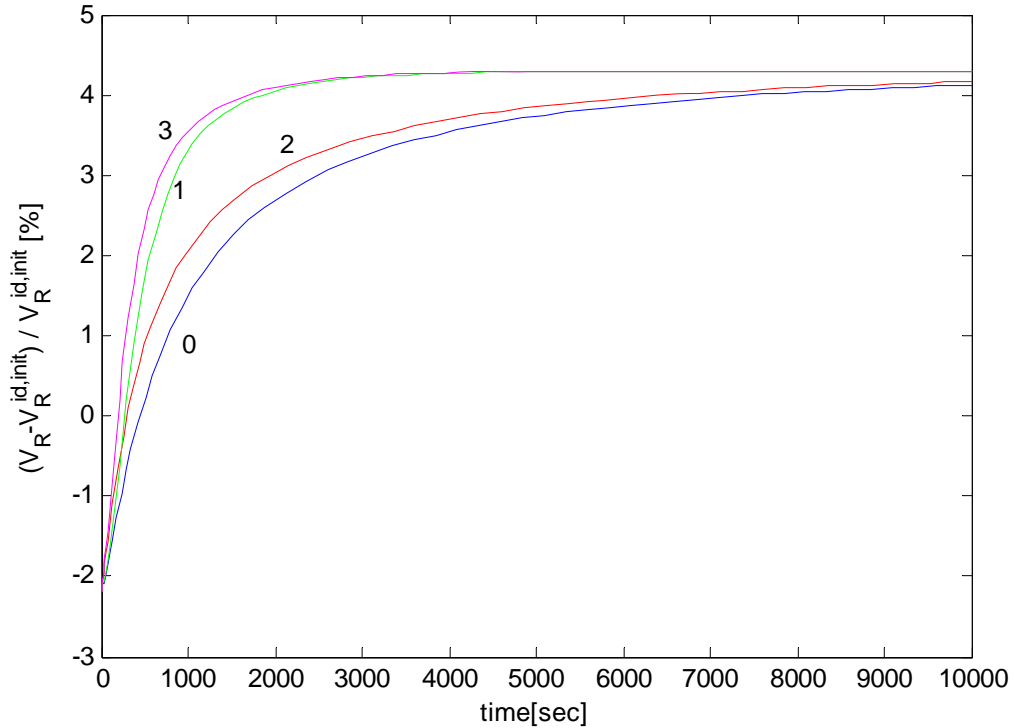


Figure 2.15 Comparison between courses of the normalized reaction volumes due to different effects for the considered case study with kinetic parameter values given in Table 2.5: 0 - volume change for isothermal case, 1 - volume change considering just the thermal effect of reaction, 2 - volume change caused by enthalpy mixing, 3 - volume change due to both enthalpy mixing and enthalpy reaction.

In Figure 2.16, the corresponding temporal concentration profiles of reactant A and product C are shown. Rather large differences in the concentration profiles can be noticed indicating the relevance of the problem studied in this thesis. The same relative trends as for the reaction volumes can be indentified. The fastest approaches to the final states of completed reaction are reached for the two cases taking the thermal effects of the reaction into account (1) and (3).

The results of the parametric study summarized in Figure 2.14, 2.15 and 2.16 clearly emphasize the importance of taking real phase effect into account in studying liquid phase reactions seriously. Careful integration of volume and enthalpy changes due to both mixing and reaction into reactor model gives an improved understanding of the underlying processes. The goal of this work is to evaluate kinetic parameters of two specific reactions from experimental data taking into account volume and thermal effects of mixing. The correct

incorporation of reaction and mixing should deliver better kinetic parameters than ideal (neglecting mixing) and constant volume considerations.

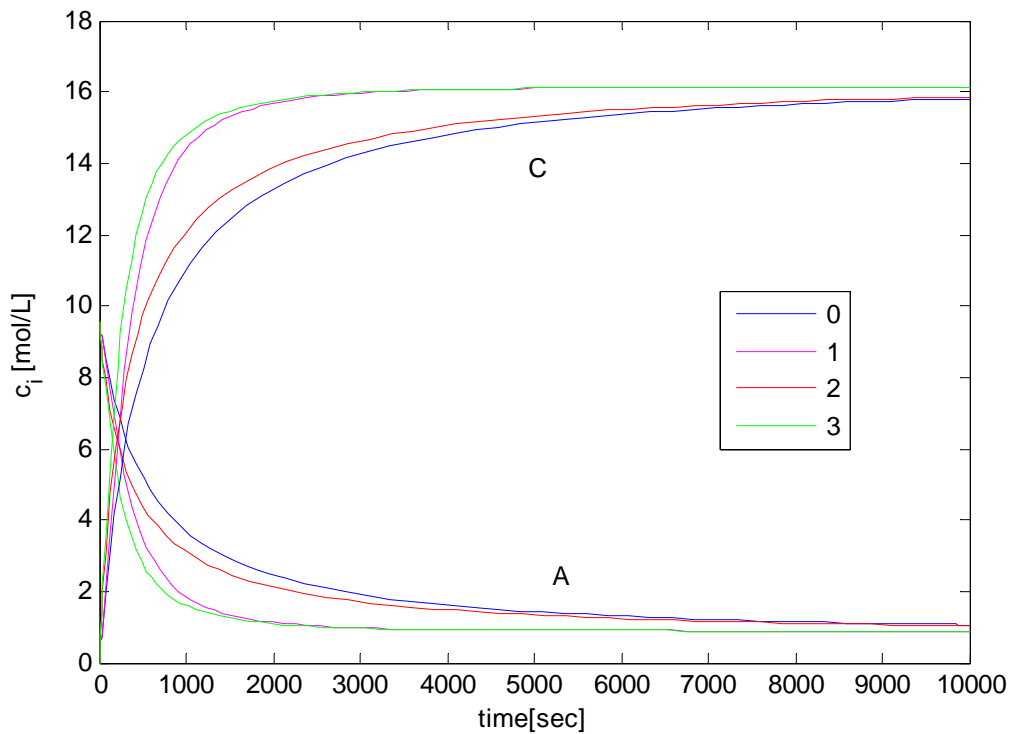


Figure 2.16 Temporal courses of concentrations versus reaction time for reactant A and product C. Concentration for different thermal effects for the considered case study with kinetic parameter values given in Table 2.5. 0 – concentration changes for isothermal conditions, 1 – concentration changes considering just the thermal effect of reaction, 2 – concentration changes considering just the thermal effect of mixing, 3 – concentration changes considering both thermal effects of mixing and reaction.

CHAPTER 3

MODEL REACTIONS

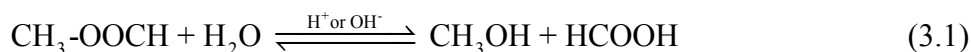
This chapter introduces the investigated two model reactions and the physical and thermodynamic properties of all components involved.

3.1 MODEL REACTIONS

In this work the hydrolysis reactions of two esters, methyl formate and ethyl formate, into alcohols and carboxylic acids are selected as the model reactions. Regarding these simple reactions, there are several reports in the literature e.g. [Weth74], [Falk02] and [Jogun10].

In general, the rates of hydrolysis reaction of esters with pure water are so slow, that they are not performed in the chemical process industry.

Below are given the two reversible hydrolysis reactions with their stoichiometric equations



These reactions can be catalysed by acids (H^+) or base (OH^-). All components in these reactions are abbreviated for the sake of brevity as shown in Table 3.1.

Table 3.1 List of compound abbreviations used.

Compounds	Specific Abbreviations	Overall Abbreviations
Methyl formate	MF	Es
Ethyl formate	EF	
Methanol	M	Al
Ethanol	E	
Formic acid	F	Ac
Water	W	-

3.2 PHYSICAL AND THERMODYNAMIC PROPERTIES

Relevant data for the components can be found in special handbooks (eg., [CRC05], [Perry99], [Barin93], and [Yaws99]).

3.2.1 Physical properties

Selected data related to the physical properties of all components in the reactions are shown in Table 3.2. Values of molar mass M_i , density ρ_i and solubility in water c_{sol,H_2O} were collected from literatures.

Table 3.2 Selected physical properties of the components [Jose06], [Jiri72] and [Perry99].

Compound	M_i [g/mol]	ρ_i^{298K} [g/mL]	V_i^0 [mL/mol]	c_{sol,H_2O} (293K)	
				[g/L]	[mol/L]
MF	60.053	0.9668	62,12	300	5.00
EF	74.079	0.9158	80,89	105	1.42
M	32.042	0.7866	40,74	<i>soluble</i>	<i>soluble</i>
E	46.069	0.7850	58,69	<i>soluble</i>	<i>soluble</i>
F	46.026	1.2138	37,99	<i>soluble</i>	<i>soluble</i>
W	18.015	0.9970	18,07	-	-

Infrared spectroscopy

Molecular vibrations and rotations give rise to absorption bands throughout most of the infrared region of the electromagnetic spectrum. Detection of absorption in the infrared spectrum is one of two possible ways to measure such molecular vibrations and rotations. Characteristic absorption peaks of all compounds are summarized in Table 3.3

Table 3.3 Absorption peaks of the components [Klau88].

Compound	Absorption peak [cm^{-1}]
MF	2958, 1729, 1434, 1381, 1215, 1162, 1030, 911, 769
EF	2988, 1726, 1389, 1192, 1156, 1011, 841
M	3329, 2942, 2832, 2522, 2045, 1449, 1115, 1033,663
E	3342, 2974, 2928, 2884, 1456, 1381, 1091, 1050, 881
F	3114, 2951, 1722, 1393, 1339, 1180, 1062, 817, 607
W	3350, 1640

3.2.2 Thermodynamic properties

In engineering design of chemical processes, thermodynamic properties such as heat capacities, $C_{P,i}$, standard enthalpies of formation $\Delta H_{f,i}^*$, and standard Gibbs energies of formation $\Delta G_{f,i}^*$ are very important. These properties are shown in Tables 3.4, 3.5 and 3.6 for reactants and products present in the systems.

Table 3.4 The heat capacity of the investigated liquid compounds at 298K from [Yaws99, Perr99 and Bari93].

Compound	$C_{P,i}$ [J/molK]		
	[Yaws99]	[Perr99]	[Bari93]
MF	122.71	146.6328	-
EF	167.4	119.6448	-
M	83.23	81.1447	81.588
E	304.52	112.2845	111.420
F	100.21	99.3789	90.161
W	76.392	75.3866	75.288

As shown in eq. (2.192) presented in chapter 2, to determine the heat of reaction, ΔH_R^* and associated heating or cooling requirements, the enthalpy of formation for individual components in chemical reaction are required. If $\Delta H_R^* < 0$, then the chemical reaction is exothermical, and it is required to withdraw heat from reaction to limit the reaction temperature. On the other hand, if $\Delta H_R^* > 0$ then the chemical reaction is endothermical and heating is needed to maintain the chemical reaction. The values for enthalpies of formation are presented in Table 3.5

Table 3.5 Standard enthalpies of formation of the investigated components from [CRC06], [Perr99], [Stull69], [Yaws99] and [Bari93].

Comp.	$\Delta H_{f,i}^*, T = 298K$ [kJ/mol]							
	Liquid				Gas			
	[CRC06]	[Stull69]	[Hine74]	[Bari93]	[CRC06]	[Stull69]	[Perr99]	[Yaws99]
MF	-386.1	-376.73	-391.0	-	-357.4	-349.78	-352.40	-349.70
EF	-	-399.32	-430.5	-	-	-371.29	-388.30	-388.30
M	-239.2	-238.57	-	-238.572	-201.0	-201.17	-200.94	-201.17
E	-277.6	-276.98	-	-276.981	-234.8	-234.81	-234.95	-235.00
F	-425.0	-425.04	-	-424.760	-378.7	-378.61	-378.60	-378.60
W	-285.8	-	-	-285.830	-241.8	-241.84	-241.81	-241.83

One of the most important values in the analysis of chemical reactions is Gibbs energy of formation. From these values, the change in Gibbs energy ΔG_R^* for the reactions can be calculated. This change is very significant because it determine the chemical equilibrium for the chemical reaction. If the change in Gibbs energy is negative, the thermodynamics for reaction are favourable and the reaction will proceed. Nevertheless, if the change in Gibbs is high positive, the thermodynamics for the reaction are not favourable. The values for Gibbs energy of the components investigated are shown in Table 3.6.

Table 3.6 The standard free Gibbs energies of formation of the investigated components [CRC04, Perr84, Perr99 and Stull89].

Comp.	$\Delta G_{f,i}^*, T = 298K$ [kJ/mol]					
	Liquid			Gas		
	[CRC06]	[Perr84]	[Bari93]	[CRC06]	[Perr99]	[Stull69]
MF	-297.44 ^a	-	-	-	-295.00	-297.19
EF	-305.9	-	-	-	-303.10	-
M	-166.6	-166.52	-166.152	-162.3	-162.32	-162.51
E	-174.8	-174.72	-173.991	-167.9	-167.85	-168.28
F	-361.4	-346.02	-361.368	-	-351.00	-351.00
W	-237.1	-237.19	-237.141	-228.6	-228.59	-228.61

^acalculated as described in Appendix A

The result of Gibbs energies and enthalpies of hydrolysis reactions are estimated by eq. (2.184) and (2.192) using values shown in Tables 3.5 and 3.6

Table 3.7 Standard reaction enthalpies and Gibbs energies of hydrolysis reactions in the liquid phase from various data in Tables 3.5 and 3.6.

Reactant	$\Delta H_R^*, T = 298K$ [kJ/mol]		$\Delta G_R^*, T = 298K$ [kJ/mol]	
	[CRC06, Hin74]	[Ola10]	[Perr99, CRC06]	[Ola10]
MF	+7.7	+ 5.44	+6.54	+6.74
EF	+13.7	+7.91	+6.8	+9.25

UNIQUAC and UNIFAC parameters

In this work, non-ideal behaviour of solutions is considered. That means, the activities a_i are used instead of concentrations c_i and the reaction kinetics are expressed in term of activity. The activity coefficients are calculated from values of pure components, component-component interaction parameters [Gmeh02], group contribution parameter, group-group interaction

parameter [Robe87] by using the UNIFAC model. All data used in this thesis are listed in Tables 3.8 and 3.9.

Table 3.8. UNIFAC parameters [Robe87] for Methyl formate and Ethyl formate hydrolysis.

Molecules	Group identification			R _i	Q _i
	Name	Main No.	Sec. No		
HCOOCH ₃	CH ₃	1	1	0.9011	0.848
	HCOO	12	24	1.2420	1.188
HCOOC ₂ H ₅	HCOO	12	24	1.2420	1.188
	CH ₃	1	1	0.9011	0.848
	CH ₂	1	2	0.6744	0.540
H ₂ O	H ₂ O	7	17	0.9200	1.400
CH ₃ OH	CH ₃ OH	6	16	1.4311	1.432
C ₂ H ₅ OH	CH ₃	1	1	0.9011	0.848
	CH ₂	1	2	0.6744	0.540
	OH	5	15	1.0000	1.200
HCOOH	HCOOH	20	44	1.5280	1.532

Table 3.9 UNIFAC group-group interaction Parameters from Kelvins [Robe87] related to Table 3.8.

Main group numbers	1	5	6	7	12	20
1	0	986.500	697.200	1318.000	741.400	663.500
5	156.400	0	-137.100	353.500	193.100	199.000
6	16.510	249.100	0	-181.000	193.400	-289.500
7	300.000	-229.100	289.600	0	0	-14.090
12	90.490	191.200	155.700	0	0	-356.300
20	315.300	-151.000	1020.000	-66.170	312.500	0

These data are used in UNIFAC eq. (2.124) to calculate activity coefficients γ_i . Unfortunately

there is no information regarding $\frac{\partial \gamma_i}{\partial T}$ and $\frac{\partial \gamma_i}{\partial P}$ to get directly H^E and V^E in literatures.

3.3 CHEMICAL EQUILIBRIA

3.3.1 Chemical reaction equilibrium

As introduced above, if the standard Gibbs energies of reaction are given, the chemical reaction equilibrium constants at 298K can be determined using eq. (2.185). Applying this method using the values of standard Gibbs energies of reaction given in Table 3.7, the values of thermodynamic equilibrium constants of reactions in the liquid phase, K_a , at 298K can be determined. To get a rough result regarding the reaction equilibrium at different temperatures, eq. (2.198) is used.

All the results of the chemical reaction equilibrium constants at different temperatures are shown in the following table

Table 3.10: Reaction equilibrium constants K_a of reversible hydrolysis of esters (MF and EF) in the liquid phase at differential temperatures.

Reactant	15°C	20°C	25°C	30°C
MF	0.063	0.067	0.071	0.074
EF	0.053	0.058	0.064	0.070

Another way to determine the chemical reaction equilibrium constants is based on experiments [Weth75], [Falk99]. Hereby typically equilibrium concentrations c_i^{eq} are measured and corresponding equilibrium constant K_c are determined. Applying eq. (2.222) and eq. (2.225) given in Chapter 2, the chemical reaction equilibrium constants for hydrolysis of esters in the liquid phase in ideal and non-ideal liquid system are expressed as,

$$K_c = \frac{c_{Al}^{eq} c_{Ac}^{eq}}{c_{Es}^{eq} c_W^{eq}} \quad (3.3)$$

and

$$K_a = \frac{a_{Al}^{eq} a_{Ac}^{eq}}{a_{Es}^{eq} a_W^{eq}} \quad (3.4)$$

A modified form of equilibrium constant was used in the literature [Weth75] when the concentration of the ester (methyl formate) is small and the concentration of water is in excess. Following the evolution of the reaction the concentration of water will be almost constant and near the one of pure water (55.4mol/L). Then it can be defined

$$K_c^{mod} = \frac{c_{Al}^{eq} c_{Ac}^{eq}}{c_{Es}^{eq}} = K_c c_w^{eq} \quad (3.5)$$

The chemical equilibrium of the methyl formate hydrolysis for different concentrations of acid catalyst (HCl) used as a typical catalyst in a temperature range of 22 to 24°C was

experimentally investigated [Weth75]. The values of equilibrium constants were determined by using the modified form given above. In Table 3.11, the results reported were converted to K_c for comparison.

Table 3.11: Equilibrium constants K_c^{mod} and K_c of hydrolysis of methyl formate [Weth75].

c_{HCl} [mol/L]	K_c^{mod} [eq. (3.5)] [mol/L]	K_c [eq. (3.3)] [-]
0.054	9.29	0.167
0.54	8.36	0.151
1.06	6.75	0.122

Falk et al. [Falk99] also estimated the chemical reaction equilibrium constant of the hydrolysis of methyl formate at 295K from the equilibrium compositions in several experiments. A value of $K_c = 0.12$ was obtained in relative good agreement with the value given by Wetherold et al. [Weth75] (Table 3.11).

3.3.2 Dissociation equilibrium

To explore the above model reactions further, a possible autocatalytic effect of the generated H^+ ions dissociated from acids and alcohols was considered. We can presume that the reaction rate depends on the concentrations of the H^+ ions (catalyst). The rate law expression for homogeneously catalysed hydrolysis reactions may be written as

$$r = kc_{H^+} \left(c_{Es}c_W - \frac{c_{Ac}c_{Al}}{K_c} \right) \quad (3.6)$$

In this work, relevant components can be dissociated to form H^+ ions by the following reactions



These dissolution solutions are characterized by a constant pK_{Ac}^{diss} which is defined as the negative logarithm of the corresponding equilibrium constant K_{Ac}^{diss}

$$pK_{Ac}^{\text{diss}} = -\lg K_{Ac}^{\text{diss}} \quad (3.11)$$

Table 3.12 shows the acid dissociation equilibrium constants of the hydrolysis products and water at different temperatures [CRC93] and [CRC05].

Table 3.12: The acid dissociation equilibrium constants pK_{Ac}^{diss} eq. (3.11) of the alcohols, the acid and water at different temperatures (298~328K) [CRC93], [CRC05].

Compound	pK_{Ac}^{diss} [-]			
	298K	308K	318K	328K
M	15.5	-	-	-
E	15.5	-	-	-
F	3.752	3.758	3.773	-
W	13.995	13.685	13.405	13.152

From definition eq. (3.11) and the values above can be seen that formic acid has the strongest acidity. The acidic strengths of methanol and ethanol are almost the same and weaker than the one of water.

The collected parameters of the components present in the model reactions investigated are available and useful for ideal case. In order to understand the relevance of mixing effects in real solutions on reaction kinetics, volume and heat changes due to mixing effects are quantified and incorporated into a reactor model, applied to estimate kinetic parameters from experimentally observed concentration transients.

CHAPTER 4

EXPERIMENTAL INVESTIGATIONS

The goal of this chapter is to describe the techniques applied experimentally to quantify molar excess volumes V^E and molar excess enthalpies H^E and reaction enthalpies ΔH_R^0 . The molar excess volumes are directly calculated from measured densities of mixtures using eq. (2.137). The molar excess enthalpies and reaction enthalpies are determined exploiting a differential reaction calorimeter.

In section 4.1, the experimental equipment and the measurement principles are introduced. Then, in section 4.2, the preliminary experiments carried out to get information about the kinetics of reactions are presented.

4.1 EXPERIMENTAL EQUIPMENT

4.1.1 Equipments to determine molar excess volumes

A density meter DM40 measures the density of the components ρ_i and their binary mixtures ρ_{12} by tube method with an accuracy of $\pm 0.0001 \text{ g.cm}^{-3}$. The temperature is controlled to $\pm 0.05\text{K}$. The masses are weighed on Sartorius electronic balance with an uncertainty of $\pm 0.0001\text{g}$. Figure 4.1 shows the design of the density meter DM40.

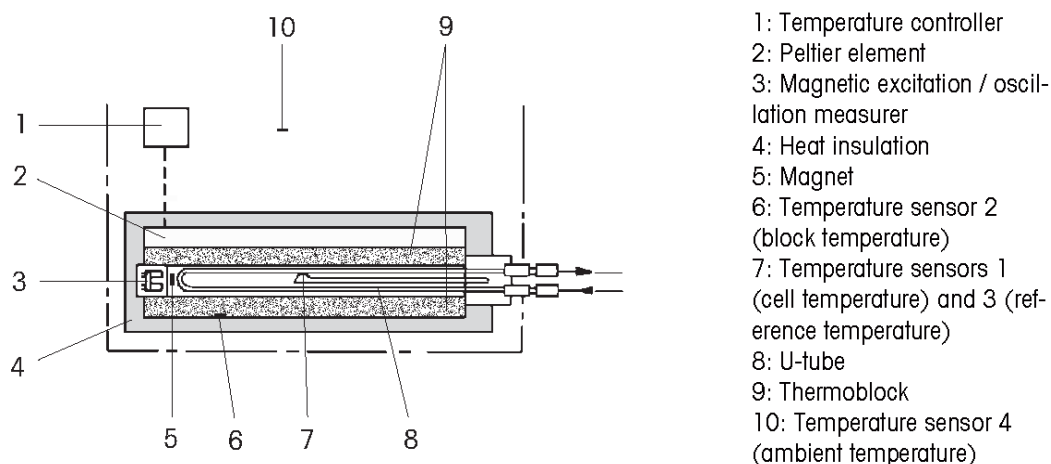


Figure 4.1 The design of the measuring cell and the temperature controller.

The principle of the density meter is based on the electromagnetically induced oscillation of U-form tube made of glass. A magnet is joined to the U-tube and a transmitter makes the oscillation and a sensor measures the period of oscillation. The period of oscillation depends on the total mass and changes when the tube is filled with a liquid. If the mass increase, the period of oscillation is bigger. The density is a function of the period of oscillation.

In this work, the molar excess volume for binary systems: methyl formate/water, ethyl formate/water, methyl formate/formic acid, ethyl formate/formic acid, methanol/formic acid, ethanol/formic acid are carried on in our laboratory. The molar excess volumes data of methyl formate/methanol, ethyl formate/ethanol, methanol/water, ethanol/water and formic acid/water are collected from literature (Appendix B).

4.1.2 Equipments to measure molar excess enthalpies and reaction enthalpies

A Differential Reaction Calorimeter (DRC) was used to determine enthalpies of mixing, reaction and heat capacity of the reaction mass. The differential thermal analysis is based on evaluating continuously a difference of temperature ΔT between a measure reactor and a reference reactor. The reactor is the place of the mixing process or reaction to be investigated. The reference reactor comprises a solvent which has chemical and physical properties close to the ones of component introduced in the study reactor.

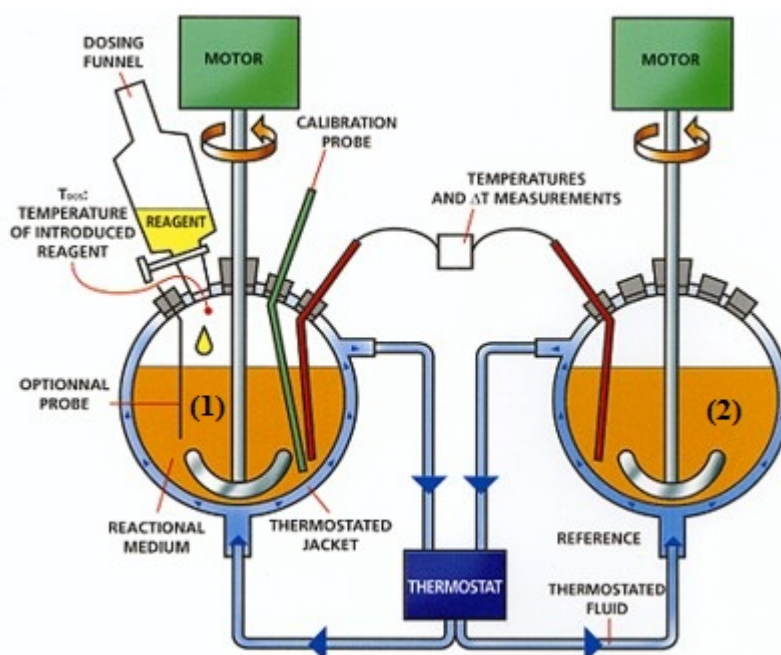


Figure 4.2 Principle scheme of Differential Reaction Calorimeter (DRC).

The two reactors are connected double-enveloped balloons. A heat exchanging fluid flowing in the jackets allows to work at a determined temperature. This experimental mode is called isoperibolic (the environment is at a constant temperature).

In this work, the difference of temperature between the reaction blend and the reference is measured by using the Platinum 100Ω tantalum-cased probes. The difference of temperature is recorded as a function of time to obtain characteristic thermograms.

The DRC is connected with a personal computer and controlled by the SETSOFT 2000 software.

The measurement principles of DRC base on the difference between the two balance of heat flux in the study reactor and reference reactor.

Index 1 and 2 refer to the properties related to the study reactor and reference reactor respectively. The study reactor can operate as semi-batch reactor.

Eq. (2.286) is used for the heat balance for the study reactor (1)

$$\dot{\mathcal{H}}_{chem-mix} + \dot{\mathcal{H}}_{mix} = \dot{\mathcal{H}}_{wall1} + \sum_{i=1}^N n_i C_{P,i} \frac{dT_1}{dt}$$

Rearranging the term $\dot{\mathcal{H}}_{wall1}$ in the study reactor

$$\dot{\mathcal{H}}_{wall1} = (UA)_1 (T_1 - T_{jack}) \quad (4.1)$$

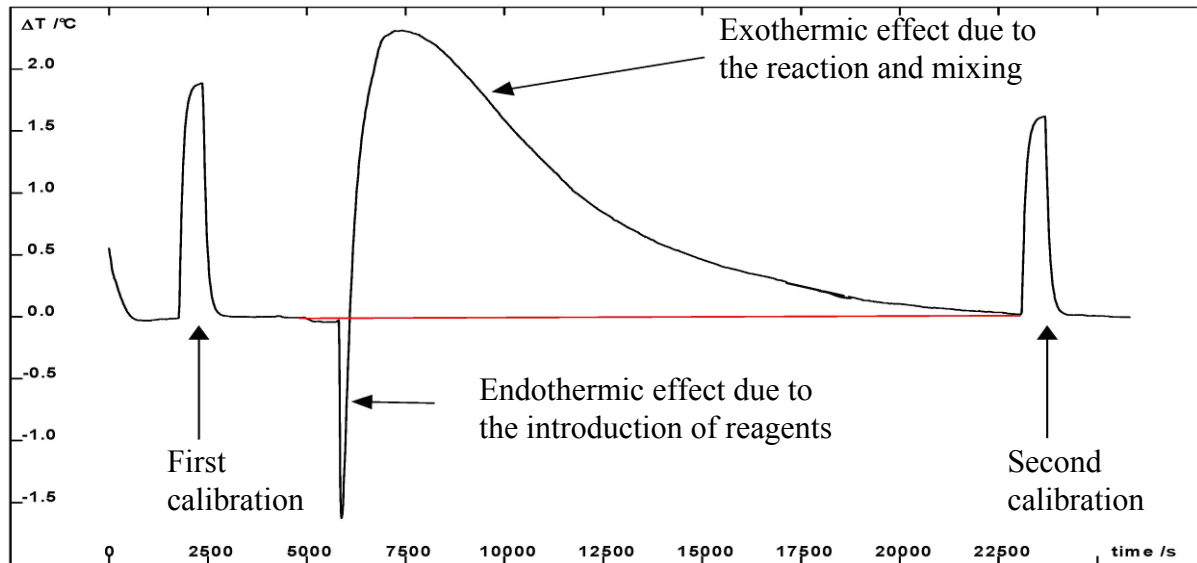


Figure 4.3 Typical curve obtained with Differential Reaction Calorimeter (DRC).

The balance of heat flux in the reference reactor (2), in which no chemical reaction occurs, from eq. (2.289) at a time t can be written

$$0 = \dot{\mathcal{H}}_{wall2} + \sum_{i=1}^N n_i C_{P,i} \frac{dT_2}{dt} \quad (4.2)$$

Quantity of heat dissipated be the walls of the reactor

$$\dot{\mathcal{H}}_{wall2} = (UA)_2 (T_2 - T_{jack}) \quad (4.3)$$

Supposing that two reactors have exactly the same thermal characteristic $(UA)_1 = (UA)_2 = (UA)$. Taking the reaction and reference media have the same thermodynamic properties, and the same mass. With these assumptions and when the temperatures are uniform inside each reactor, making the difference between the two heat balances

$$\dot{\mathcal{K}}_{chem-mix} + \dot{\mathcal{K}}_{mix} = (\dot{\mathcal{K}}_{wall1} - \dot{\mathcal{K}}_{wall2}) + (\dot{\mathcal{K}}_{accu1} - \dot{\mathcal{K}}_{accu2}) \quad (4.4)$$

or

$$\dot{\mathcal{K}}_{chem-mix} + \dot{\mathcal{K}}_{mix} = UA(T_1 - T_2) + \sum_{i=1}^N n_i C_{P,i} \frac{d(T_1 - T_2)}{dt} \quad (4.5)$$

The value of the heat resulting from the chemical reaction or mixing can be determined as follows

$$\dot{\mathcal{K}}_{chem-mix} + \dot{\mathcal{K}}_{mix} = UA\Delta T + \left(\sum_{i=1}^N n_i C_{P,i} \right) \frac{d(\Delta T)}{dt} \quad (4.6)$$

where ΔT_R is difference of temperature between the sample and the reference [K]

Integrating both sides of eq. (4.6)

$$\int_{t=0}^{\infty} (\dot{\mathcal{K}}_{chem-mix} + \dot{\mathcal{K}}_{mix}) dt = \int_{t=0}^{\infty} UA\Delta T dt + \int_{t=0}^{\infty} \left(\sum_{i=1}^N n_i C_{P,i} \right) d(\Delta T) \quad (4.7)$$

Have

$$\mathcal{K}_{chem-mix} + \mathcal{K}_{mix} = UA \int_{t=0}^{\infty} \Delta T_R dt + \left(\sum_{i=1}^N n_i C_{P,i} \right) [\Delta T_R]_{t=0}^{\infty} \quad (4.8)$$

Yet $\Delta T_R = 0$ at $t = 0$ and $\Delta T_R = 0$ at $t = \infty$

So

$$\mathcal{K}_{chem-mix} + \mathcal{K}_{mix} = UA \int_{t=0}^{\infty} \Delta T_R dt \quad (4.9)$$

If no reaction occurs in the mixture, the molar excess enthalpy is determined as

$$H^E = \frac{\mathcal{K}_{mix}}{n} \quad (4.10)$$

and if there is a reaction, assumed that the heat changes due to mixing of introduced components is negligible, the value calculated is the quantity of heat produced during reaction for Δn mole of product formed, thus, the value of chemical reaction and mixing molar enthalpy can be expressed as

$$\Delta H_{chem-mix} = \frac{\mathcal{H}_{chem-mix}}{\Delta n} \quad (4.11)$$

4.1.3 Batch reactor and equipment to measure heat fluxes

The goal of the batch reactor is to measure heat fluxes over the reaction time. The complete METTLER TOLEDO Reaction Calorimeter (RC1) system includes the actual RC1 reaction calorimeter (with thermostat, stirrer, and electronics cabinet), a glass chemical reactor and personal computer which can be used in the evaluation of the experimental data and for preprogramming of an experiment. The RC1 uses a double-jacketed vessel as a reactor. The temperature of reaction can be controlled by the thermostat. In a closed circulation system, the silicon oil used as heat transfer agent is pumped through the double jacket of the reactor. This keeps the temperature of reaction contents T at the set temperature.

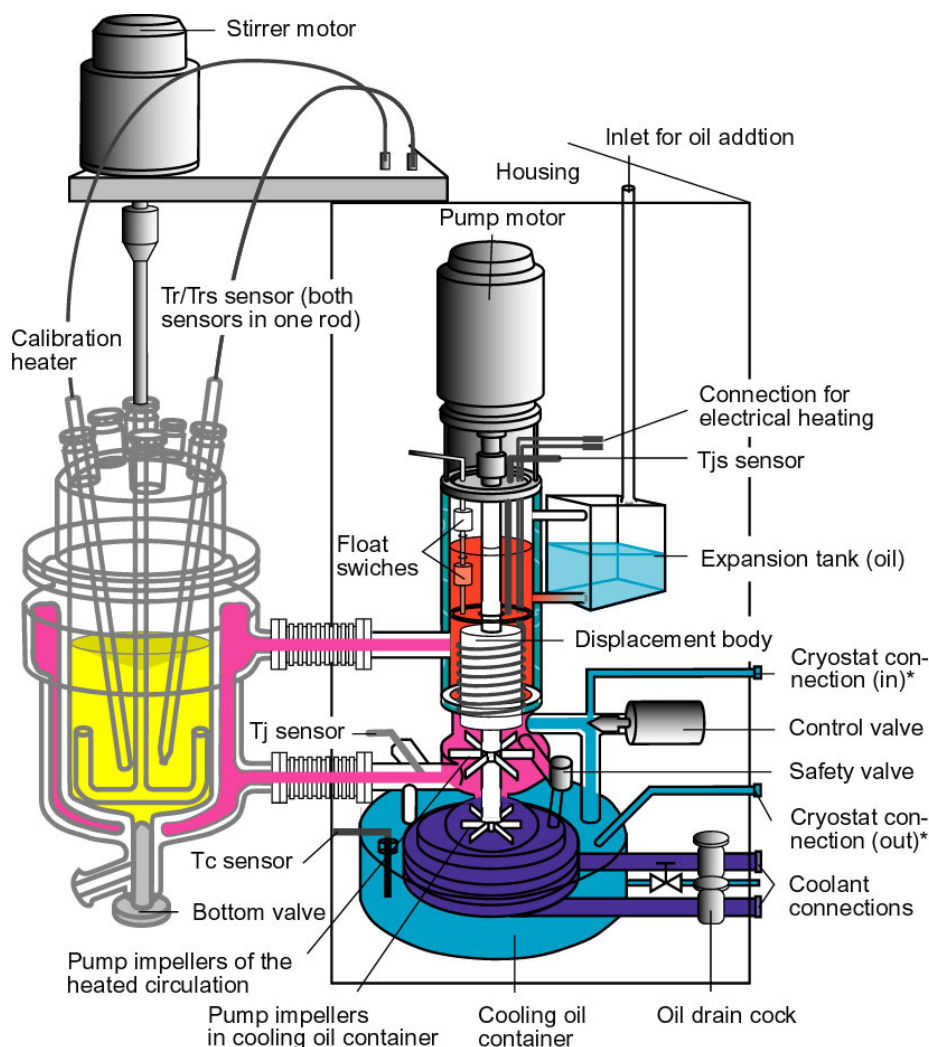


Figure 4.4 Thermostat and pump for the circulating oil.

The reaction calorimeter is computer-controlled that enables experimenter to operate the investigated chemical reaction under isothermal, isoperibolic, adiabatic and temperature

programmed condition. The different operation models of a reaction calorimeter is shown in Table 4.1

Table 4.1 Different operation models of a reaction calorimeter.

Operation mode	Principle
Isothermal	Constant T by varying T_{jack}
Isoperibolic	Constant jacket temperature T_{jack}
Adiabatic	Continuous readjustment of T_{jack} to be equal T
Temperature programmed	Linear heating to a final temperature

In this work, the isothermal mode is applied to perform experiments in order to measure concentration profiles and heat fluxes over the time. Figure 4.5 shows the operating principle of the RC1 in T mode. The temperature of the reaction is held constant or changed with a ramp. Deviation of the temperature of reaction contents from the set value (through heat of reaction) are compensated by appropriate correction of the jacket temperature, i.e. the heat generated is dissipated.

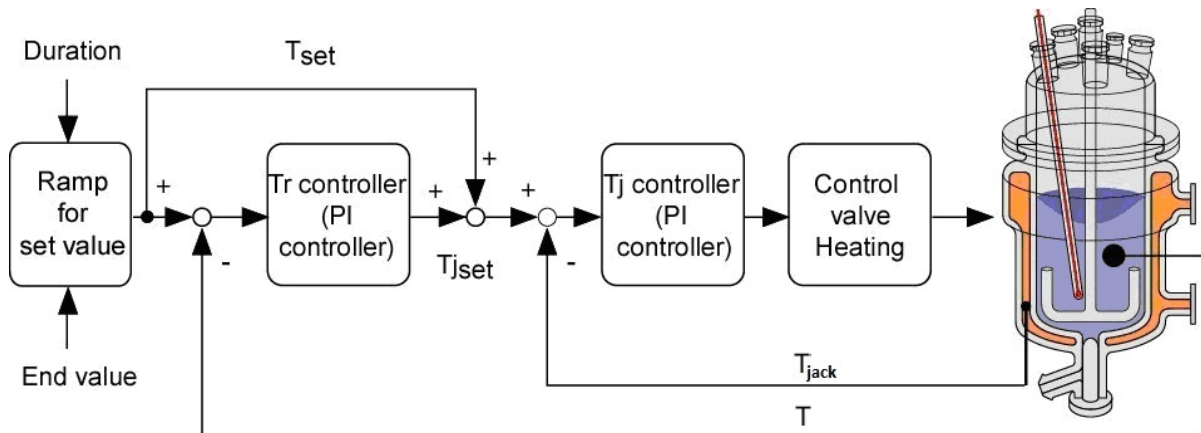


Figure 4.5 Operating principle of the RC1 in isothermal mode ($T = \text{constant}$).

The measurement principle of RC1 based on the jacket temperature T_{jack} and the reaction temperature T can be measured very accurately. This allows the heat flow through the reactor wall to be computed.

$$\dot{\mathcal{K}}_{wall} = UA(T - T_{jack}) \quad (4.12)$$

Where $\dot{\mathcal{K}}_{wall}$ is again the heat flow through the reactor wall [J/s]

Like DRC, two calibrations, before and after reaction with the assumption that no reaction occurs, the applied calibration power $\dot{\mathcal{K}}_C$ can only be dissipated via the wall. This allows the UA factor to be calculated.

Under isothermal condition, From eq. (2.276), the heat fluxes measured include heat flow of reaction and mixing during the time.

4.1.4 Concentration analysis

Fourier transform infrared spectroscopy (FTIR) is the most advanced method of infrared spectroscopy. This is the ideal analysis tool for understanding chemical reactions by real-time data and without disturbing the reaction mixture. This technique allows the reaction kinetics to be observed under experimental conditions.

Principle of FTIR is based on absorptions of molecular vibrations and rotations directly in the infrared spectrum. Many functional groups in organic molecules show characteristic vibrations, which correspond to absorption bands in defined regions of the IR spectrum. These molecular vibrations are essentially localised within the functional groups and do not extend over the rest of the molecule. Thus such functional groups can be identified by their absorption bands. This fact, together with the simple measurement technique, makes IR spectroscopy the easiest, quickest, and often most reliable method to assign a substance to a particular class of compounds. Usually it is possible to decide immediately if an alcohol, amine, etc. is present [Man97].

In this work, chemical reaction model systems employed by the Mettler-Toledo ReactIR iC10 for monitoring concentration are performed. The Mettler-Toledo ReactIR iC10 is a FTIR spectrometer that measures chemical species as they react over a period of time. It uses a Mercury Cadmium Telluride (MCT) detector which is cooled by liquid nitrogen. Measurements are taken optically using a diamond tipped probe with a mirror based optical conduit.

The small size and relatively light weight of the system enable it to be used in many laboratory and industrial settings. The liquid nitrogen supply is sufficient for 24 hours. A basic power supply, USB cable and a supply of instrument grade air or nitrogen are all that is necessary for reliable operation and accurate chemical analysis.

Quantitative IR spectroscopy

The concentration of a substance in a solution or mixture can be determined with the assistance of IR spectroscopy. Based on UV spectroscopy the Beer-Lambert law [Man97] describes the relationship between absorbed light and concentration

$$\lg \frac{I_0}{I} = \varepsilon cd = E_\lambda \quad (4.13)$$

Where I_0 and I is radiant power of the light before and after its passage through the sample, E_λ is the absorbance, ε is the molar absorptivity or extinction coefficient with units of [$\text{Lmol}^{-1}\text{cm}^{-1}$], d is the thickness of the cell [cm] and c is the concentration of a pure compound in the solution, expressed in [molL^{-1}].

The mid-infrared wavelength bands lie in the region from $\lambda = 2.5$ to $25.0\mu\text{m}$. However, it is usual to quote the inverse of wavelength, so-called wavenumber

$$\tilde{\lambda} = \frac{1}{\lambda} \quad (4.14)$$

Therefore, the region of mid-infrared wavenumber bands is from 400 to 4000 [cm^{-1}]

The concentration of the component in a solution can be determined from a measurement of absorbance E_λ by using an empirical calibration curve. It is generated by plotting the absorbances against concentration.

In the IR spectra of the reaction mixtures, the peaks of methanol and ethanol are isolated. Thus, two alcohols (Methanol and ethanol) are chosen to construct calibration curves.

4.2 EXPERIMENTAL PROCEDURES AND PROGRAM

4.2.1 Measurement of molar excess volumes V^E

The molar excess volumes of several binary systems were investigated. Methyl formate and ethyl formate, ethanol, methanol and formic acid were supplied by MERCK with stated purities of 97% and 97%, 99.8%, 99.8%, 99% respectively. All measurements were made at atmospheric and 298K.

Firstly, the first component was filled with amount desired in a 100mL glass flask, and then introduces the quantity of the second component desired into the flask. All the mass of dry flask, flask with the first component and flask with total mixture mass were measured. The mixture was closed by glass stopper for preventing evaporation, and immediately used after it was well mixed by shaking. The density of each mixture was performed on DM40 density meter and from eq. (2.144) the binary molar excess volumes were calculated by the experimental density

$$V_{12}^E = \frac{x_1 M_1 + x_2 M_2}{\rho} - \frac{x_1 M_1}{\rho_1} - \frac{x_2 M_2}{\rho_2} \quad (4.15)$$

Since solubilities of methyl formate and ethyl formate in water are limited (solubilities of MF and EF in water at 20°C are 300 and 105g/L respectively see Table 3.2), so only the molar excess volumes V^E in a dilute aqueous solution were measured. A summary of the experiments is shown in Table 4.2.

Table 4.2 Summary of preliminary density measurements to estimate values for molar excess volumes of MF and EF in 50mL water at 298K.

N ^o	MF [mL]	EF [mL]
1	0	0
2	2	2
3	4	5
4	6	7
5	8	10
6	10	12
7	12	
8	14	
9	16	

The other system: MF(1)/F(2), EF(1)/F (2), M(1)/F(2), and M(1)/F(2) were summarised in Table 4.3.

Table 4.3. Summary of compositions for density measurements to estimate other values for molar excess volumes at 298K.

N ^o	1 st component [mL]	2 nd component [mL]
1	0	100
2	5	95
3	10	90
4	20	80
5	30	70
6	40	60
7	50	50
8	60	40
9	70	30
10	80	20
11	90	10
12	95	5
13	100	0

4.2.2 Measurement of molar excess enthalpies H^E

The heat of mixing of binary system has been performed at 298K. Firstly, the quantity of the first component desired was introduced in the measure and reference reactor. It is important

that in the measure reactor, the Joule Effect calibration probe needs to be immersed enough in the solution. Perform a Joule Effect calibration when the base line is stable. This calibration will be able to determine the UA product, typical of the reaction with U is the transfer coefficient of the reaction wall and A is the exchange area. Once the Joule Effect is over, and the calorimetric signal is back to the base line, the second component can be introduced in the reactor. When the reaction is gone, wait until it returns to the based line. Make the second of Joule Effect calibration at the end of the experiment. The total heats of mixing are obtained by integration of the temperature difference with time using both the Joule Effect calibration. The values for molar excess enthalpies are determined by eq. (4.10).

Table 4.4. Summary of compositions for measurements to get values for binary molar excess enthalpies in reaction (3.1) at 298K.

MF [g]	W [g]	MF [g]	F [g]	M [g]	F [g]	M [g]	W [g]	MF [g]	M [g]	F [g]	W [g]
0.0	10.0	100	0	100	0	0.0	100.0	100.0	0.0	0.0	100.0
2.4	197.1	80.1	7.2	120	19	14.0	150.0	80.0	5.0	43.0	150.0
3.8	190.0	80	27	80	29	30.0	150.0	79.9	11.0	75.0	117.0
4.9	195.1	79.9	27	65	40	55.0	120.1	80.0	19.0	100.2	90.0
7.9	155.1	80.2	41	52	50	61.0	80.0	80.0	29.0	120.0	70.2
12.1	140.0	80.1	62	70	100	81.0	84.0	80.0	43.0	119.9	47.0
20.0	165.0	87	100	46	100	90.1	75.1	80.7	65.0	120.2	31.0
21.1	140.1	56	100.1	30.1	100.1	100.0	56.0	52.0	65.0	120.0	20.0
27.0	150.1	32.1	100	17	100	135.0	50.2	30.0	65.0	130.0	12.1
30.8	150.0	13.9	100	7.1	100.1	85.0	20.2	13.0	65.0	145.0	6.0
23.1	100.1	0	100	0	100	110.0	15.1	0.0	100.0	100.0	0.0
29.0	100.1					100.0	6.0				
1.0	0.0					100.0	0.0				

Table 4.5. Summary of preliminary measurements to get values for binary molar excess enthalpies in reaction (3.2) at 298K.

EF [g]	W [g]	EF [g]	F [g]	E [g]	F [g]	E [g]	W [g]	EF [g]	E [g]	F [g]	W [g]
10.5	100	0.0	100.0	0	100	0.0	100.0	0.0	100.0	0.0	100.0
8.4	100	18.0	100.0	11.1	100	26.0	90.0	12.9	70.0	43.0	150.0
6.2	100	40.9	100.0	25	100	51.0	80.0	28.0	70.0	75.0	117.0
4.1	100	69.0	100.0	43	100	88.0	80.0	48.0	70.0	100.2	90.0
2.1	100	75.0	70.0	67	100	70.0	41.1	75.0	70.0	120.0	70.2
0	100	75.0	46.0	65	65	70.0	27.0	75.0	46.0	119.9	47.0
		75.0	31.0	65	42	70.0	18.0	75.0	31.0	120.2	31.0
		75.0	20.0	65	27	70.0	12.1	75.0	20.0	120.0	20.0
		75.0	11.0	65	16	70.0	7.0	75.0	11.0	130.0	12.1
		75.0	5.0	65	7	70.0	3.0	75.0	5.0	145.0	6.0
		100	0.0	100	0	100.0	0.0	100.0	0.0	100.0	0.0

4.2.3 Measurement of reaction enthalpies ΔH_R

Like measuring enthalpies of mixing, the DRC was used to measure the reaction enthalpies of hydrolysis of esters for investigating the reaction model in isothermal condition. The total enthalpies of reaction are obtained by integration of the temperature difference with time using both the Joule Effect calibration. The values for reaction enthalpies are determined by eq. (4.11).

Table 4.6 Overview of initial composition for reaction enthalpy measurements for methyl formate and ethyl formate hydrolysis at 298K.

N ^o	Reaction	W[g]	Es[g]
1	MF	122	27.0
2	EF	120	11.8

4.2.4 FTIR calibration

To determine the concentrations of components of analyses in the reaction mixtures, calibration curves are needed. The calibration curves are plots of how the FTIR signal response changes with the concentrations based on eq. (4.13). The ranges of concentrations for calibration curves lie near the working concentrations expected in experiments.

The concentrations near the expected working concentrations are given in Table 4.7.

Table 4.7 Concentration of methanol c_M and ethanol c_E for calibration curves.

N ^o	c_M [mol/L]	c_E [mol/L]
1	0.0	0
2	0.5	0.2
3	1.0	0.4
4	1.5	0.8
5	2.0	1.0
6	2.5	1.2
7	3.0	1.4
8	3.5	-
9	4.0	-

4.2.5 Measurement of reaction equilibrium constants

The chemical equilibriums were measured by using the same experimental set up as for the kinetic measurements. The reaction was observed until it reached equilibrium state in which there is no net change in composition. The value of equilibrium constant of hydrolysis of ester reactions is calculated from equilibrium concentration of all components measured by FTIR.

4.2.6 Reaction kinetics experiments in batch reactor

In order to record transient concentrations, heat fluxes, experiments for kinetic analysis of hydrolysis of ester were performed in the Batch Reactor RC1. Water and homogeneous catalyst were placed and heated up or cooled down to desired reaction temperature in the RC1. The first calibration is performed when reaction temperature was stable. The ester was heated up or cooled down until it reached the desired reaction temperature in second separate thermostat and introduced in the BR once the first calibration was over. A second calibration at the end of the experiment was performed when the reaction was extinguished. All these processes are controlled by a program made by experimenter. During the experiment, FTIR spectrum is real time monitored every 1 minute for whole experimental time.

To get good rates of ester hydrolysis reactions, the concentration of homogeneous catalyst hydrochloric acid was always 0.05mol/L.

The initial conditions for kinetic measurements for methyl formate and ethyl formate hydrolysis at different temperatures are given in Table 4.8.

Finally, to evaluate the kinetic results estimated, two more experiments under different initial conditions have to be performed. These initial conditions are shown in Table 4.9.

Table 4.8 Initial conditions for kinetic measurements for methyl formate and ethyl formate hydrolysis at different temperatures.

	Methyl formate	Ethyl formate
Reaction temperature [K]	288-303	288-303
n_{Es}^{init} [molL ⁻¹]	2.878	1.191
n_W^{init} [molL ⁻¹]	46.905	50.513
n_{Al}^{init} [molL ⁻¹]	0.167	0.039
n_F^{init} [molL ⁻¹]	0	0
n_{HCl}^{init} [molL ⁻¹]	0.05	0.05
$V_R^{id,init}$ [L]	1.033	1.011

Table 4.9 Reactant concentrations for validating the kinetics results of hydrolysis of ester performed in BR catalysed by 0.05M HCl acid at 298K.

	Methyl formate	Ethyl formate
Reaction temperature [K]	298	298
Stirrer speed [rpm]	200	200
n_{Es}^{init} [molL ⁻¹]	3.73	1.98
n_W^{init} [molL ⁻¹]	43.63	47.18
n_{Al}^{init} [molL ⁻¹]	0.216	0.065
n_F^{init} [molL ⁻¹]	0	0
n_{HCl}^{init} [molL ⁻¹]	0.05	0.05
$V_R^{id,init}$ [L]	1.029	1.017

CHAPTER 5

RESULTS AND DISCUSSION

In this chapter the results obtained in this work based on experiments described in chapter 4 are presented and discussed. Section 5.1 describes the measured molar excess volumes and enthalpies for all binary systems considered. In addition, the determined reaction enthalpies of the methyl formate and ethyl formate hydrolysis reactions are given together with the chemical reaction equilibrium constants estimated. In section 5.2, the reaction kinetic parameters obtained by analysing the transients measured are summarized. They are based on *i*) neglecting and *ii*) incorporating the volume changes of the reaction mixture due to mixing. Results of a more comprehensive sensitivity analysis of the kinetic parameters are presented in section 5.3 focusing on a comparison of simulated and experimental data of the temporal concentration profiles during the reaction. Finally in section 5.4, comparisons of simulated and measured heat fluxes through the wall of the reactor are made for the hydrolysis of methyl formate. Theoretical reaction temperature profiles for this reaction performed under adiabatic condition are generated and interpreted.

5.1 EXPERIMENTAL RESULTS

5.1.1 Molar excess volumes

The molar excess volume is defined by eq. (2.36) in chapter 2. For a binary mixture, at given temperature and pressure, the molar excess volume is directly computed by eq. (4.15) from measured densities ρ . The way to measure these densities is presented in chapter 4. The different values of molar excess volumes range were fitted as a function of composition by the Redlich/Kister formula, eq. (2.151).

The results for molar excess volumes of binary mixtures of MF/W, EF/W, MF/F, EF/F, M/F and E/F were calculated based on densities measured by eq. (4.15). The experiments were carried out at 298K and atmospheric pressure. Values for binary molar excess volumes V^E of M/W, E/W [Jose06], MF/M [Jiri71], EF/E [Jian96] and F/W [Apel87] were collected from literature. All V^E values determined are listed in tabulated form in Appendix B.

Figure 5.1 shows the molar excess volumes V^E of the binary systems relevant for methyl formate hydrolysis as a function of composition at 298K. The values of V^E are always negative

over the entire range of composition and quite symmetrical. Extreme values for V^E occur near equimolar compositions. However, the corresponding behaviour of M/F, MF/F and F/W is not fully symmetrical. The values for V^E of M/F are smallest and the values for V^E of M/W are the biggest with an extreme $-1.01\text{cm}^3/\text{mol}$. The different intermolecular forces and packing states of the molecules (different sizes and shapes of the molecules mixed) cause the different values of molar excess volumes.

The positive contribution arises where dipole-dipole interactions between like molecules predominate. The negative can be attributed to strong unlike interactions between molecules [Hars09].

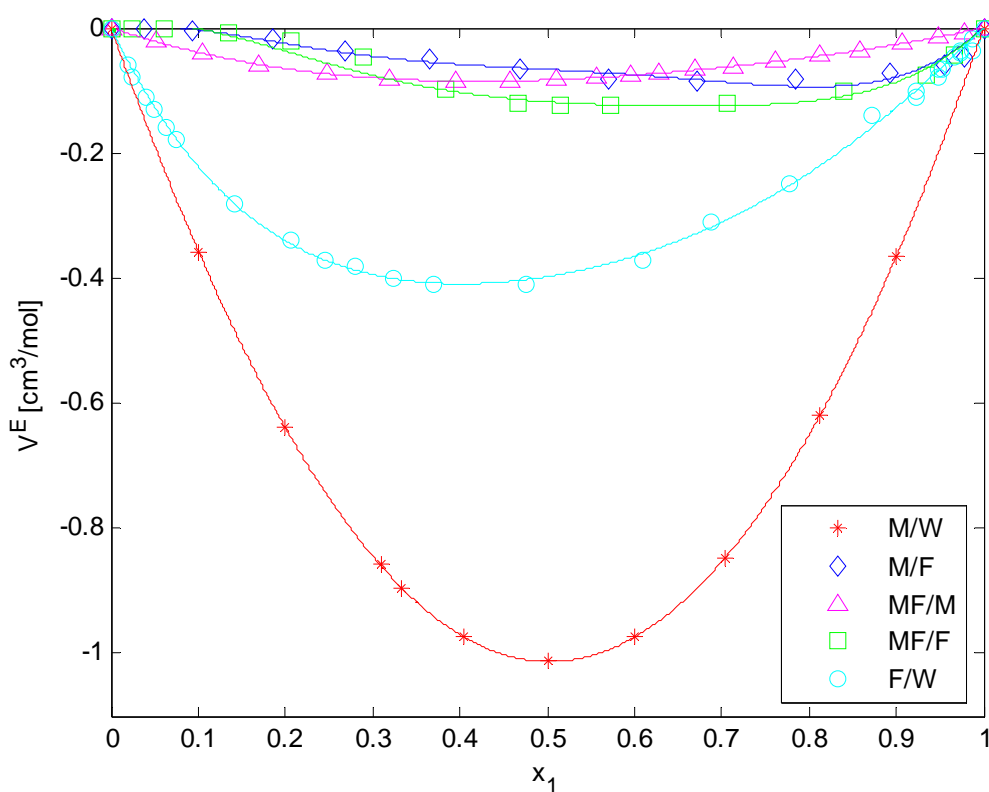


Figure 5.1 Measured molar excess volumes V^E over the mole fraction x_1 of M, MF and F for the binary mixtures of M/W(*), M/F(\diamond), MF/M (Δ), MF/F(\square), and F/W(o) respectively, at 298K. Lines are calculated using the Redlich/Kister eq. (2.151).

In Figure 5.2 are given the values of determined molar excess volumes of binary systems relevant in ethyl formate hydrolysis as a function of composition at 298K. The molar excess volumes are negative for E/W, EF/E, and F/W but positive for E/F over the whole composition regions. The minimum value for V^E of E/W is $-1.04\text{cm}^3/\text{mol}$ and the maximum V^E value of E/F is $+0.27\text{cm}^3/\text{mol}$.

The molar excess volumes of EF/F are positive in the regions of small ethyl formate fractions, and negative in the regions of high ethyl formate fractions. There is no molar excess volume at

approximately equimolar composition. The minimum value for V^E of EF/F is $-0.06\text{cm}^3/\text{mol}$ and the maximum is $+0.066\text{cm}^3/\text{mol}$.

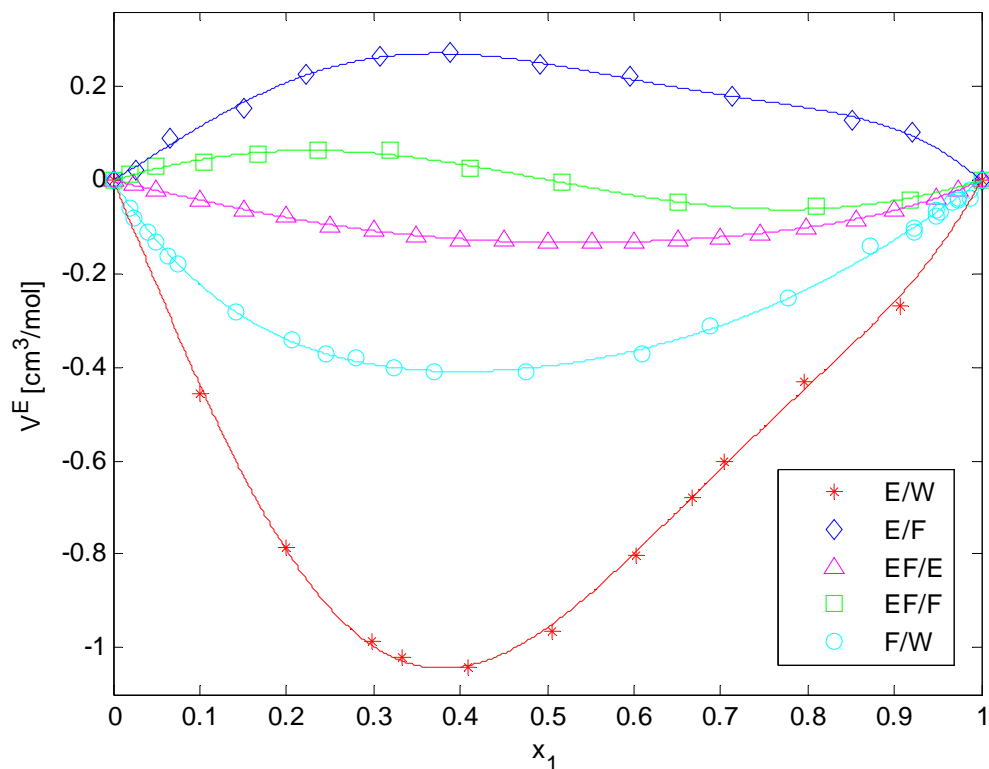


Figure 5.2 Measured molar excess volumes V^E over the mole fraction x_1 of M, MF and F for the binary mixtures of E/W(*), E/F(\diamond), EF/M (Δ), EF/F(\square), and F/W(o) respectively, at 298K. Lines are calculated using the Redlich/Kister eq.(2.151).

As can be observed in Figure 5.3, the values of molar excess volumes in a very dilute solution of esters are negative and can be represented approximately by linear expressions.

There is satisfactory agreement between the values for molar excess volumes in this works and the values provided in different literature sources [Smith05], [Albe01], [Rui07], etc. The observed small differences may be caused by differences of the purity of the components applied.

The Redlich/Kister model was found suitable to fit the data measured and to predict the molar excess volumes. The values of the parameters were evaluated using the least squares method. Table 5.1 summarizes the values of the free parameters A_{p_i} and corresponding R^2 values determined.

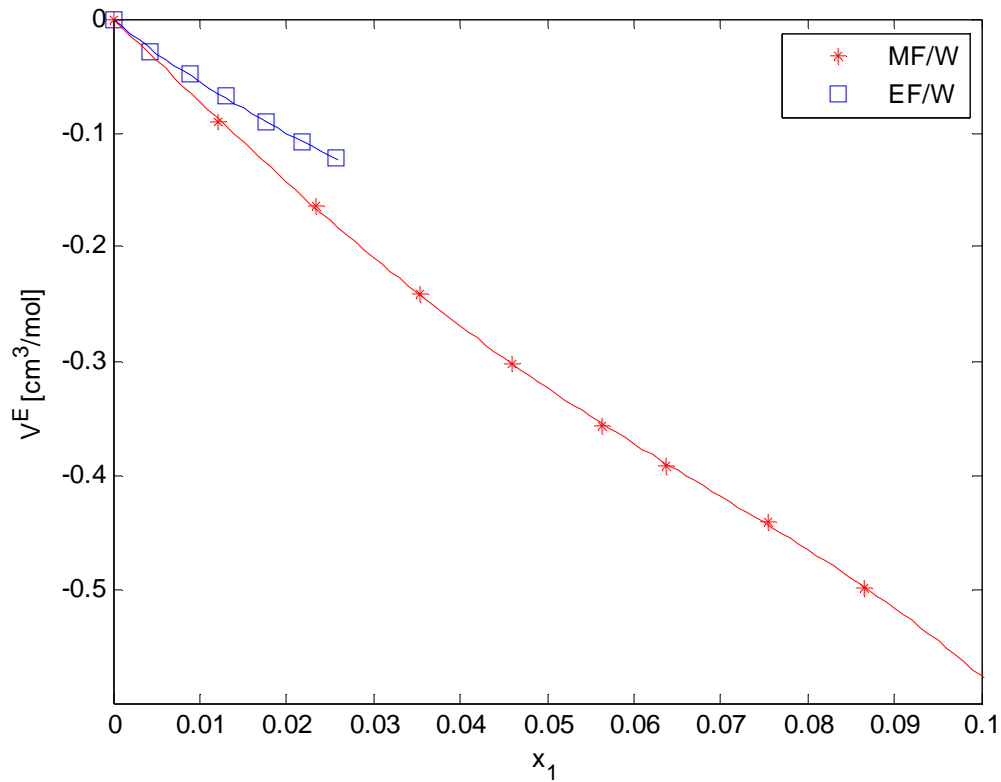


Figure 5.3 Measured molar excess volumes V^E over the mole fraction x_1 of MF and EF for the binary mixtures of MF/W(*) and EF/W(□) respectively at 298K. Lines are calculated using the Redlich/Kister eq.(2.151).

Table 5.1 Pressure derivatives of coefficients of the Redlich/Kister eq. (2.151) for molar excess volumes V^E of binary mixtures at 298K.

Mixture	$A_{P,12,0}$	$A_{P,12,1}$	$A_{P,12,2}$	$A_{P,12,3}$	R^2
MF/W	-457.1	-1520.1	-1698.8	-628.5	0.99
EF/W	6112.9	19208	20122	7033.5	0.99
MF/F	-0.4722	-0.1946	-0.0299	-0.6221	0.99
EF/F	0.0086	-0.7002	-0.0021	0.1408	0.99
M/F	-0.2661	-0.1478	-0.2933	-0.5885	0.99
E/F	0.9996	-0.6080	0.3938	0.9116	0.99
M/W	-4.0518	-0.0530	0.0573	-0.0145	0.99
E/W	-3.8349	2.5993	-0.0602	-2.1470	0.99
MF/M	-0.3326	0.1016	-0.0515	-0.0266	0.99
EF/E	-0.5295	-0.0556	-0.0868	-0.1566	0.99
F/W	-1.5911	0.4438	-0.5497	0.3223	0.99

It would be desirable to have these derivatives of the $A_{p,12,i}$ values interpreted to calculate directly G_{12}^E values or corresponding activity coefficients γ . However, this would require four values of the $A_{12,i}$ as a function of pressure, which could not be determined in this work.

5.1.2 Molar excess enthalpies

The molar excess enthalpy is defined by eq. (2.37). As described in chapter 4, from eq. (4.9), the value for total excess enthalpies can be obtained by multiplying values of integrate temperature transient based on DRC measurement and UA values computed from two Joule effect calibration performed before and after the experiments. Then values of molar excess enthalpies are calculated by eq. (4.10). The values of molar excess enthalpies over the composition range were fitted also by the Redlich/Kister formula eq. (2.160). The results obtained of H^E for all binary systems are listed in tabulated form Appendix C. All experiments have been performed at 298K and atmospheric pressure.

The sensitivity of the calorimeter RC1 applied was limited and the values of the heat fluxes of ethyl formate hydrolysis were formed to be very weak and influenced by significant noises. In this work, only the measured heat fluxes of methyl formate hydrolysis is used to evaluate “correct” enthalpy of reaction based on the heat balance.

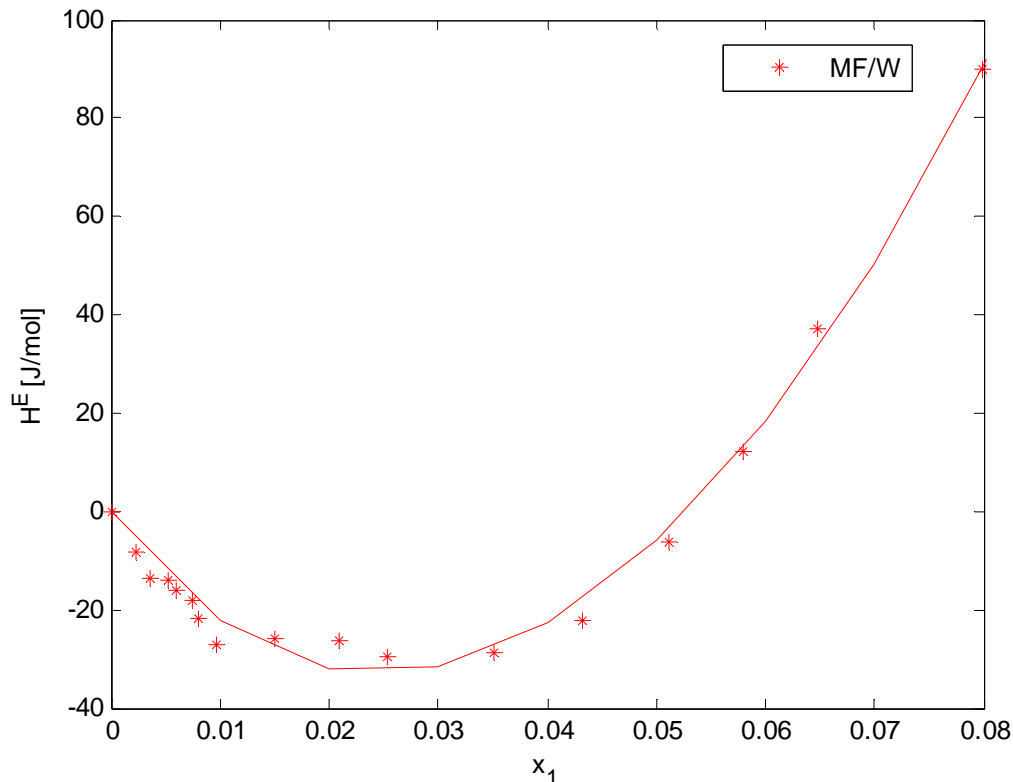


Figure 5.4 Measured molar excess enthalpies H^E over the mole fraction x_1 of MF for binary mixtures of MF/W(*), at 298K. The line is calculated using the Redlich/Kister eq. (2.160).

As can be seen in Figure 5.4, the molar excess enthalpies of methyl formate/water are negative (exothermic) at low x_1 regions and positive (endothermic) at other regions of methyl formate fraction ($x_{MF} > 0.05$). There is no heat of mixing when x_{MF} is approximately 0.05.

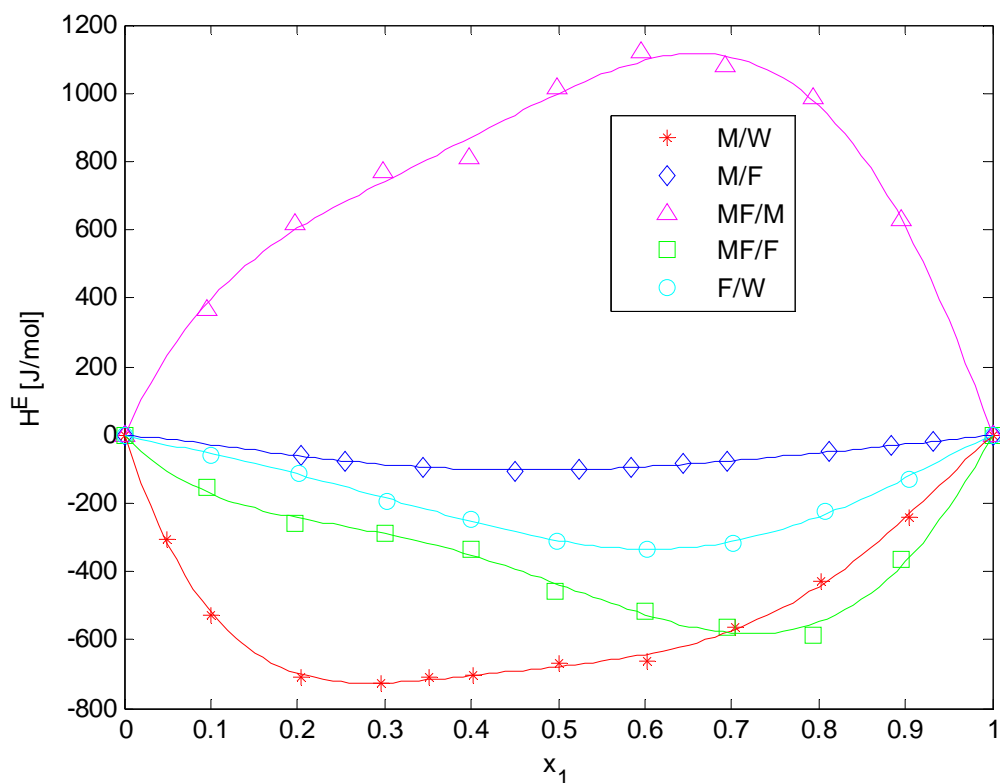


Figure 5.5 Measured molar excess enthalpies H^E over the mole fraction x_1 of M, MF, and F for binary mixtures of M/W(*), M/F(◇), MF/M(△), MF/F(□), F/W(o) respectively, at 298K. Lines are calculated using the Redlich/Kister eq.(2.160).

In Figure 5.5, the molar excess enthalpy values are negative over the complete range of composition for all mixtures except for the MF/M mixture. The values of molar excess enthalpies for methanol/water are in good agreement with the ones reported in literature [Batt85]. The small differences may be again caused by differences in the purity of the methanol.

The actual specific values of molar excess enthalpy can be explained in terms of negative contributions due to the formation of interactions between unlike molecules and of positive contributions due to the breaking of interactions between like molecules [Enri95]

Like in case of representing the molar excess volumes, the Redlich/Kister model used in fitting the data measured, is also appropriate in fitting the molar excess enthalpies. The model parameters for all binary mixtures and the corresponding R^2 values are given in Table 5.2.

Table 5.2 Temperature derivative coefficients of the Redlich/Kister eq.(2.160) for molar excess volumes H^E of binary mixtures at 298K.

Mixture	$A_{T,12,0}$	$A_{T,12,1}$	$A_{T,12,2}$	$A_{T,12,3}$	R^2
MF/W	279097	904072	1000000	377993	0.99
MF/F	-1750.3	-1843.3	-2000.7	715.2	0.99
M/F	-7301.7	7184.6	-1295.5	-4075.5	0.99
M/W	-2713.7	565.8	-2373.3	2105.5	0.99
MF/M	3996.5	2398.3	2507.9	-1451.1	0.99
F/W	-1238.3	-854.6	347.0	567.1	0.99

Inspecting the determined V^E and H^E values it would be desirable to have further the corresponding pressure and temperature dependences in order to generate directly G_{12}^E values or corresponding activity coefficients γ . However, this would require more tedious and difficult experiments which were not possible in the frame of this work.

5.1.3 Reaction equilibrium constants and reaction enthalpies

The reversible hydrolysis reactions, can be described by (Table 3.1)



The equilibrium constant was determined at 288, 293, 298 and 303K. The values of K_c were calculated from measured concentrations at equilibrium by eq. (3.3). The corresponding values of activity coefficient were computed with UNIFAC method using the measured equilibrium concentrations. Then, the values K_a were computed from eq. (3.4). The results were summarized in Tables 5.3 and 5.4.

Table 5.3 Effect of temperature on equilibrium compositions and constants K_c and K_a of methyl formate hydrolysis at initial concentration of methyl formate $c_{MF}^{init} : 2.84 \text{ molL}^{-1}$.

T [K]	Equilibrium concentrations $c_i^{eq} [\text{molL}^{-1}]$					Activities $a_i^{eq} [-]$				
	MF	W	M	F	K_c	MF	W	M	F	K_a
288	0.719	44.529	2.293	2.132	0.153	0.061	0.905	0.086	0.046	0.071
293	0.692	44.502	2.319	2.259	0.163	0.059	0.904	0.087	0.047	0.076
298	0.668	44.478	2.344	2.184	0.172	0.057	0.903	0.088	0.047	0.081
303	0.643	44.453	2.369	2.208	0.183	0.055	0.903	0.089	0.048	0.086

The values of the equilibrium constant of two ester hydrolysis reactions are small. This indicates that the reactants (ester and water) are favored at equilibrium and the reactions are unlikely to form much products. The reaction equilibrium constants increase with increasing temperature. Therefore, from definition of reaction equilibrium constant, eq. (2.222), the rate of

the forward reaction is more sensitive than reverse reaction with respect to temperature and this denote the reactions are endothermic ones. Raising the temperature of an endothermic reaction favors the formation of products [Akins99].

Table 5.4 Effect of temperature on equilibrium compositions and constants K_c and K_a ethyl formate hydrolysis at initial concentration of ethyl formate $c_{EF}^{init} : 1.187 \text{ molL}^{-1}$.

T [K]	Equilibrium concentrations c_i^{eq} [molL ⁻¹]					Activities a_i^{eq} [-]				
	EF	W	E	F	K_c	EF	W	E	F	K_a
288	0,175	49,498	1,054	1,015	0,123	0.039	0.961	0.117	0.021	0.066
293	0,165	49,488	1,065	1,025	0,134	0.037	0.960	0.118	0.022	0.072
298	0,157	49,479	1,073	1,034	0,143	0.035	0.960	0.119	0.022	0.076
303	0,149	49,471	1,081	1,042	0,153	0.034	0.960	0.120	0.022	0.082

Since the water amounts in the reaction mixtures are superior to other components, the changes of concentrations of water at equilibrium are negligible. Furthermore, for nearly pure water, $a_w \approx 1$. Therefore, in ethyl formate hydrolysis, which starts with a dilute solution of ethyl formate, the activity of water in this solution is always approximately one.

At 298K, for the methyl formate hydrolysis, the K_c value computed has good agreement with results in literature [Rober75]: $K_c = 0.167$, [Weth74]: $K_c = 0.169$ and [Falk02] $K_c = 0.12$ and the K_a value given in Tables 5.3 and 5.4 has also good agreement with data in Table 3.10 obtained by eq. (2.185) $K_a = 0.071$. For ethyl formate hydrolysis, the K_a value obtained is in an acceptable agreement with that estimated from thermodynamic data illustrated in Table 3.10, $K_a = 0.064$.

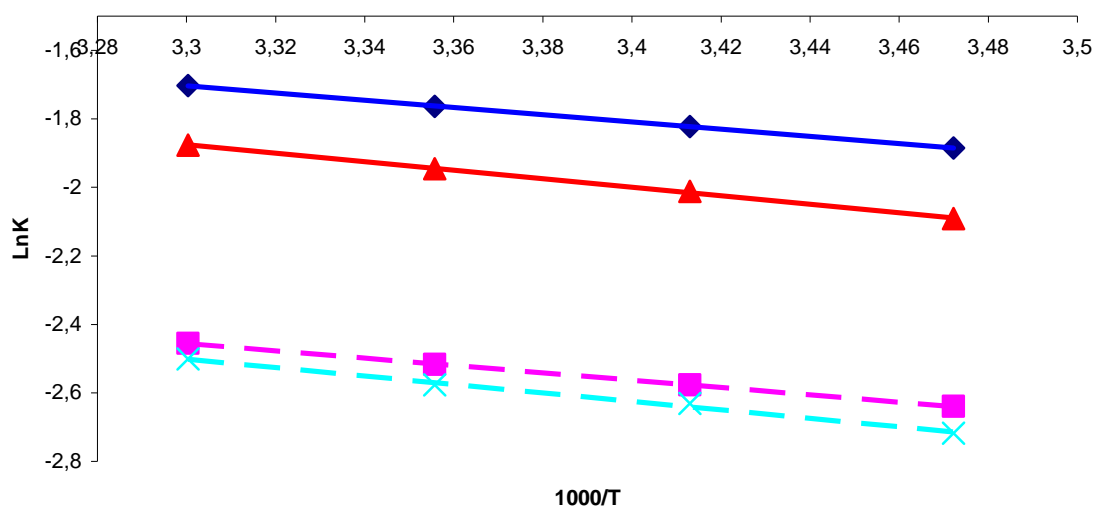


Figure 5.6 Temperature dependence of the equilibrium constant $K_c(\text{MF})$: \square , $K_a(\text{MF})$: Δ , $K_c(\text{EF})$: \times , $K_a(\text{EF})$: \diamond , full lines: K_c , dashed lines: K_a .

All equilibrium constants determined increase when raising the temperature. However, the temperature interval is relative small. Van't Hoff eq. (2.198) enables to estimate a reaction enthalpy. A plot of $\ln K_c$ and $\ln K_a$ against the value of $(1000/T)$ is depicted in Figure 5.6. The results of reaction enthalpy were calculated based on linear regression (the slope equals to $-\Delta H_R^0 / R$)

Table 5.5 ΔH_R^0 values of hydrolysis for two esters obtained from different sources.

Source	ΔH_R^0 [kJ/mol]	ΔH_R^0 [kJ/mol]
	MF hydrolysis	EF hydrolysis
HSC chemistry 7.0 database	+5.44	+7.91
CRC handbook	+7.70	+13.7
[Vu07]	+9.75	+7.64
[Mai06]	+8.19	+4.28
K_c (Figure 5.6)	+8.76	+10.33
K_a (Figure 5.6)	+8.87	+10.24

The slopes of the lines in Figure 5.6 from measured K_c and K_a for the two esters are similar, indicating an agreement of ΔH_R^0 values. Table 5.5 displays the reaction enthalpy values of two ester hydrolysis reactions calculated from the experimental concentrations at equilibrium and literature data are in a good agreement.

5.1.4 Reaction enthalpies from calorimetric measurements

Working temperature of experimental procedure for determination of reaction enthalpies is 298K. Like molar excess enthalpy, the total reaction enthalpy results from multiplication of integration the temperature transients and an UA value calculated from two Joule effect calibrations performed before and after reaction time. From eq. (4.11), the reaction enthalpies of hydrolysis reactions and mixing measured by DRC are given in Table 5.6

Table 5.6 Measured reaction enthalpies of hydrolysis of two esters combined with mixing enthalpies at 298K.

Hydrolysis reaction	$\Delta H_{chem-mix}$ [kJ/mol]
Methyl formate	+3.18
Ethyl formate	+2.16

The value for methyl formate is satisfactory agreement with one measured by [Mai06]. However both values have poor agreement with values obtained from different sources in Table 5.5.

To explain this difference, as presented in chapter 4, when ester previously heat up at the same reaction temperature is introduced into water in reactor, immediately mixing effect happens and last until reaction finish. In the beginning, there is a significant drop in temperature due to the mixing between the ester and water. After that, due to the combination of reactants together to form new products, the mixing effect is also presented. Therefore, the enthalpy values measured include both reaction and mixing enthalpy.

In order to evaluate the correct reaction enthalpy, the mixing enthalpies are computed by using molar excess enthalpy. The correct reaction enthalpy is the difference between the value of reaction enthalpy measured and the enthalpy due to mixing. It will be described in detail in section 5.4.

5.2 ESTIMATION OF REACTION KINETIC PARAMETERS FROM CONCENTRATION PROFILES

The determination of the reaction kinetic parameters is usually a two-step procedure; first the concentration dependency is found at a fixed temperature. This means the reactor needs to be operated isothermally.

$$\frac{dT}{dt} = 0 \quad (5.2)$$

Then, the temperature dependence of the kinetic parameters is found from results for different (constant) temperatures yielding the complete rate equation [Leve99].

In this work, the reaction kinetic parameters were estimated by following the concentration of a given component based on the mass balance eq. (2.229) rewrites for the model reactions

$$\frac{dn_i}{dt} = v_i r V_R \quad i = \text{Es, W, Al, Ac} \quad (5.3)$$

In parallel, three reaction volume V_R options are studied: “*Const*” - no volume change, “*Ideal*” - volume change just by the reaction, “*Real*” – volume change due to the reaction and mixing.

Because of autocatalytic effects of the generated H^+ ions, the kinetic equations of the model reaction does depend on the concentrations of reactants, products and the H^+ ions as well. Therefore, the concentration of the catalysing hydrogen proton in reaction mixture was additionally taken into account in the rate of reaction. For ideal solution behaviour, according to eq. (2.223), the reaction rate of the model reaction (3.1) and (3.2) can be expressed by

$$r(\bar{c}) = k c_{H^+} \left(c_{Es} c_W - \frac{c_{Al} c_{Ac}}{K_c} \right) \quad (5.4)$$

where k is the reaction rate constant, K_c is the concentration-based on reaction equilibrium constant (Tables 5.3 and 5.4).

Protons H^+ are created by the dissociation of eventually externally added acids (catalyst) and the carboxylic acids, which is formed in the reaction system. The concentration c_{H^+} can be calculated as

$$c_{H^+} = \frac{n_{H^+}^{sys} + n_{H^+}^{ext}}{V_R} \quad (5.5)$$

where $n_{H^+}^{sys}$, $n_{H^+}^{ext}$ are the H^+ mole number contributed by the acids which are part of the reaction system: $n_{H^+}^{sys} = c_{H^+}^{sys,eq} V_R$ and the eventually externally added acids.

For established dissociation equilibrium the concentrations $c_{H^+}^{sys,eq}$ depend on the dissociation constants K_{Ac}^{diss} of acids as follows

$$c_{H^+}^{sys} = \sqrt{K_{Ac}^{diss} c_{Ac}} \quad (5.6)$$

Values constant K_{Ac}^{diss} were listed in Table 3.12.

Alternatively, for non-ideal phases kinetic expressions, the reaction rate can be expressed in terms of activities applying eq. (2.224).

$$r = k_a c_{H^+} \left(a_{Es} a_W - \frac{a_{Al} a_{Ac}}{K_a} \right) \quad (5.7)$$

Here K_a is the activity-based on reaction equilibrium constant (Tables 5.3 and 5.4). The activity coefficients were estimated by again using the UNIFAC method [Fred77]

5.2.1 Constant volume (“Const”)

Most liquid-phase reactions occur on an assumption that the volume of reaction mixture is constant [Leve99]. The constant reaction volume actually means the density of reaction system which is constant, eq. (2.230).

Thus, for a constant volume system, combining eq. (2.230) and mass balance eq. (5.3) then the problem can be expressed as an ODE system.

5.2.2 Varying volume due to reaction (“Ideal”)

This case is much more complex than the simple constant reaction volume. In such systems, even for ideal solutions, the volume of reaction mixture is not constant because of the composition changes caused by chemical reactions.

For the model reactions, eq. (2.241) is replaced as

$$\frac{dV_R}{dt} = r V_R \sum_{i=1}^N \nu_i V_i^0 \quad i = Es, W, Al, Ac \quad (5.8)$$

The values for molar volumes of pure components were given in Table 3.2. Therefore, the ODE system is built by combining eq. (5.8) and mass balance eq. (5.3)

For “*Const*” and “*Ideal*” cases, to quantify the temporal change of the concentration of one component i , in each case, the ODE have to be solved with the following initial conditions:

$$t = 0 : \begin{cases} n_i = n_i^{init} \\ V_R = V_R^{id,init} \end{cases} \quad (5.9)$$

The initial conditions for two ester hydrolysis reactions were given in Table 4.8.

More pronounced volume change effects can occur in case on real mixtures. In this case, significant volume changes can be caused just by mixing. Hence, more complicated forms have to be considered.

5.2.3 Varying volume due to mixing and reaction (“*Real*”)

From eq. (2.252) the varying volume change for this reacting system can be expressed as

$$\frac{dV_R}{dt} = rV_R \sum_i v_i V_i^0 + rV_R \sum_i v_i V_i^E \quad i = \text{Es, W, Al, Ac} \quad (5.10)$$

In real systems, the reaction volume is not constant because of mixing and composition changes due to reaction. From the reduced version of the Ulrici *et al.* model (2.156) ($\delta_{ijk} = 0, \Delta_{1234} = 0$), the molar excess volume for a quaternary system is simplified as determination of the volume of reaction mixture from the corresponding binary

$$V_R^E = V_{Es-W}^E + V_{Al-F}^E + V_{Es-F}^E + V_{Al-W}^E + V_{F-W}^E + V_{Es-M}^E \quad (5.11)$$

Then, the partial molar excess volume of each component was calculated by eqs. (2.76) and (2.77).

Thus, for real systems, the ODE system is built up by combining mass balance eq. (5.3) and eq. (5.10)

To quantify the temporal change of the concentration of one component i , in this case, the ODE have to be solved with the following initial conditions:

$$t = 0 : \begin{cases} n_i = n_i^{init} \\ V_R = V_R^{init} \end{cases} \quad (5.12)$$

The values for initial volumes in “*Real*” case for methyl formate and ethyl formate hydrolysis reactions are 1.014 L and 1.003 L. The values for number of moles n_i^{init} were again given in Table 4.8.

Under isothermal condition, the reaction rate is related to concentrations c_i and reacting volume V_R . Thus, to find out the constant of reaction rate, the mass balance has to be solved simultaneously with reacting volume equation. This is provided by three options (“*Const*”, “*Ideal*” and “*Real*”)

5.2.4 Parameter fitting

Following the progress of the reaction, the concentration profiles measured have to be eventually related to the rate of reaction. To find out the best values of the reaction rate constant (k or k_a), firstly, one k or k_a value is estimated and put into the rate equation (5.4) or (5.7) to predict time dependence of the concentration versus reaction time curve, then the reaction product alcohol profile are compared with the experimental data by using the following objective function of relative concentrations eq. (2.293)

$$OF_c = \frac{1}{NUM} \sum_{k=1}^{NUM} \left[\frac{c_{Al}^{exp}(t_k) - c_{Al}^{cal}(t_k)}{c_{Al}^{exp}(t_k)} \right]^2 \longrightarrow \min \quad (5.13)$$

Hereby, it is respected that no values $c_{Al}^{exp} = 0$ can be processed.

If the fit is unsatisfactory, another reaction rate constant is appraised and tested. This procedure runs till the best-fit value of the reaction rate constant is found out.

Consequently, there are three ways to gain the kinetic parameters: “*Const*”, “*Ideal*” and “*Real*”. Kinetic parameters of the model reaction are determined analysing the transients concentrations measured based on neglecting or incorporating the volume changes of the reaction mixture due to reaction and mixing in the following. To solve these problems, the MATLAB program is employed. The errors of parameters are estimated by comparing the precision of difference between alcohol concentrations measured and its values predicted from kinetic model.

5.2.5 Determined reaction rate constants

Determined rate constants are presented in this section together with component concentration transients measured and predicted. The comparisons of the simulation of two alcohol (methanol and ethanol) concentration profiles and measured data are shown for the three cases: “*Const*”, “*Ideal*” and “*Real*” respectively. Then volume changes of the reaction mixtures in each case are drawn.

Free parameters of kinetics are found out for the three cases of considering V_R described above.

The results obtained by assuming constant reaction volume (“*Const*”) serve as references, to compare with two other ones gained from different Cases (“*Ideal*” and “*Real*”)

$$\Delta k^{Ideal/Real} = \frac{k^{Ideal/Real} - k^{Const}}{k^{Const}} \times 100 [\%] \quad (5.14)$$

and

$$\Delta k_a^{Ideal/Real} = \frac{k_a^{Ideal/Real} - k_a^{Const}}{k_a^{Const}} \times 100 [\%] \quad (5.15)$$

The results of reaction rate constants of two esters hydrolysis reaction at different temperatures are shown from Table 5.7 to 5.10. The differentials of reaction rate constants between “Const” and “Ideal” cases are small and negligible but the values between “Const” and “Real” cases are significant. The different values between “Const” and “Real” cases for methyl formate hydrolysis are bigger than for ethyl formate hydrolysis. The maximum value of the differential is up to 8.6% and thus quite remarkable.

At the same concentration, but at two different temperatures, Arrhenius equation (2.218) indicates that [Leve99]

$$\ln \frac{r_2}{r_1} = \ln \frac{k_2}{k_1} = \frac{E}{R} \left(\frac{1}{T_1} - \frac{1}{T_2} \right) \quad (5.16)$$

That means when the reaction temperature increases the rate of reaction increases. As a rough approximation, the reaction rates of two reactions double for 10K rise in reaction temperature. The difference in values of reaction rate between “Const” and “Ideal” case are negligible but ones between “Const” and “Real” case are considerable.

Table 5.7 The reaction rate constant $10^5 \times k [L^2 mol^{-2} s^{-1}]$ of methyl formate hydrolysis in an ideal kinetic expression, eq. (5.4).

$T[K]$	“Const”	“Ideal”		“Real”	
	$10^5 \times k$	$10^5 \times k$	$\Delta k^{Ideal} [\%]$	$10^5 \times k$	$\Delta k^{Real} [\%]$
288	1.430±0.010	1.422±0.014	-0,5	1.316±0.009	-7,9
293	2.634±0.021	2.620±0.021	-0,5	2.430±0.016	-7,7
298	3.997±0.025	3.974±0.023	-0,6	3.652±0.021	-8,6
303	6.343±0.048	6.307±0.043	-0,6	5.812±0.024	-7,9

Table 5.8 The reaction rate constant $10^5 \times k [L^2 mol^{-2} s^{-1}]$ of ethyl formate hydrolysis in an ideal kinetic expression, eq. (5.4).

$T[K]$	“Const”	“Ideal”		“Real”	
	$10^5 \times k$	$10^5 \times k$	$\Delta k^{Ideal} [\%]$	$10^5 \times k$	$\Delta k^{Real} [\%]$
288	1.984±0.045	1.971±0.041	-0,7	1.892±0.030	-4,6
293	3.117±0.080	3.094±0.071	-0,7	2.963±0.067	-4,9
298	5.221±0.011	5.183±0.010	-0,7	4.959±0.005	-5,0
303	7.758±0.047	7.701±0.035	-0,7	7.378±0.011	-4,9

Table 5.9 The reaction rate constant $k_a[s^{-1}]$ of methyl formate hydrolysis in a non-ideal kinetic expression, eq. (5.7).

$T[K]$	“Const”		“Ideal”		“Real”	
	k_a	k_a	$\Delta k_a^{Ideal} [\%]$	k_a	$\Delta k_a^{Real} [\%]$	
288	0.0078±0.0001	0.0078±0.0001	-1,2	0.0075±0.0001	-4,7	
293	0.0144±0.0002	0.0144±0.0001	-0,7	0.0138±0.0001	-4,2	
298	0.0219±0.0001	0.0218±0.0001	-0,5	0.0210±0.0001	-4,1	
303	0.0347±0.0003	0.0346±0.0002	-0,6	0.0333±0.0001	-4,1	

Table 5.10 The reaction rate constant $k_a[s^{-1}]$ of ethyl formate hydrolysis in a non-ideal kinetic expression, eq. (5.7).

$T[K]$	“Const”		“Ideal”		“Real”	
	k_a	k_a	$\Delta k_a^{Ideal} [\%]$	k_a	$\Delta k_a^{Real} [\%]$	
288	0.0043±0.0001	0.0043±0.0001	0	0.0042±0.0001	-3,8	
293	0.0067±0.0002	0.0067±0.0001	0	0.0065±0.0001	-4,2	
298	0.0113±0.0004	0.0112±0.0003	0	0.0109±0.0001	-4,1	
303	0.0168±0.0009	0.0167±0.0007	0	0.0163±0.0002	-4,0	

Case “Const”: Figure 5.7 shows the comparisons of the measured and the simulated methanol and ethanol concentration profiles for hydrolysis of methyl formate and ethyl formate at 298K based on constant volume of the reaction mixture (“Const”). The concentrations in this case are smaller than measured concentrations. It can be depicted that there is not good agreement with the measured alcohol concentration profiles.

Case “Ideal”: Figure 5.8 shows the comparisons of the measured and the simulated methanol and ethanol concentration profiles for hydrolysis of methyl formate and ethyl formate at 298K based on neglecting the volume changes of the reaction mixture due to mixing (“Ideal”). It can be viewed that the simulation is in slightly better agreement with the measured alcohol concentration profiles than “Const” case.

The first reason for the differences is reaction volumes in both cases (“Const” and “Ideal”) are bigger than one in “Real” case. The second reason is values of reaction equilibrium constants (K_c and K_a) calculated based on “Real” case.

Case “Real”: Figure 5.9 shows comparisons of the measured and the simulated methanol and ethanol concentration profiles for hydrolysis of methyl formate and ethyl formate at 298K based on incorporating the volume changes of the reaction mixture due to reaction and mixing (“Real”). It can be observed that the simulation is in great better agreement with the measured alcohol concentration profiles than “Const” and “Ideal” case.

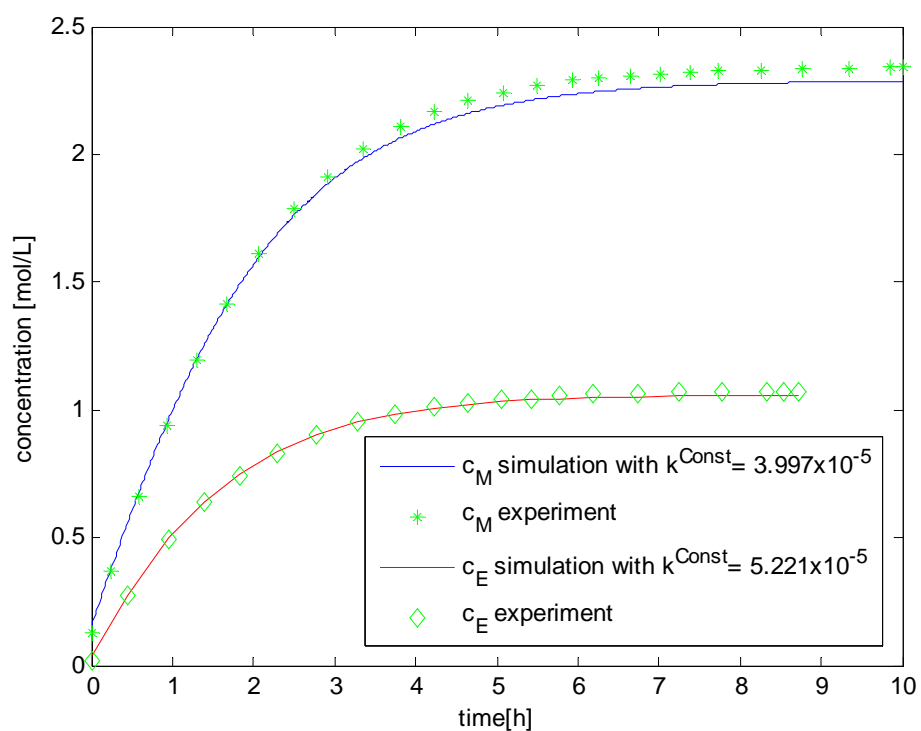


Figure 5.7 Comparison of the measured (symbol) and simulated (“Const”) methanol concentrations for the hydrolysis reaction of methyl formate at 298K performed in the BR.

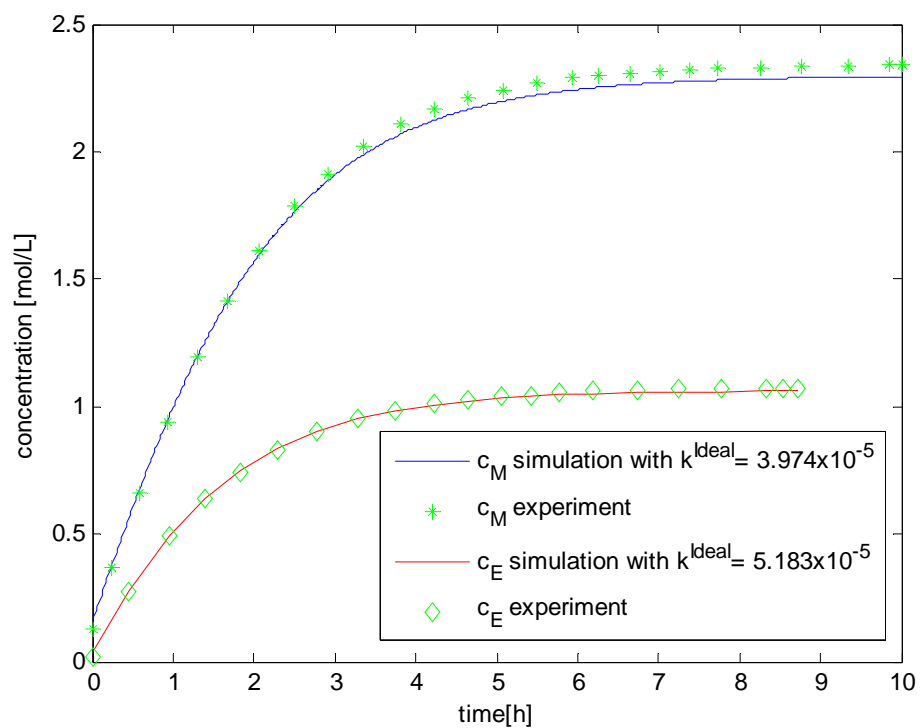


Figure 5.8 Comparison of the measured (symbol) and simulated (“Ideal”) methanol concentration for the hydrolysis reaction of methyl formate at 298K performed in the BR.

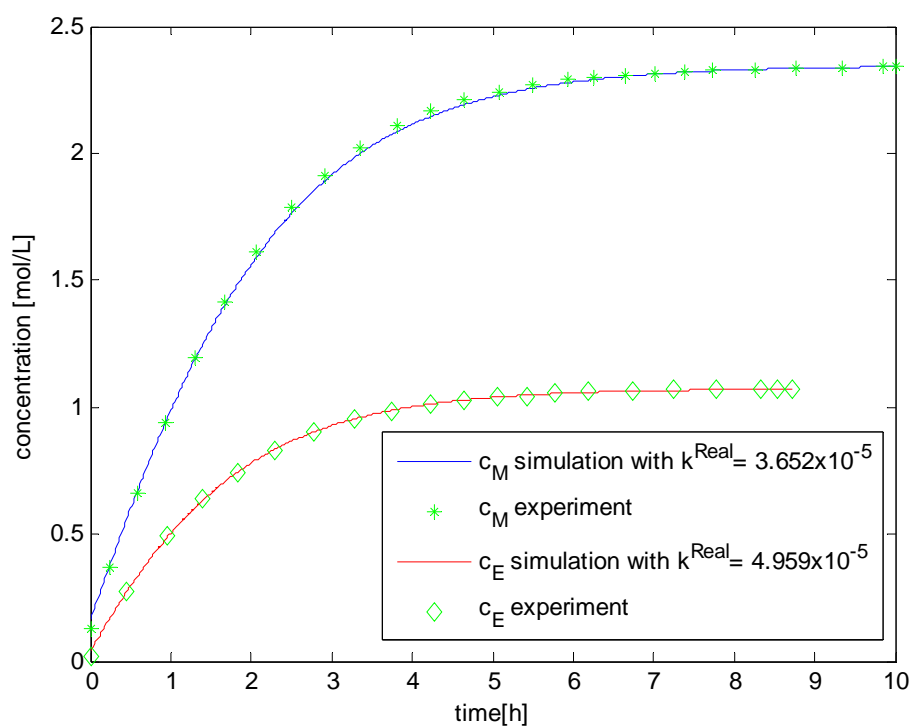


Figure 5.9 Comparison of the measured (symbol) and simulated (“Real”)methanol concentration for the hydrolysis reaction of methyl formate at 298K performed in the BR.

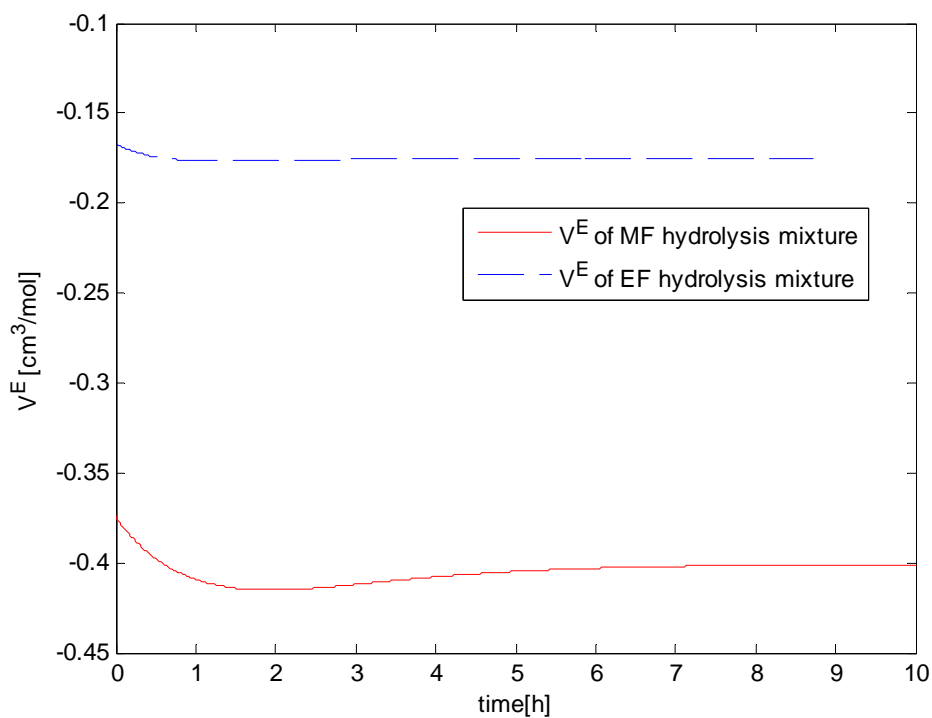


Figure 5.10 Molar excess volumes for the methyl formate (MF) and ethyl formate (EF) hydrolysis mixtures as predicted using eq. (2.156).

At given temperature and pressure, V^E is a function of composition. Following the progress of the reactions, the amounts of reactants are consumed to form the products so molar excess volumes V^E are changed. Figure 5.10 shows the values of V^E changes due to composition changes caused by chemical reactions at 298K and atmospheric pressure. The values of V^E drop when two reactants are mixed together then change smoothly due to both reaction and mixing until the end of the reactions.

The volumes of the reaction mixtures determined for methyl formate and ethyl formate hydrolysis reactions at 298K by using “Const”, “Ideal” and “Real” case are drawn in Figure 5.11 and 5.12. The volumes of the reaction mixtures in “Const” case are used as a reference. It can be seen that, for “Ideal” case, volume changes occur due to composition changes caused by chemical reactions and reach constant at equilibrium when no composition changes. For “Real” case, from beginning of reaction time, when reactants are introduced into reactor, the volume changes of the reaction mixture due to mixing occur immediately. Because of the negative molar excess volume of ester and water mixture, there is a considerable drop in reaction volume. Then, when the reactions occur, composition changes make the volume of reaction mixture happen due to mixing and reaction. The deviations of volume changes of reaction mixture in “Real” case are 2.3% and 1.1% at equilibrium for methyl formate and ethyl formate respectively.

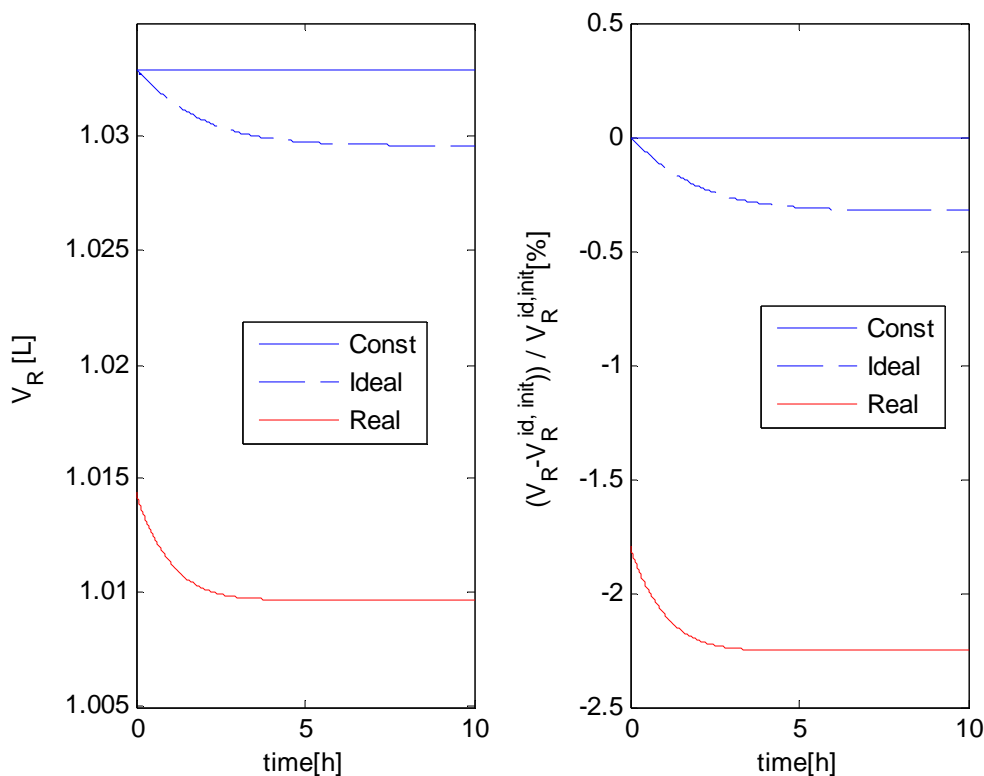


Figure 5.11 Methyl formate hydrolysis comparison between reaction volumes due to different volume changing causes and ideal constant volume versus reaction time.

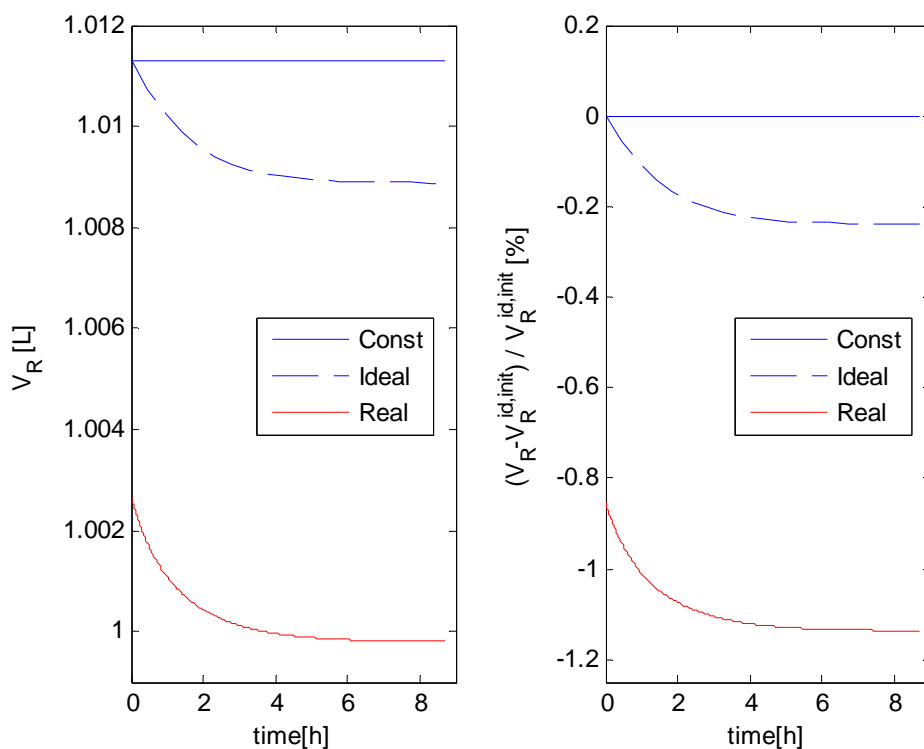


Figure 5.12 Ethyl formate hydrolysis comparison between reaction volume due to different volume changing causes and ideal constant volume versus reaction time.

When the reaction volume changes significantly, it effects the result of kinetic computation. The consideration of the real phenomenons helps us to solve problem clearly and precisely.

In addition, Figures 5.11 and 5.12 clearly show that reaction volumes in “*Ideal*” and “*Real*” models decrease following the course of reactions. When the reaction volume reduces, the concentrations of components in the reaction mixture determined by eq. (2.217) increase. In the kinetic expressions eq. (5.4) and eq. (5.7), since the reaction rates and reaction equilibrium constants are fixed, the reaction rate constants must decrease. The results gained agree with that and list from Table 5.7 to 5.10.

According to the Arrhenius’s law eq. (2.218), a plot of $\ln k$ vs $1/T$ gives a straight line, with large slope for large E and small slope for small E [Leve99]. Thus, Arrhenius parameters can be determined by using the linear regression and the slope of a straight line is $(-E_A/R)$. Figures 5.13 and 5.14 show the best fit lines of Arrhenius equation for two ester hydrolysis reactions.

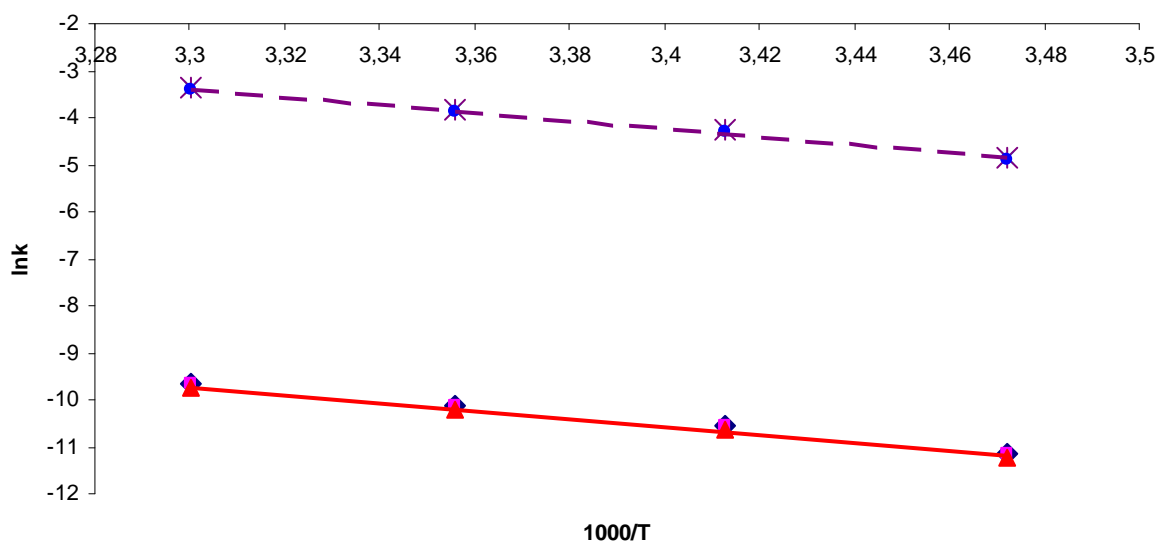


Figure 5.13 Temperature dependence of the reaction rate constants of methyl formate. k^{Const} : \diamond , k^{Ideal} : \square , k^{Real} : Δ , k_a^{Const} : \times , k_a^{Ideal} : $*$, k_a^{Real} : \circ , full lines: k , dashed lines: k_a .

Figures 5.13 and 5.14 provide the rates of reactions go faster as the temperature is raised. Combining the Arrhenius's law and Figures 5.13, 5.14, the activation energy E_a and k_0 quantified are summarized in Tables 5.11 and 5.12

The similar slopes of straight line based on ideal and non-ideal kinetic expression in Figures 5.13, 5.14 indicate an agreement of the Arrhenius parameters of hydrolysis reactions obtained from k and k_a values.

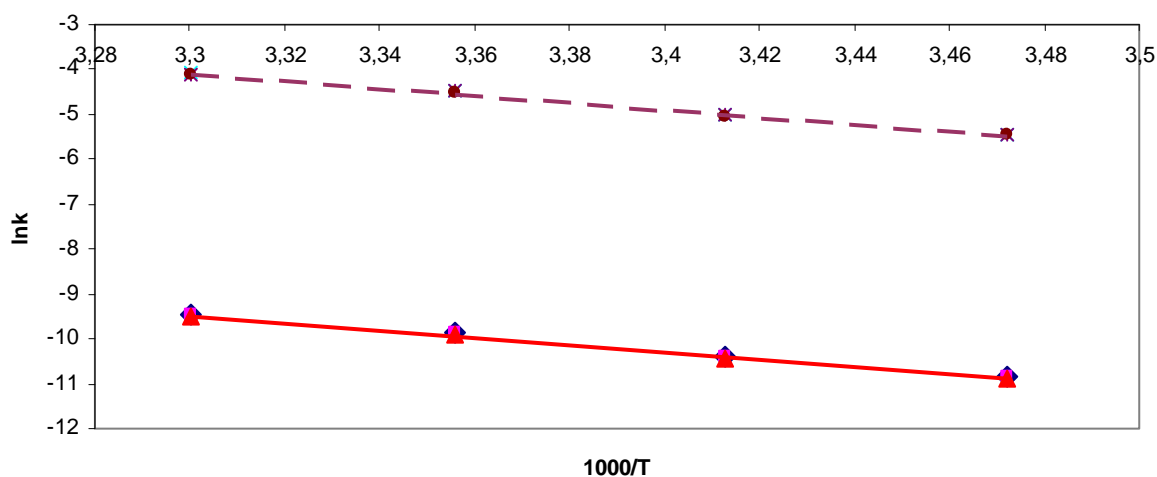


Figure 5.14 Temperature dependence of the reaction rate constants of ethyl formate. k^{Const} : \diamond , k^{Ideal} : \square , k^{Real} : Δ , k_a^{Const} : \times , k_a^{Ideal} : $*$, k_a^{Real} : \circ , full lines: k , dashed lines: k_a .

Table 5.11 The results of kinetic parameters of methyl formate hydrolysis.

<i>Reaction volume</i>	<i>Ideal kinetic expression</i>		<i>Non-Ideal kinetic expression</i>	
	$E_a[\text{kJ/mol}]$	$\ln k_0 [-]$	$E_a[\text{kJ/mol}]$	$\ln k_0 [-]$
<i>Const</i>	70.971 ± 2.932	18.5 ± 1.2	71.122 ± 2.957	24.9 ± 1.2
<i>Ideal</i>	70.949 ± 2.938	18.5 ± 1.2	70.929 ± 2.995	24.8 ± 1.2
<i>Real</i>	70.841 ± 3.026	18.4 ± 1.4	71.043 ± 2.879	24.8 ± 1.2

Table 5.12 The results of kinetic parameters of ethyl formate hydrolysis.

<i>Reaction volume</i>	<i>Ideal kinetic expression</i>		<i>Non-Ideal kinetic expression</i>	
	$E_a[\text{kJ/mol}]$	$\ln k_0 [-]$	$E_a[\text{kJ/mol}]$	$\ln k_0 [-]$
<i>Const</i>	66.867 ± 1.601	17.1 ± 0.7	66.918 ± 1.739	22.5 ± 0.7
<i>Ideal</i>	66.833 ± 1.604	17.1 ± 0.7	66.528 ± 1.561	22.3 ± 0.6
<i>Real</i>	66.719 ± 1.576	16.9 ± 0.7	66.537 ± 1.628	22.3 ± 0.7

These reactions have rates that depend significantly on temperature and they have rather high activation energies.

5.3 SENSITIVITY OF KINETIC PARAMETERS

In order to evaluate the reaction rate constants gained in different ways, two new experiments of hydrolysis of methyl formate and ethyl formate were performed for different initial compositions. New initial experimental conditions for hydrolysis of methyl formate and ethyl formate are shown in Table 4.9.

The results of testing for calculating the methanol concentration profile at initial condition shown in Table 4.9 are depicted in Figures 5.15. The result of evaluation for ethyl formate hydrolysis is shown in Figure 5.16. The concentrations in “*Const*” and “*Ideal*” cases have differences from ones in “*Real*” case. The values for concentration simulated based on “*Real*” case have relatively very good agreements with measured data.

To verify more clearly, for methyl formate hydrolysis, volume changes due to mixing are significant ($\approx 3\%$), whose model can be used to describe properly the features of the batch reactors and generalize well, we take a cross-curve of Figure 5.15 at selected reaction time

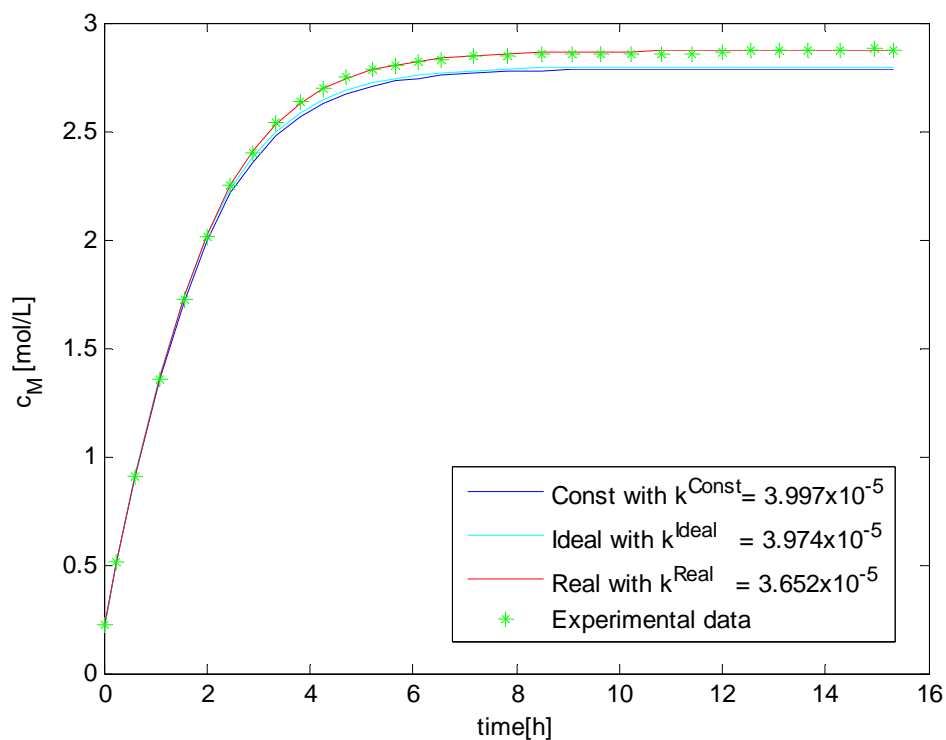


Figure 5.15 Comparisons of the concentration of methanol calculated by using the obtained value of k , and its measured concentrations for hydrolysis of methyl formate at 298K.

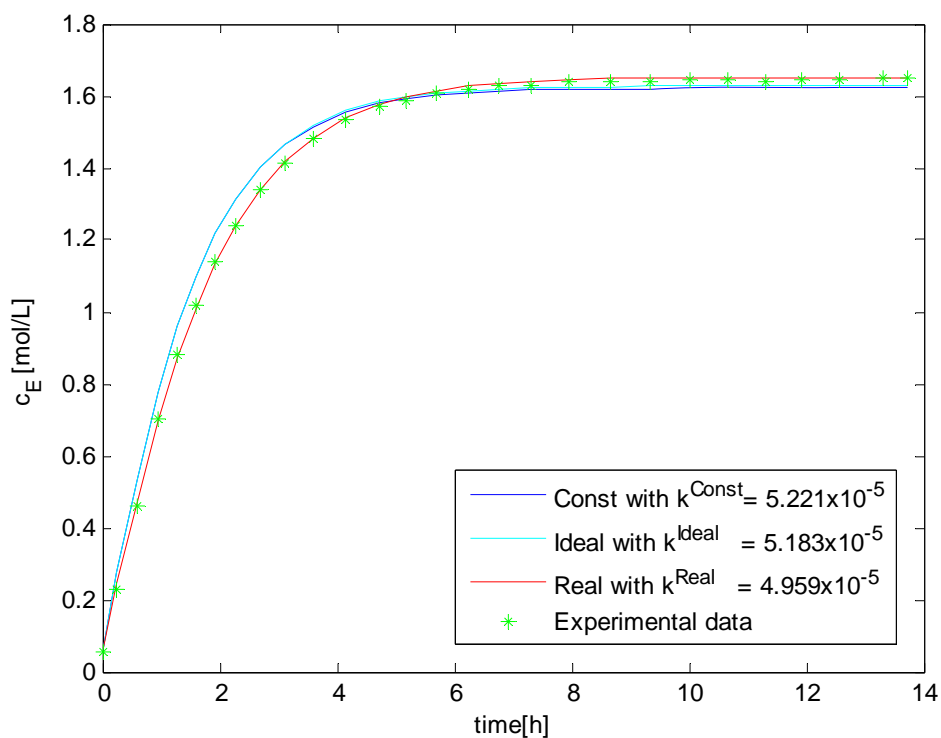


Figure 5.16 Comparisons of the concentration of ethanol calculated by using the obtained value of k , and its measured concentration for hydrolysis of ethyl formate at 298K.

Table 5.13 The comparison between methanol concentrations calculated and their experimentally measured values at different reaction times.

Model	$t = 3h$		$t = 6h$		$t = 15h$	
	c_M [molL ⁻¹]	$\frac{c_M^{cal} - c_M^{exp}}{c_M^{exp}} \%$	c_M [molL ⁻¹]	$\frac{c_M^{cal} - c_M^{exp}}{c_M^{exp}} \%$	c_M [molL ⁻¹]	$\frac{c_M^{cal} - c_M^{exp}}{c_M^{exp}} \%$
<i>Const</i>	2,357	-1,914	2,746	-3,037	2,785	-3,164
<i>Ideal</i>	2,382	-0,874	2,760	-2,542	2,796	-2,781
<i>Real</i>	2,404	0,042	2,824	-0,283	2,87	-0,208
Experiment	2,403	0	2,832	0	2,876	0

From Figures 5.15 and the data shown in Table 5.13, it can be seen that the results gained from “*Const*” and “*Ideal*” case are almost the same and not in good agreement with measured ones, but the “*Real*” model give us the best result and have a great agreement with experimental data.

Therefore, in general, if the changes of volumes are considerable, studies reaction kinetics should be based on incorporating the volume changes of the reaction mixture due to reaction and mixing.

5.4 CORRECTION OF THE REACTION HEAT BY THE HEAT OF MIXING AND SIMULATION OF TEMPERATURE PROFILES

5.4.1 Correction of the reaction heat by the heat of mixing

Now we come back to the results of section 5.1.4. Under isothermal conditions, from the heat balance of a batch reactor eq. (2.276), the heat flux through the wall of reactor $\dot{\mathcal{K}}_{wall}$ measured are included heat of reaction and mixing during reaction process.

As mentioned earlier, since there is significant noise in the low heat flux measurements for the ethyl formate hydrolysis, only the heat flux for hydrolysis of methyl formate are measured with the reaction calorimeter. Thus, the quantitative analysis of experimental heat flux in this section is applied to methyl formate hydrolysis only.

The values for heat flux measured through the wall of reactor are compared with simulated results based on the experimental reaction enthalpy and shown in Figure 5.17. The values computed have a good relatively agreement with the measured values.

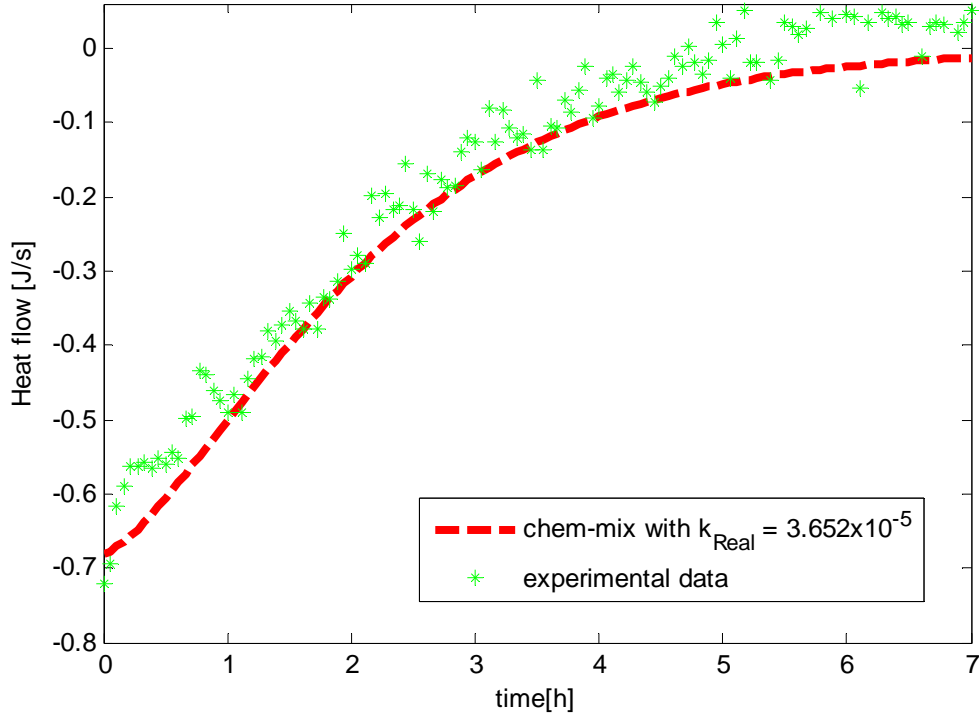


Figure 5.17 Comparisons of simulated $\dot{\mathcal{K}}_{chem-mix}$ and measured $\dot{\mathcal{K}}_{wall}$ (*) heat flux of methyl formate hydrolysis reaction at 298K.

In order to analyse in more detail the heat changes due to mixing and to determine the heat of reaction for methyl formate hydrolysis. As mentioned earlier, the value of measured heat of reaction does not represent the correct heat of reaction but includes heat of mixing. To calculate the reaction enthalpy of this reaction, eq. (2.280) is used. The partial molar excess enthalpy of each component are calculated from eqs. (2.76) and (2.77) with the molar excess enthalpy of quaternary system is simplified from Ulrici *et al* model eq. (2.166)

$$H^E = H_{MF-W}^E + H_{M-F}^E + H_{MF-F}^E + H_{M-W}^E + H_{F-W}^E + H_{MF-M}^E \quad (5.17)$$

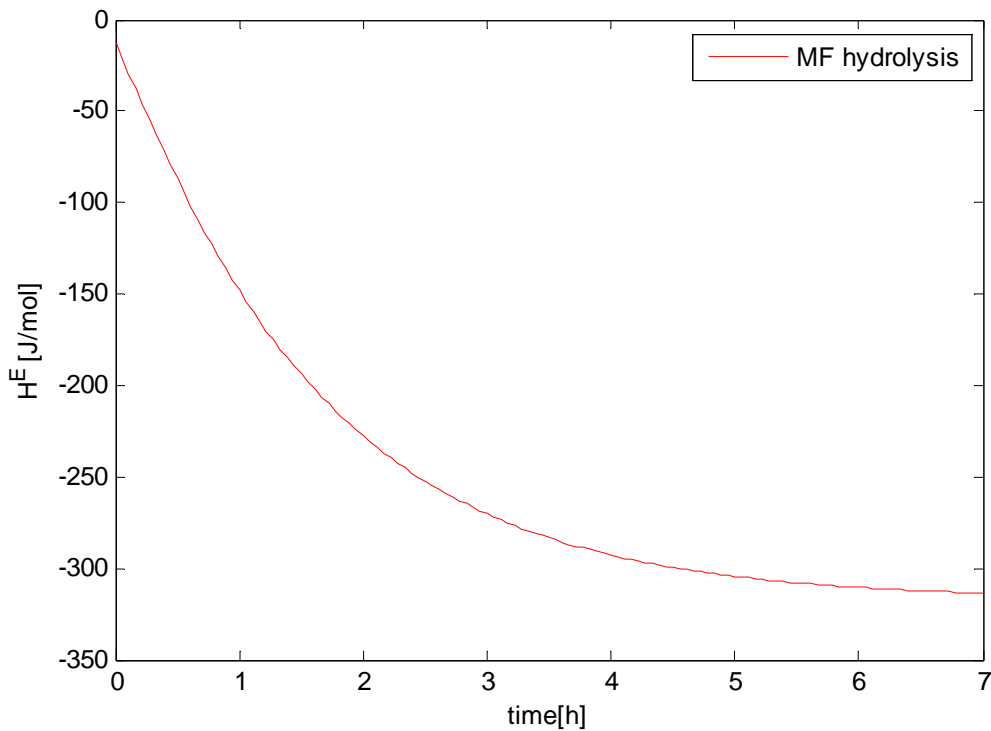


Figure 5.18 Molar excess enthalpies H^E for the methyl formate hydrolysis mixtures. This Figure is linked with V^E shown in Figure 5.10.

At given temperature and pressure, H^E is a function of composition. When the reaction between reactants to form products, the molar excess enthalpies H^E are changed following the progress of the reactions. Figure 5.18 shows the values of H^E changes due to composition changes caused by chemical reactions at 298K and atmospheric pressure. The values of H^E drop when two reactants are mixed together then change smoothly due to both reaction and mixing until the end of the reactions.

Figure 5.19 shows the heat flux of reaction and/or mixing. The differential between heat flux of both reaction and mixing and heat flux of mixing is “correct” reaction heat flux. The quality of reaction heat produced during reaction time can be computed from the area of integration of the reaction heat flow $\dot{\mathcal{H}}_{chem}$ and reaction time. To determine “correct” reaction enthalpy of the reaction, the integration value is then divided by the mole number of reactant consumed from starting time until the reaction reaches equilibrium state.

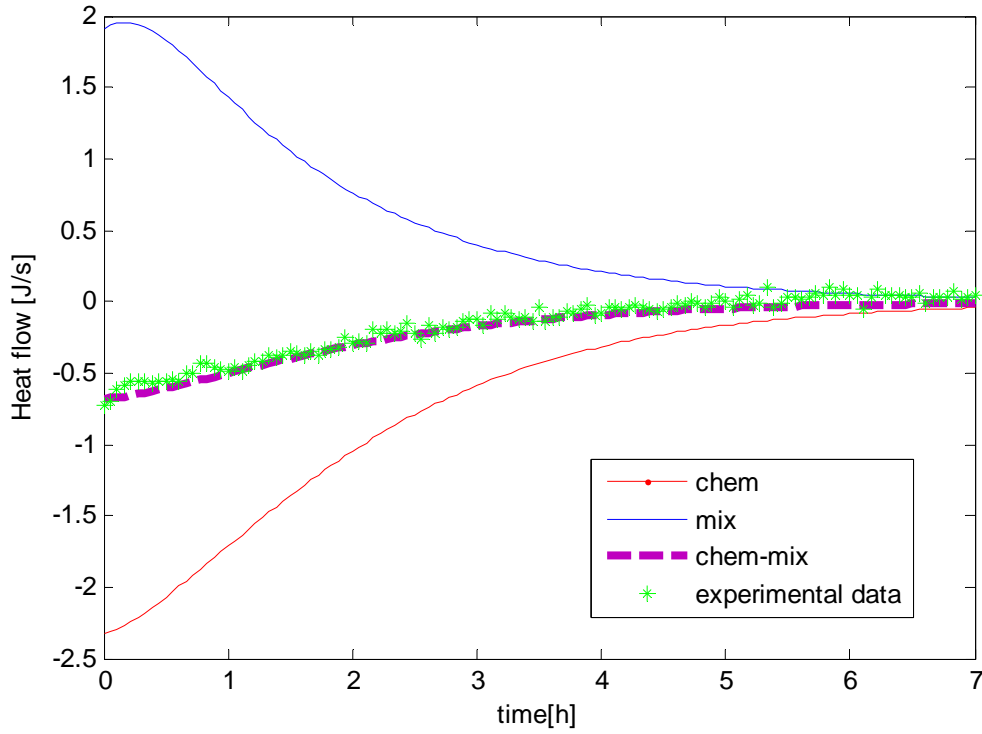


Figure 5.19 Determination of the corrected reaction enthalpy for methyl formate hydrolysis at 298K.

This result in a reaction enthalpy for MF hydrolysis, $\Delta H_R = 9.60$ [kJ/mol], which is good agreement with the values calculated from different sources shown in Table 5.5.

5.4.2 Adiabatic conditions

To evaluate finally the magnitude of the adiabatic temperature rise the result of reaction enthalpy is applied. To quantify the effects of temperature changes of methyl formate hydrolysis, the mass balances and an energy balance has to be solved simultaneously. Adiabatic conditions mention that overall heat transfer across the boundary between the reactor and the surroundings is absent, then leads to $\dot{\mathcal{K}}_{wall} = 0$ and eq. (2.313) becomes

$$\frac{dT}{dt} = \frac{-V_R r \Delta H_R^0 - V_R r \sum_{i=1}^4 \nu_i H_i^E}{\sum_i n_i C_{P,i}} \quad i = \text{Es, W, Al, Ac} \quad (5.18)$$

If we assume the values of $\sum_{i=1}^4 \nu_i H_i^E$ to be negligible, then eq. (5.18) can now be written as

$$\frac{dT}{dt} = \frac{-V_R r \Delta H_R^0}{\sum_i n_i C_{P,i}} \quad i = \text{Es, W, Al, Ac} \quad (5.19)$$

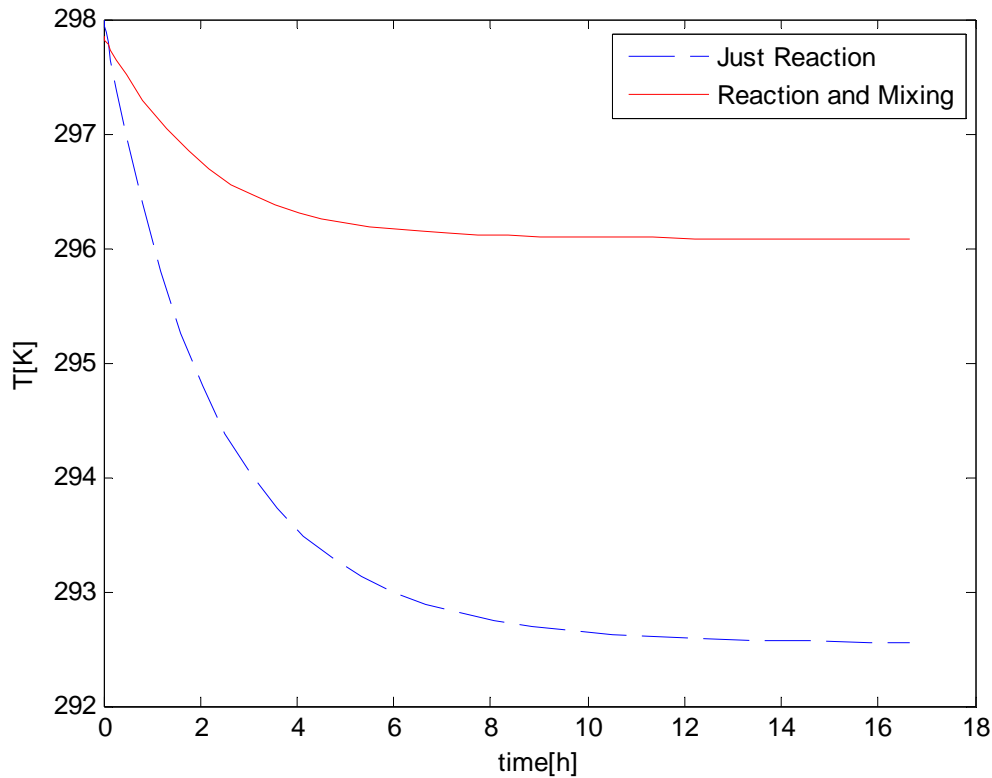


Figure 5.20 The adiabatic temperature decrease of the methyl formate hydrolysis from the initial reaction temperature at $T^{init} = 298\text{K}$ to the minimum temperature at equilibrium.

Figure 5.20 represents the reaction temperature under the adiabatic condition. The results in temperature decrease from initial reaction temperature to minimum reaction temperature when the reaction reaches equilibrium. If the heat of mixing is not considered, the reaction temperature just depends on reaction heat. The value of reaction enthalpy is positive. Thus, the reaction temperature decreases until minimum value at equilibrium. The adiabatic temperature fall $\Delta T \approx -5\text{K}$ is predicted. In reality, the reaction temperature depends on the heat of reaction and mixing. The values for heat of mixing shown in Figure 5.18 are negative. This means mixing is exothermic in this case study. The temperature of reaction mixture in the real case decreases slightly until a minimum value is reached at equilibrium. The slope is smaller than the one for the case assuming temperature dependence of reaction. The adiabatic temperature fall ΔT is approximately -2K . This small difference justifies the validity of the assumptions made regarding V_i^0 and $C_{P,i}$.

The temperature effect observed in this case study might appear small. However it can already influence rates of reaction significantly, as demonstrated for the examples described above (see section 5.2).

CHAPTER 6

CONCLUSIONS AND OUTLOOK

Real phase effects related to volume and temperature changes are often neglected in analysing mixing and reaction processes in solutions. Even for ideal solutions volume changes can occur just due to composition changes caused by chemical reactions. In real solutions considerable additional volume and temperature changes can be caused by mixing.

In this dissertation, the kinetics of two reactions were studied experimentally and theoretically based on neglecting and incorporating the volume changes and heat effects due to mixing and reaction in real solutions.

There is a well established theory available to describe molar excess volumes V^E and molar excess enthalpies H^E . It is based on Gibbs energies, G^E , and activity coefficients, γ , models. To use these models to predict V^E and H^E the parameters should be known as a function of temperature T and pressure P . This theory was summarized in this dissertation. However, for most liquid mixtures the parameters required to apply the theoretical framework are not available.

The effects of mixing in real mixtures on reaction kinetics were analysed first theoretically by using mass and energy balances valid for well-mixed batch reactors. Systematic simulations were performed based on *i*) neglecting and *ii*) incorporating volume and temperature changes due to reaction and mixing effects.

To study the phenomena experimentally the hydrolysis reactions of two esters (methyl formate and ethyl formate) were investigated. The specific values for molar excess volumes V^E and molar excess enthalpies H^E were measured. Concentration profiles of alcohols and heat fluxes were measured in a batch reactor as a function of time quantifying the courses of the reactions.

The observed transients were analysed to find out kinetic parameters *i*) neglecting molar excess volumes V^E and *ii*) incorporating them. The reaction volume changes due to three different cases (“*Const*”, “*Ideal*” and “*Real*”) were simulated and interpreted.

For the methyl formate hydrolysis, the volume changes due to mixing were found to be approximately 3% compared to the volume in the “*Const*” case. Concentration transients

simulated based on neglecting and incorporating the volume changes due to mixing were different but rather comparable. For the ethyl formate hydrolysis, since the volume changes of mixing were found to be ignorable (1.1%), the values of concentrations simulated based on incorporating the volume changes of mixing are almost perfectly the same as those for the case neglecting the volume changes valid for ideal solutions.

Reaction rate constants were quantified by analysing the measured transient concentration profiles. The results gained by assuming constant reaction volume (“*Const*”) served as standard to be compared with cases based on different assumptions (“*Ideal*” and “*Real*”). In the “*Real*” case, the simulated concentration profiles gave the best agreement fit with the measured data.

For different temperatures, the reaction equilibrium constants were computed from component concentrations at equilibrium. For the determination of the equilibrium constants K_a , activity coefficients were calculated using UNIFAC method. The values of reaction equilibrium constants determined were in relative good agreement with literature data.

From the temperature dependence of the equilibrium constants reaction enthalpies were calculated, which were found to be in relative agreement with literature data.

Furthermore, heat fluxes measured calorimetrically for methyl formate hydrolysis gave after correcting mixing effects access to calculate reaction enthalpy. The value for reaction enthalpy is satisfactory agreement with the ones determined from the temperature dependence of K_a .

Temperature profiles in the batch reactor under adiabatic conditions based on incorporating the enthalpy changes due to reaction and mixing were simulated and interpreted exploiting the different sets of kinetic parameters obtained.

This dissertation described then a way to estimate kinetic parameters taking mixing effects into account. Predictions with kinetics based on incorporating molar excess volumes were found to be in a good agreement with concentrations measured. A detail validation of the thermal effects was not possible due to restricted resolution of the calorimetric equipment used in this study.

This work has confirmed that effects of non-idealities in liquid phase reactions for a first coarse analysis of system behaviour can be often neglected. However, a careful consideration appears to be necessary in each specific case to confirm this.

This study illustrated and applied concepts how to incorporate real phase effects and it provided tools and illustrations how to implement them. If changes of volume or enthalpy due to mixing are significant, the behaviour of real solutions should be considered instead of using simplified ideal models. The results should lead to improved calculations, simulations and optimizations of chemical engineering processes.

Future works may deal with extending the results described to the analysis of continuously operated tank reactors and tubular reactors, where feed and product flows are introduced and

withdrawn continuously. Then, volume changes and heats effects due to mixing can be triggered by composition changes caused not only by chemical reactions but also by the inlet flows. Also non-isothermal systems should be evaluated more systematically.

Nomenclature

Latin symbols

a_i	Activity of component i	-
A	Heat transfer area	m^2
c	Concentration	molL^{-1}
C_P	Specific heat capacity	$\text{Jmol}^{-1}\text{K}^{-1}$
E_a	Activation energy	Jmol^{-1}
G	Molar Gibb's free energy $\equiv H - TS$	Jmol^{-1}
G^E	Excess Gibbs energy	Jmol^{-1}
G_i	Partial Gibbs energy of species i in solution	Jmol^{-1}
\mathcal{G}	Total Gibb's free energy	J
ΔG_R^0	Standard Gibbs energy change of reaction	Jmol^{-1}
H	Molar enthalpy $\equiv U + PV$	Jmol^{-1}
H_i	Partial enthalpy of species i in solution	Jmol^{-1}
H^E	Excess enthalpy	Jmol^{-1}
H_i^E	Partial molar excess enthalpy of component i in solution	Jmol^{-1}
ΔH	Enthalpy change of mixing	Jmol^{-1}
ΔH_R^0	Standard enthalpy change of reaction	Jmol^{-1}
\mathcal{K}	Total enthalpy	J
f_i	Fugacity of species i in solution	bar
f_i^0	Fugacity of pure species i	bar
k	Reaction rate constant	$\text{L}^2\text{mol}^{-2}\text{s}^{-1}$
k_a	Reaction rate constant in real kinetic form	s^{-1}
K_a	Thermodynamic equilibrium constant	-
K_c	Concentration –based equilibrium constant	-
n	Number of total moles	mol

n_i	Number of moles of species i	mol
M_i	Molar mass of component i	gmol ⁻¹
P	Pressure	Pa
r	Reaction rate	molL ⁻¹ s ⁻¹
R	Gas constant	Jmol ⁻¹ K ⁻¹
S	Molar Entropy	Jmol ⁻¹ K ⁻¹
S_i	Partial entropy of species i in solution	Jmol ⁻¹ K ⁻¹
S^E	Excess entropy	Jmol ⁻¹ K ⁻¹
T	Absolute temperature	K
T_{jack}	Jacket temperature	K
t_R	Reaction time	s
V	Molar volume	Lmol ⁻¹
V_i	Partial volume of species i in solution	Lmol ⁻¹
V^E	Molar excess volume	Lmol ⁻¹
V_i^E	Partial molar excess volume of component i in solution	Lmol ⁻¹
U	Overall heat-transfer coefficient for the reactor wall	J s ⁻¹ m ⁻² K ⁻¹
V_R	Volume of reaction mixture	L
ΔV	Volume change of mixing	Lmol ⁻¹
x_i	Mole fraction	-

Greek Letter

ν_i	Stoichiometric coefficient of species i	-
γ_i	Activity coefficient of species i in solution	-
ρ	Density	gcm ⁻³
$\xi(t)$	The extent of reaction.	mol
μ	Chemical potential	Jmol ⁻¹
Ω	Molar value of thermodynamic property	-

Ω_i	Partial properties of species i in solution	-
Ω_i^0	Pure species i properties	-

Superscripts and subscripts

a	Activity, activation
Ac	Acid
Al	Alcohol
$chem$	Chemical
E	Excess
eq	Equilibrium
Es	Ester
f	Formation
i	i^{th} component
id	Ideal
$init$	initial
$jack$	Jacket
mix	Mixing
R	Reaction
W	Water
$wall$	Wall
$*$	Standard
0	Pure

References

- [Abbot89] M. M. Abbott, Hendrick C. Van Ness, *Theory and Problems of Thermodynamics*, 2nd edition; McGraw Hill, New York, USA, 1989.
- [Agui09] F. Aguilar, F. E. M. Alaoui, C. Alonso-Trista'n, J. J. Segovia, M. A. Villamana'n, and E. A. Montero, Excess enthalpies of binary and ternary mixture containing dibutyl ether, cyclohexane, and 1-butanol at 298.15K, *J. Chem. Eng. Data* **2009**, *54*, 1672-1679.
- [Akints99] P. W Atkins, L. L. Jones, *Chemical Principles The Quest for Insight*, 1st edition; W. H. Freeman and Company: New York, 1999.
- [Albe01] A. Alberto, A. J. Alberto, R. Eva, and S. Ana, Physical properties and their changes on mixing at 298.15K and atmospheric pressure for the 2-ethoxy-2-methylbutane + methanol + water system; *Journal of Chemical & Engineering Data*, **2001** *46* (5), 1261-1265.
- [Alkis00] Alkis Constantinides, Navid Mostoufi, *Numerical Methods for Chemical Engineerings with MATLAB Aplications*, Prentice-Hall International (UK) Limited, London, 2000.
- [Apel87] A. Apelblat, E. Mansurola, Molar excess volumes of formic acid + water, acetic acid + water and propionic acid + water systems at 288.15, 298.15 and 308.15K. *Fluid Phase Equilibria*, **1987**, *32*, 163-193.
- [Bari93] I. Bari, *Thermochemical data of pure substances*, VHC, Weiheim, 1993.
- [Batt85] J. R. Battler, R. L. Rowley, Excess enthalpies between 293 and 323K for constituent binaries of ternary mixtures exhibiting partial miscibility, *J. Chem. Thermodyn.* **1985**, *17*, 719-732.
- [Ben63] L. Benjamin, G. C. Benson , A deuterium isotope effect on the excess enthalpy of methanol-water solutions; *Canadian Journal of Chemistry*, **1963**.
- [Bouk09] Boukais-Belaribi, Ghénima, Mohammadi ,Amir H., Belaribi, Farid B., Richon, Dominique, Molar excess enthalpies for the binary and ternary mixtures of cyclohexane, tetrahydropyran, and 1,4-dioxane at 308.15K and atmospheric pressure: experimental measurements and correlations. *J. Chem. Eng. Data*, **2009**.
- [Cibul82] I. Cibulka, Estimation of excess volume and density of ternary liquid mixtures of non-electrolytes from binary data, *Coll. Czech. Chem. Commun.* **1982**, *47*, 1414–1419.

- [Coke01] A. K. Coker, *Modeling of Chemical Kinetics and Reactor Design*, Gulf Professional Publishing, Boston, 2001.
- [Coop71] A.R. Cooper, G. V. Jeffreys, *Chemical Kinetics and Reactor Design*, Oliver & Boyd, Edinburgh, UK, 1971.
- [Coto91] B. Coto, J. A.G. Calzon, C. Pando, and J. A. R. Renucio, Prediction of ternary excess enthalpy data by the UNIFAC group contribution method, *Journal of Solution Chemistry*, **1991**, 20, 71-68.
- [CRC05] David R. Lide, *CRC Handbook of Chemistry and Physics, Internet version 2005*; <<http://www.hbcnpnetbase.com>>, CRC Press, Boca Raton, FL, 2005.
- [Domi95] M. Domingesz, A. Camacho, M.C. Lo'pez, F.M. Royo, and J.S. Urieta, Molar excess volumes and viscosities of ternary mixtures (2-butanol + 1-chlorobutane + 1-butylamine) and (2-methyl-2propanol + 1-chlorobutane + 1-butylamine) at 298.15K, *Can. J. Chem.* **1995**, 73, 896-901, Printed in Canada.
- [Don08] H. Dong, L. Shengying, Y. Weidong, Molar excess enthalpies of n,n-dimethylethanolamine with (methanol, ethanol, 1-propanol, and 2-propanol) at T (298.2, 313.2, and 328.2K) and P (0.1 and 10.0 MPa). *J. Chem. Eng. Data*, **2008**, 53, 1927–1931.
- [Enri95] R. L. Enriqueta, G. Josefa, L. L. Jose', C. Alberto and F. Josefa, Experimental and predicted excess enthalpies of the 2,2,2-trifluoroethanol – water –tetraethylene glycol dimethyl ether ternary system using binary mixing data, *J. Chem. Soc., Faraday Trans.* **1995**, 91, 2071-2079.
- [Falk02] T. Falk, A. Seidel-Morgenstern, Analysis of a discontinuously operated chromatographic reactor. *Chem. Eng. Sci.* **2002**, 57, 1599-1606.
- [Gmeh02] J. Gmehling, U. Onken, and W. Arlt, *Vapor-Liquid Equilibrium Data Collection*, Chemistry Data Series, vol. I, parts 1-8, DECHEMA, Frankfurt/Main, 2002.
- [Gmeh93] J. Gmehling, J. D. Li, M. Schiller, A modified UNIFAC model present parameter matrix and results for different thermodynamic properties. *Ind. Eng. Chem. Res.* **1993**, 32, 178–193.
- [Hars09] K. Harsh, K. Bhupinder, K. Ashvinder, A. Tenzin, Y. Surekha. Density and molar excess volume of cyclopentane (1)+ 1-Alkanol (2) systems at (298.15 and 308.15)K, *J. Chem. Eng. Data* **2009**, 165-267.

- [Hemm84] W. Hemminger, G. Höhne, *Calorimetry Fundamentals and Practice*, Verlag Chemie, Germany, 1984.
- [Höhn96] G. Höhne, W. Hemminger, H. J. Flammersheim, *Differential Scanning Calorimetry*, Springer, Berlin, Germany 1996.
- [Illiu00] C. M. Illiuta, K. Thomsen, P. Rasmussen, Extended UNIQUAC model for correlation and prediction of vapour-liquid-solid equilibria in aqueous salt systems containing non-electrolytes. Part A. Methanol-water-salt systems; *Chemical Engineering Science*, **2000**, *55*, 2673-2686.
- [Jac77] R. K. Jacob and K. Fitzner, The estimation of the thermodynamic properties of ternary alloys from binary data using the shortest distance composition path. *Thermochim. Acta*. **1977**, *18*, 197–206.
- [Jian96] H. Jianhua, T. Katsutoshi, M. Sachio, Excess thermodynamic properties of binary mixtures of ethyl formate with benzene, ethanol, and 2,2,2-trifluoroethan-1-ol at 298.15K, *Fluid Phase Equilibria* **1996**, *131*, 197-221.
- [Jiri72] P. Jiri and B. C.-Y.Lu; Excess Gibbs free energies and excess volumes of methyl formate + methanol and methyl formate + ethanol at 298.15K. *J. Chem. Thermodynamics* **1972**, *4*, 469-476.
- [Jogun10] O. Jogunola; T. Salmi; K. Eränen; J. Wärnä; M. Kangas, and J.-P. Mikkola. Reversible autocatalytic hydrolysis of alkyl formate: Kinetics and reactor modelling, *Ind. Eng. Chem. Res.* **2010**, *49*, 4099-4106.
- [John99] M. P. John, N. L. Rüdiger, G. A. Edmundo, *Molecular Thermodynamics of Fluid-Phase Equilibria*, 3rd edition; Prentice Hall International: London, UK, 1999.
- [Jose06] V. H. Jose, R. Belda, Refractive indices, densities and molar excess volumes of monoalcohols + water. *J. Solution Chem.* **2006**, *35*, 1315–1328
- [Klau88] G. R. P. Klaus, M. Franz, G. Hans-Ulrich, *Merck FT-IR Atlas*, VCH, 1988.
- [Kohl60] F. Kohler, Estimation of the thermodynamic data for a ternary system from the corresponding binary systems, *Monatsch. Chem.* **1960**, *91*, 738–740.
- [Kriiss01] H. Kirss, M. Kuus, E. Siimer, L. Kudryavtseva, Molar excess enthalpies of ternary system o-xylene + hexan-2-one + nonane at 298.15K, *Proc. Estonian Acad. Sci. Chem.* **2001**, *50*, 89-94.

- [Kriss96] H. Kirss, L. Kudryavtseva, M. Kuus, E.Siimer, Excess enthalpies for ternary mixtures phenol-3-methylphenol-1-hexanol, 3-mehtylphenol-1-hexanol-cyclohexanol and their constituent binaries at 318.15K, *Chem. Eng. Comm.* **1996**, *146*, 139-147.
- [Lang99] *Langer's Handbook of chemistry 15th*, edited by Dean, J.A.; McGraw Hill, Inc.: New York, 1999.
- [Leve99] O. Levenspiel, *Chemical Reaction Engineering*, 3rd edition; John Wiley & Sons, 1999.
- [Luci98] L. Luciano, M. Enrico, Excess volumes of the ternary system ethanol + tetrahydrofuran + cyclohexane at 298.15K. *Fluid phase equilibria.* **1998**, *145*, 69-87.
- [Mai06] T. P. Mai, *Experimental investigation of heterogeneously catalysed hydrolysis of ester*, Dissertation, 2006, Uni-Magdeburg.
- [Man97] H. Manfred, M. Herbert, Z. Bernd, *Spectroscopic Methods in Organic Chemistry*, Georg Thieme Verlag Stuttgart, 1997.
- [Medin02] C. Medina, J. Fernandez, J. Legido, A. M. I. Paz, Determination of molar excess enthalpies of α,ω -dichloroalkane +1-butanol or 1-heptanol mixtures at 298.15K. analysis and comparison with predicted values of UNIFAC; *J. Chem. Eng. Data.* **2002**, *47*, 411-415.
- [Miss99] R. W. Missen, C. A. Mims, B. A. Saville, *Introduction to Chemical Reaction Engineering and Kinetics*; John Wiley&Son, Inc: New York, USA, 1999.
- [Ness82] H. C. Van Ness, M. M. Abbott, *Classical Thermodynamics of Nonelectrolyte Solutions*, 1st edition; McGraw-Hill: New York, USA, 1982.
- [Never02] N. D. Never, *Physical and Chemical Equilibrium for Chemical Engineering*; John Wiley & Sons, New York, USA, 2002.
- [Ola10] J. Olatunde, S. Tapio, E. Kari, W. Johan, K. Matias, and J.-P. Mikkola. Reversible Autocatalytic Hydrolysis of Alkyl Formate: Kinetic and Reactor Modeling, *Ind. Eng. Chem. Res.* **2010**, *49*, 4099-4106.
- [Orye65] R. V. Orye, J. M. Prausnitz, Multicomponent equilibria with the Wilson equation. *Ind. Eng. Chem.* **1965**, *57*, 18-26.
- [Perry99] R. H. Perry, D. W. Grenn, and J. O. Maloney, *Perry's Chemical Engineers'*

Handbook, 7th edition; McGraw-Hill, 1999.

- [Rado77] N. Radojkovic, A. Tasic, D. Grozdanic, B. Djordevic, and M.M.Malic, Excess volumes of acetone + benzene, acetone + cyclohexane, and acetone + benzene + cyclohexane at 298.15K, *J. Chem. Thermodyn.* **1977**, *9*, 349–356.
- [Rasto77] R. P. Rastogi, J. Nath, S. S. Das, *J. Chem. Data.* **1977**, *22*, 249.
- [Renon68] H. Renon, J. M. Prausnitz, Local composition in thermodynamic excess function for liquid mixtures. *AIChE J.* **1968**, *14*, 134–144.
- [Robe87] C. R. Robert, M. P. John, P. E. Bruce, *The Properties of Gases and Liquids*, 4th edition; McGraw-Hill: New York, USA, 1987.
- [Rober75] G. W. Robert, and H. W. Eugene, An experimental and computational study of the Hydrolysis of methyl formate in a chromatographic reactor, *Advances in chemistry series*, **1975**, *13*, 181-190.
- [Rui07] M. P. Rui, F. C. Henrique, G. M. F. Abel, and M. A. F. Isabel, Viscosity and density of water + ethyl acetate + ethanol mixtures at 298.15 and 318.15 K and Atmospheric Pressure; *Journal of Chemical & Engineering Data*, **2007** *52* (4), 1240-1245.
- [Sand99] S. I. Sandler, *Chemical and Engineering Thermodynamics*, 3rd edition; John Wiley&Sons, Inc., New York, USA, 1999.
- [Scat52] G. Scatchard, L. B. Ticknor, J. R. Goates, E. R. McCartney, *J. Am. Chem. Soc.* **1952**, *74*, 3721.
- [Schm98] L. D. Schimidt, *The Engineering of Chemical Reactions*, Oxford University Press, New York, 1998.
- [Silb01] R. J. Silbey, R. A. Alberty, *Physical chemistry*: John Wiley & Son, Inc.: New York, USA, 2001.
- [Singh84] P. P. Singh, R. K. Nigam, S. P. Sharma, and S. Aggarwal, *Fluid Phase Equil.* **1984**, *18*, 333.
- [Smith05] J. M. Smith, H. C. Van Ness, M. M. Abbott, *Introduction to Chemical Eng. Thermodynamics*, 6th edition; McGraw-Hill: Boston, USA, 2005.
- [Smith81] J. M. Smith, *Chemical Engineering Kinetics*, 3rd edition; McGraw Hill, New York, USA, 1981.

- [Stoess08] F. Stoessel, *Thermal Safety of Chemical Processes*, Wiley-VCH Verlag GmbH & Co. KGaA, Germany, 2008.
- [Stull69] D. R. Stull, E. F. Westtrum, G. C. Sinke, *The Chemical Thermodynamics of Organic Compounds*, John Wiley&Son, New York, 1969.
- [Tami09] R. Tamilarasan, A. Anand Prabu, M. Raajenthiren, M. Dharmendra Kumar, Chang Kyoo Yoo, Effect of dissolved salts on the enthalpy of mixing of the methanol + formic acid system at 303.15 K. *J. Chem. Eng. Data*, **2009**, *54*, 4–7.
- [Tej99] M. A. Tejjraj, Thermodynamic interactions in binary mixtures of ethenylbenzene with methanol, ethanol, butan-1-ol, pentan-1-ol, and hexan-1-ol in the temperature range 298.15-308.15K. *J. Chem. Eng. Data* **1999**, *44*, 1291-1297.
- [Toop65] G. W. Toop, *Trans. TMS-AIME*, **1965**, *233*, 850.
- [Tsao53] C. C. Tsao, J.M. Smith, *Chem. Eng. Prog. Symp.* **1953**, *49*, 107.
- [Ulri06] A. Ulrici, M. Cochi, G. Foca, M. Manfredini, A. Marchetti, S. Sighinolfi, and L. Tassi, Study of the dependence on temperature and composition of the volumic properties of ethane-1,2-diol + 2-methoxyethanol + 1,2-dimethoxyethane +water solvent system and graphical representation in the quaternary domain, *Journal of solution chemistry*, **2006**, *35*, No. 2.
- [Vu07] D. T. Vu, *Analysis of heterogeneously catalysed ester hydrolysis reactions in a fixed-bed chromatographic reactor*, Dissertation 2007, Uni-Magdeburg.
- [Weste90] K. R. Westerterp, W. P. M. Van Swaaij, A. A. C. M. Beenackers, *Chemical reactor design and operation*; John Wiley & Sons: New York, 1990.
- [Weth75] R. G. Wetherold; E. H. Wissler. An experimental and computational study of the Hydrolysis of methyl formate in a chromatographic reactor. *Advances in chemistry series*, **1975**, *13*, 181-190.
- [Yaws99] C. L. Yaws, *Chemical Properties Handbook*, McGraw Hill, New York, 1999.

Appendix A

Calculation of Gibbs energies of formation.

The ΔG_f^0 value in liquid state of methyl formate is calculated from available data of its value in gas state ($\Delta G_f^{0,gas}$) and vapor-pressure (P^{gas}) [Silb99]

$$\Delta G_f^0 = \Delta G_f^{0,gas} + RT^0 \ln\left(\frac{P}{P^{gas}}\right) \quad (\text{B.1})$$

where, $T^0 = 298\text{K}$, P is the pressure of liquid at standard state $P = 1 \text{ bar}$ ($\sim 14.5038 \text{ Psi}$).

The partial vapor-pressure is obtained by Antoine equation [Lang99]

$$\log P^{gas} = A - \frac{B}{T + C} \quad (\text{B.2})$$

Where A , B and C are the Antoine equation coefficients. These values of A , B and C for the investigated components are collected and given in Table A.1 [Lang99]

Table A.1 The coefficients of Antoine equation.

Compound	Temp. range, [K]	Antoine equation's coefficients		
		A	B	C
MF	294-306	3.0270	3.02	-11.90
EF	277-327	7.0091	1123.94	218.20

Appendix B

Molar excess volume V^E

B.1. Methyl formate/water and Ethyl formate/water

Since solubility of esters in water is limited (solubility in water at 20°C is 300g/L for methyl formate and 105g/L for ethyl formate), so we just measured the excess volume V^E in dilute aqueous solution of ester. The experimental results for the binary mixture of ester/water at 25°C and atmospheric pressure are listed in Table B.1

Table B.1 Experimental molar excess volume V^E for methyl formate/water and ethyl formate/water mixture at 298K.

Mixture	<i>Methyl formate/water</i>		<i>Ethyl formate/water</i>	
	x_{MF}	V^E [cm ³ mol ⁻¹]	X_{EF}	V^E [cm ³ mol ⁻¹]
1	0,012077	-0,09024	0,004341	-0,02853
2	0,023419	-0,16465	0,008804	-0,04854
3	0,035338	-0,24076	0,012905	-0,06771
4	0,045969	-0,30181	0,017554	-0,09054
5	0,056397	-0,35768	0,021838	-0,1087
6	0,063815	-0,39209	0,025645	-0,12172
7	0,075528	-0,44093	-	-
8	0,086441	-0,49885	-	-

B.2 Methyl formate/formic acid and Ethyl formate/formic acid

Table B.2 Experimental molar excess volume V^E for methyl formate/formic acid and ethyl formate/formic acid mixture at 298K.

Mixture	<i>Methyl formate/formic acid</i>		<i>Ethyl formate/formic acid</i>	
	x_{MF}	V^E [cm ³ mol ⁻¹]		V^E [cm ³ mol ⁻¹]
1	0,023756	-0,00076	0,018811	0,015478
2	0,061979	-0,00218	0,04971	0,028993
3	0,133784	-0,00959	0,103862	0,039424
4	0,206724	-0,02179	0,167463	0,058034
5	0,289123	-0,04528	0,235534	0,066489
6	0,384581	-0,09919	0,318507	0,063113
7	0,467142	-0,11913	0,411126	0,02515
8	0,515132	-0,12258	0,517644	-0,00376
9	0,571917	-0,1234	0,651722	-0,04585
10	0,706743	-0,12181	0,80924	-0,05659
11	0,839778	-0,10131	0,918499	-0,04134
12	0,935177	-0,07589	-	-
13	0,966877	-0,04209	-	-

B.3 Methanol/formic acid and Ethanol/formic acid

Table B.3 Experimental molar excess volume V^E for methanol/formic acid and ethanol/formic acid mixture at 298K.

Mixture	<i>Methanol/formic acid</i>		<i>Ethanol/formic acid</i>	
	x_M	V^E [cm ³ mol ⁻¹]	x_E	V^E [cm ³ mol ⁻¹]
1	0,038475	-0,00269	0,025783	-0,022789
2	0,092685	-0,00531	0,066523	-0,090981
3	0,186555	-0,0185	0,150118	-0,156399
4	0,268091	-0,03856	0,222929	-0,226382
5	0,365619	-0,05075	0,307081	-0,264850
6	0,468782	-0,06499	0,388804	-0,274093
7	0,57017	-0,08059	0,492176	-0,248824
8	0,67134	-0,08456	0,596217	-0,222626
9	0,784373	-0,08311	0,712341	-0,178456
10	0,892135	-0,07348	0,851489	-0,130847
11	0,955552	-0,05954	0,921394	-0,103272
12	0,978704	-0,04721	-	-

The molar excess volumes of the other binary system: methanol(1)/water(2), ethanol(1)/water(2) [Jose06] , formic acid(1)/water(2) [Apel87] and methyl formate(1)/methanol(2) [Jri71], ethyl formate/ethanol [Jian96] were collected from literature.

B.4 Methanol/water and Ethanol/water

The experimental data of methanol/water and ethanol/water system from literature [Joe06] was presented in Table B.4

Table B.4 Experimental molar excess volume V^E for methanol/water and ethanol/water mixture at 298K.

Mixture	Methanol/water		Ethanol/water	
	x_M	V^E [cm ³ mol ⁻¹]	x_E	V^E [cm ³ mol ⁻¹]
1	0,101	-0,35947	0,101	-0,4548
2	0,1995	-0,63911	0,2001	-0,7877
3	0,3102	-0,85815	0,2987	-0,9859
4	0,333	-0,897	0,3332	-1,0218
5	0,4054	-0,97369	0,4087	-1,0415
6	0,5006	-1,0126	0,5051	-0,9665
7	0,5998	-0,97445	0,603	-0,8037
8	0,7035	-0,84819	0,6664	-0,6773
9	0,8122	-0,6206	0,7032	-0,6033
10	0,9002	-0,36469	0,7956	-0,4312
11	1	0	0,9075	0,26738

B.5 Formic acid/water

The determined molar excess volume V^E of formic acid/water at 298K is presented in Table B.5 [Apel87].

Table B.5 Molar excess volume V^E in the formic acid + water system at 298K.

Mixture	x_M	$V^E[\text{cm}^3\text{mol}^{-1}]$
1	0,0202	-0,061
2	0,0249	-0,079
3	0,0414	-0,11
4	0,0501	-0,13
5	0,0645	-0,16
6	0,0752	-0,18
7	0,1428	-0,28
8	0,2072	-0,34
9	0,2443	-0,37
10	0,2809	-0,38
11	0,3234	-0,4
12	0,3699	-0,41
13	0,4756	-0,41
14	0,6098	-0,37
15	0,6878	-0,31
16	0,7786	-0,25
17	0,8722	-0,14
18	0,923	-0,1
19	0,9236	-0,11
20	0,949	-0,078
21	0,949	-0,065
22	0,9528	-0,066
23	0,9677	-0,048
24	0,974	-0,038
25	0,9745	-0,04
26	0,9862	-0,036
27	0,9875	-0,019

B.6 Methyl formate/methanol and ethyl formate/ethanol

The determined molar excess volume V^E of methyl formate/methanol [Jiri71] and ethyl formate/ethanol system at 298K [Jian96] were presented in Table B.6

Table B.6 Experimental molar excess volume V^E for methyl formate/methanol and ethyl formate/ethanol mixture at 298K.

Mixture	Methyl formate/methanol		Ethyl formate/ethanol	
	x_{MF}	$V^E[\text{cm}^3\text{mol}^{-1}]$	x_{EF}	$V^E[\text{cm}^3\text{mol}^{-1}]$
1	0.0517	-0.0204	0,0251	0,007
2	0.1055	-0.0411	0,05	0,019
3	0.1702	-0.0591	0,1004	0,042
4	0.2479	-0.0737	0,1502	0,063
5	0.3201	-0.0815	0,1989	0,078
6	0.3957	-0.0847	0,2502	0,096
7	0.4563	-0.0842	0,3001	0,106
8	0.51	-0.0824	0,3497	0,118
9	0.5567	-0.0798	0,3988	0,126
10	0.5961	-0.0763	0,4513	0,129
11	0.6289	-0.0729	0,5007	0,13
12	0.6689	-0.0674	0,5509	0,133
13	0.7134	-0.0613	0,5997	0,131
14	0.7623	-0.0538	0,6503	0,128
15	0.8122	-0.045	0,7004	0,122
16	0.8576	-0.0361	0,7457	0,113
17	0.9058	-0.0255	0,7995	0,1
18	0.9476	-0.015	0,8561	0,083
19	0.9784	-0.0066	0,9003	0,063
			0,9489	0,037
			0,9732	0,02

Appendix C

Molar excess enthalpy H^E

C.1 Methyl formate/water and Ethyl formate/water

Table C.1 the experimental molar excess enthalpy H^E in Jmol^{-1} at 25°C for methyl formate/water and ethyl formate/water.

Methyl formate(1)/water(2)		Ethyl formate(1)/water(2)	
x_{MF} [-]	H^E [$\text{J}\cdot\text{mol}^{-1}$]	x_{EF} [-]	H^E [$\text{J}\cdot\text{mol}^{-1}$]
0.000	0.00	0.000	0.00
0.002	-8.43	0.005	-15,8874
0.004	-13.52	0.010	-22,1466
0.005	-14.02	0.015	-28,8839
0.006	-16.19	0.020	-25,7913
0.007	-17.90	0.025	-24,7002
0.008	-21.88	1.000	0.00
0.010	-27.18		
0.015	-25.82		
0.021	-26.13		
0.025	-29.66		
0.035	-28.84		
0.043	-22.08		
0.051	-6.13		
0.058	12.24		
0.065	37.03		
0.080	89.85		
1.000	0.00		

C.2 Methanol/water and Ethanol/water

Table C.2 The experimental molar excess enthalpy H^E in Jmol^{-1} at 25°C for methanol/water and ethanol/water.

Methanol(1)/water(2)		Ethanol (1)/water(2)	
x_M [-]	H^E [$\text{J}\cdot\text{mol}^{-1}$]	x_E [-]	H^E [$\text{J}\cdot\text{mol}^{-1}$]
0.000	0.00	0.000	0.00
0.050	-304.14	0.102	-629.30
0.101	-526.02	0.200	-675.50
0.205	-709.50	0.301	-536.86
0.296	-728.67	0.400	-444.32
0.352	-708.19	0.503	-341.95
0.403	-703.14	0.603	-268.39
0.501	-669.61	0.693	-243.47
0.602	-663.76	0.796	-176.76
0.703	-563.51	0.901	-129.74
0.804	-427.21	1.000	0.00
0.904	-244.27		
1.000	0.00		

C.3Methanol/Methyl formate and ethanol/Ethyl formate

Table C.3 the experimental molar excess enthalpy H^E in Jmol^{-1} at 25°C for methnol/methyl formate and ethanol/ethyl formate.

Methanol(1)/ Methyl formate(2)		Ethanol(1)/ Ethyl formate(2)	
x_M [-]	H^E [$\text{J}\cdot\text{mol}^{-1}$]	x_E [-]	H^E [$\text{J}\cdot\text{mol}^{-1}$]
0.000	0.00	0.000	0.000
0.105	629.42	0.097	795.323
0.205	986.90	0.191	1072.630
0.308	1081.61	0.300	1365.664
0.405	1037.44	0.399	1368.931
0.502	1015.84	0.497	1275.223
0.602	812.47	0.600	1144.658
0.701	767.38	0.701	1051.334
0.802	618.14	0.801	859.044
0.904	367.34	0.897	522.007
1.000	0.00	1.000	0.000

C.4 Formic acid/ Methyl formate and Formic acid/Ethyl formate

Table C.4 The experimental molar excess enthalpy H^E in Jmol^{-1} at 25°C for Formic acid/methyl formate and formic acid/ethyl formate.

Formic acid(1)/ Methyl formate(2)		Formic acid(1)/ Ethyl formate(2)	
x_F [-]	H^E [$\text{J}\cdot\text{mol}^{-1}$]	x_F [-]	H^E [$\text{J}\cdot\text{mol}^{-1}$]
0.000	0.00	0.000	0.00
0.105	-365.62	0.097	-87.46
0.207	-584.48	0.191	-121.05
0.306	-564.92	0.300	-152.05
0.400	-514.11	0.399	-178.81
0.502	-457.27	0.497	-198.77
0.600	-336.06	0.600	-172.51
0.700	-286.41	0.700	-154.67
0.803	-261.22	0.797	-133.32
0.904	-153.63	0.899	-108.27
1.000	0.00	1.000	0.00

C.5 Formic acid/Methanol and Formic acid/Ethanol

Table C.5 the experimental molar excess enthalpy H^E in Jmol^{-1} at 25°C for Formic acid/methanol and Formic acid/ethanol.

Formic acid(1)/Methanol(2) [Tami09]		Formic acid(1)/ Ethanol(2)	
x_F [-]	H^E [$\text{J}\cdot\text{mol}^{-1}$]	x_F [-]	H^E [$\text{J}\cdot\text{mol}^{-1}$]
0	0	0.000	0.00
0,205	-19,3	0.097	-174.35
0,255	-31,4	0.198	-355.54
0,345	-50,4	0.294	-551.94
0,45	-77,9	0.393	-802.45
0,525	-85,8	0.500	-1029.02
0,585	-95,3	0.599	-1192.44
0,645	-100,9	0.699	-1316.45
0,695	-104,7	0.800	-1367.64
0,813	-94,6	0.900	-730.82
0,884	-76,2	1.000	0.00
0,932	-62,4		
1	0		

C.6 Formic acid /water

Table C.6 The experimental molar excess enthalpy H^E in Jmol^{-1} at 25°C for Formic acid/water.

Formic acid(1)/water(2)	
x_F [-]	H^E [$\text{J}\cdot\text{mol}^{-1}$]
0.000	0.000
0.101	-57.339
0.201	-113.109
0.304	-193.968
0.401	-246.555
0.500	-310.248
0.603	-336.609
0.701	-316.352
0.808	-222.176
0.904	-128.577
1.000	0.000

Appendix D

IR spectra of pure components

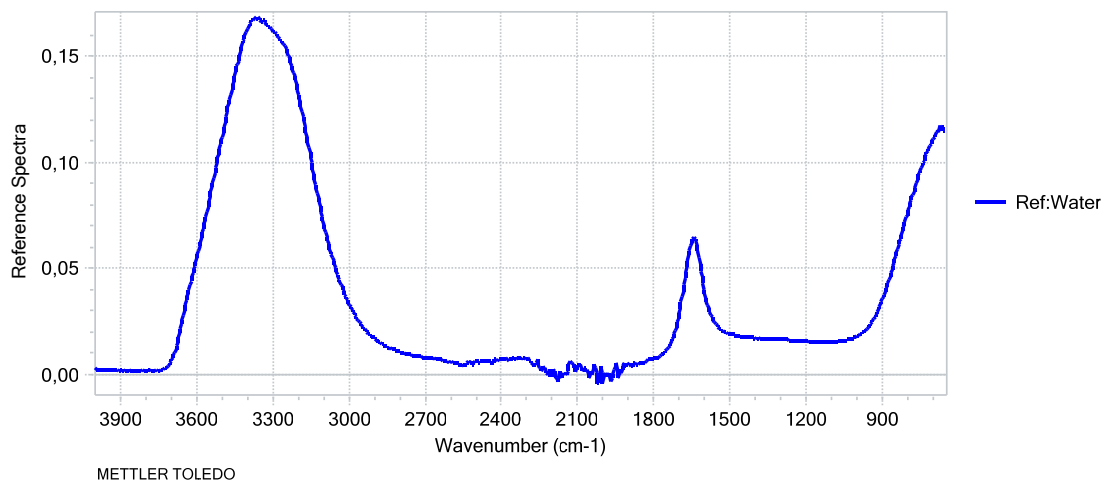


Figure D.1 IR spectra of pure water

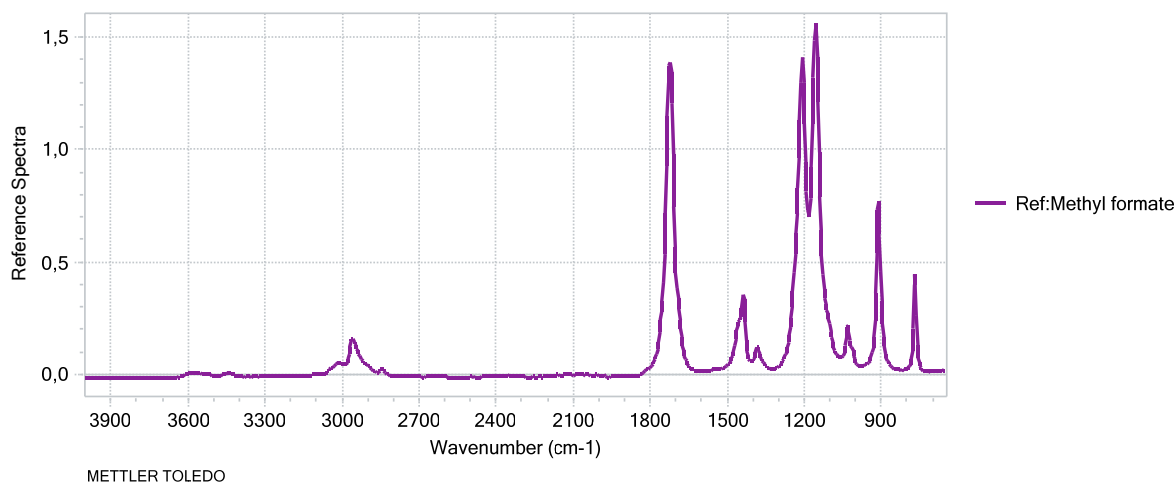


Figure D.2 IR spectra of pure methyl formate

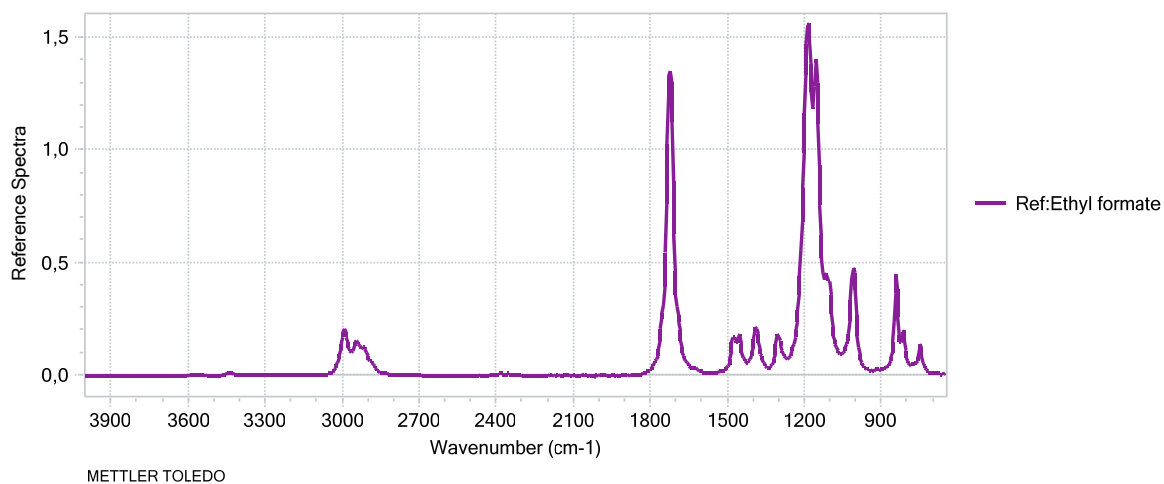


Figure D.3 IR spectra of pure ethyl formate

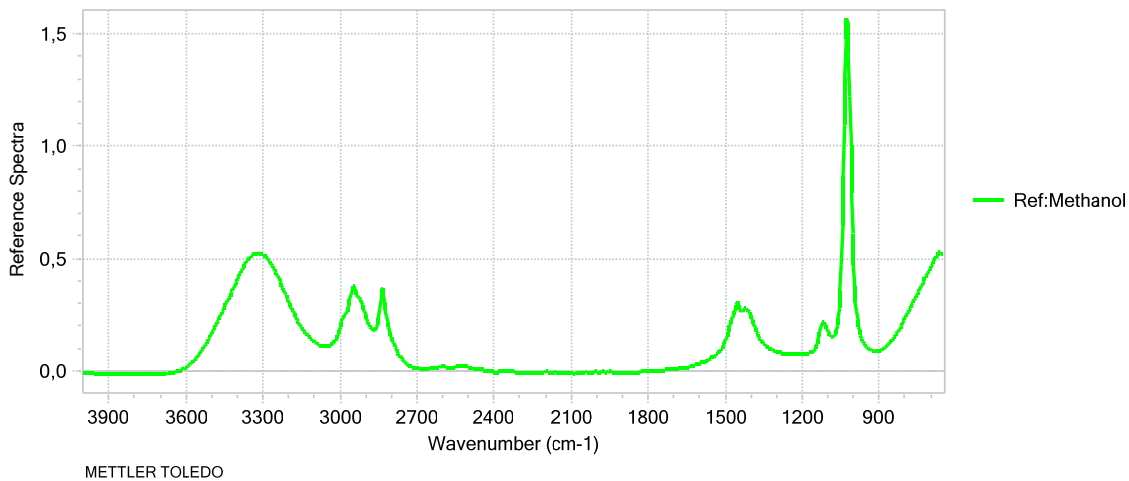


Figure D.4 IR spectra of pure methanol

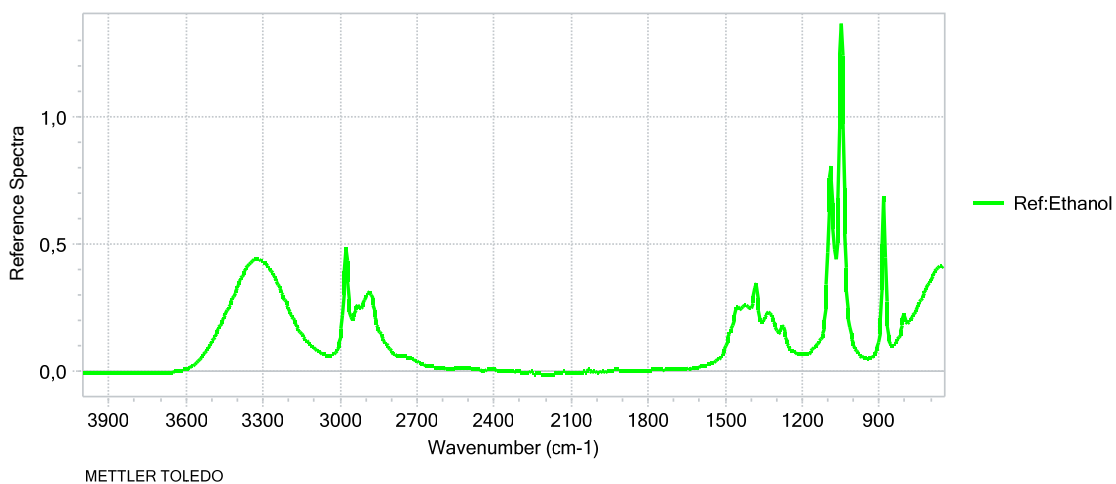


Figure D.5 IR spectra of pure ethanol

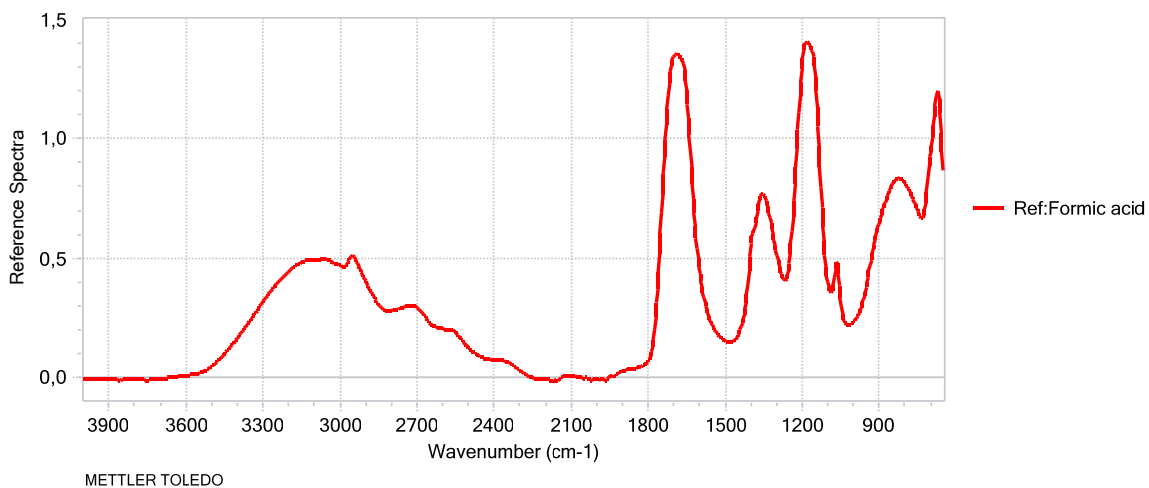


Figure D.6 IR spectra of pure formic acid

Appendix E

FTIR calibration curves

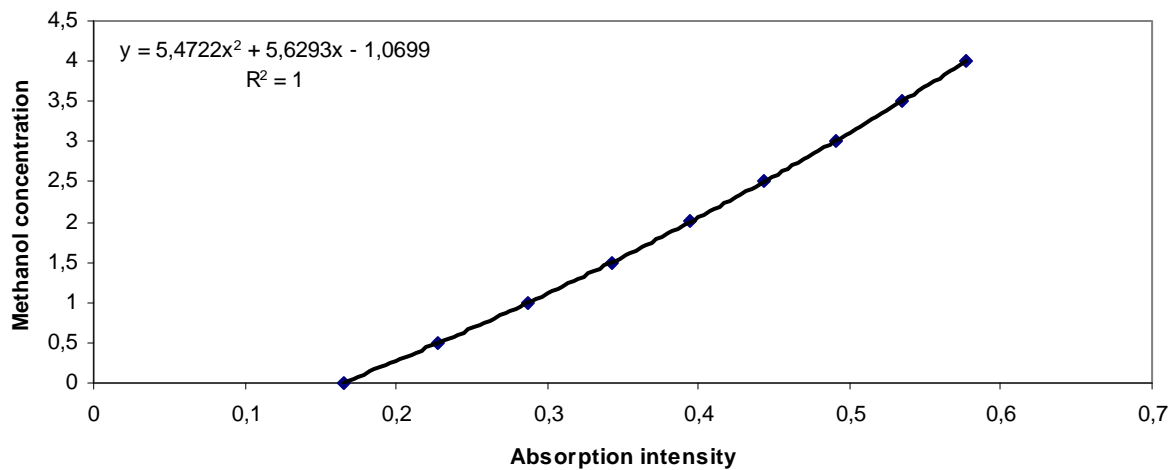


Figure E.1 FTIR calibration curves of methanol

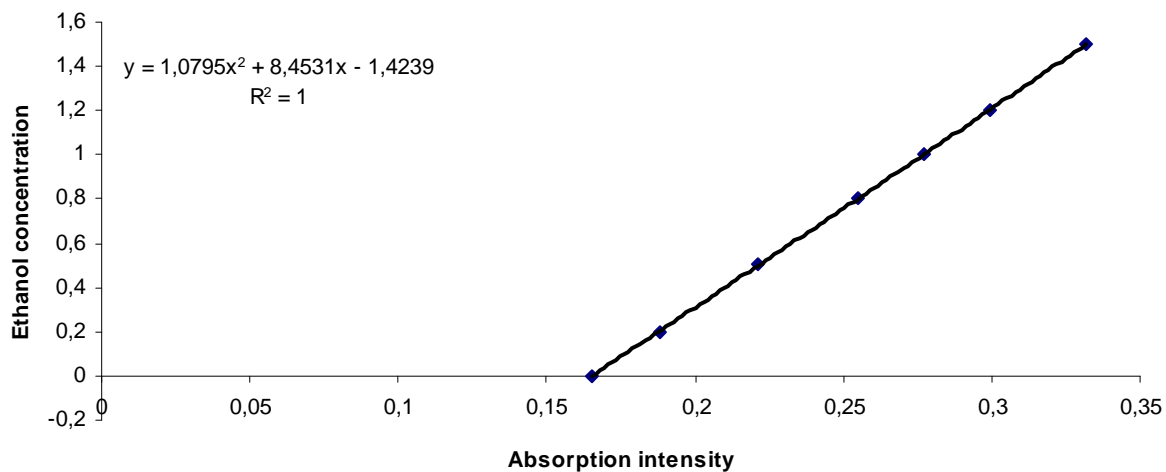


Figure E.2 FTIR calibration curves of ethanol

CURRICULUM VITAE

PERSONAL DETAILS

Full name: HONG DUC TA
Address: J. -G.- Nathusius Ring 2, Zi. 08, 39106 Magdeburg, Germany
Date of Birth: 20.02.1977
Place of Birth: Vinh Phuc, Vietnam
Nationality: Vietnamese

EDUCATION

Year	Qualification	Name of Institution/Address
1995-2000	Undergraduate degree of Chemical Engineering	Hanoi University of Science and Technology, Hanoi, Vietnam
2000-2002	Master degree of Chemical Engineering	Hanoi University of Science and Technology, Hanoi, Vietnam
2007-now	PhD research on Chemical Engineering	Otto-von-Guericke-Universität, Magdeburg, Germany

PROFESSIONAL EXPERIENCE

9.2000 – 8.2007:

Lecturer at The School of Chemical Engineering, Hanoi University of Science and Technology, Hanoi, Vietnam.

8.2007 to the present:

- Ph.D student in Chemical Process Engineering, Otto-von-Guericke-Universität, Magdeburg, Germany on topic: “A *Kinetic analysis of hydrolysis of esters considering volume and enthalpy changes due to mixing*” with Supervisor Prof. Andreas Seidel-Morgenstern
- Supervising Master students doing and writing thesis

SCHOLARSHIPS

Vietnamese Government

DAAD

Pro3-Network of Otto-von-Guericke-Universität, Magdeburg, Germany

Max Planck Society